Vesicular Loading and Synaptic Release at Central Cholinergic Synapses

A thesis submitted to the University of Manchester for the Degree of Doctor of Philosophy in the Faculty of Biology, Medicine and Health

2018

Samuel W Vernon

Division of Neuroscience and Experimental Psychology
Faculty of Biology Medicine and Health

Contents

Final Word Count: 42,873

List of Figures

List of Tables

List of Abbreviations

Abbreviation	Full Name
5Cl-CASPP	5-chloro-1=-[(E)-3-(4-chlorophenyl)allyl]spiro[indoline-3,4=-piperidine]-1-yl}-(2-chloro-4-pyridyl))
aCC	Anterior Corner Cell
Acetylcholine	ACh
AChE	Acetylcholinesterase
AEL	After Egg Laying
ATP	Adenosine Triphosphate
ChAT	Choline Acetyltransferase
ChT	Choline Transporter
CNS	Central Nervous System
CPG	Central Pattern Generator
CRISPR	Clustered Regularly Interspaced Short Palindromic Repeats
CS	Canton-S
DDT	Dichlorodiphenyltrichloroethane
DLM	Dorsal Longitudinal Flight Muscle
DMSO	Dimethyl Sulfoxide
DNA	Deoxyribonucleic Acid
EPSC	Excitatory Post-Synaptic Current
EPSP	Excitatory Post-Synaptic Potential
GABA	γ-Aminobutyric Acid
HAP1	Huntington Associated Protein
HD	Huntington's Disease
IGR	Insect Growth Regulators
IRES	Internal Ribosome Entry Site
ISN	Intersegmental Nerve
LD50	Lethal Dose = 50%
mAChR	Muscarinic Acetylcholine Receptor
mEPSC	Miniature Excitatory Post-Synaptic Current
mEPSP	Miniature Excitatory Post-Synaptic Potential
MN	Motoneuron
mRNA	Messenger Ribonucleic Acid
MVR	Multivesicular Release
nAChR	Nicotinic Acetylcholine Receptors
NMJ	Neuromuscular Junction
PAM	Protospacer Adjacent Motif
PCCAs	Polychlorocycloalkanes
PCR	Polymerase Chain Reaction
PKA	Protein Kinase A

PTx	Picrotoxin
qRT-PCR	Quantitative Reverse Transcription Polymerase Chain Reaction
RBP	RIM Binding Protein
ResP	Reserve Pool
RNA	Ribonucleic Acid
RP2	Raw Prawn 2
RRP	Readily Releasable Pool
RyP	Recycling Pool
SN	Segmental Nerve
SNAP	Synaptosomal-Associated Protein
SNARE	Soluble N-Ethylmaleimide-Sensitive Factor Attachment Protein Receptor
SRC	Spontaneous Rhythmic Current
SV	Synaptic Vesicle
TeTxLC	Tetanus Toxin Light Chain
TM	Transmembrane
TN	Transverse Nerve
TTM	Tergotrochanteral Muscle
TTX	Tetrodotoxin
UAS	Upstream Activator Sequence
UVR	Univesicular Release
VAChT	Vesicular Acetylcholine Transporter
VAMP	Vesicular Associated Membrane Protein
V-ATPase	Vesicular ATPase pump
VGAT	Vesicular GABA Transporter
VGLUT	Vesicular Glutamate Transporter
VGLYT	Vesicular Glycine Transporter
VIAAT	Vesicular Inhibitory Amino Acid Transporter
VMAT	Vesicular Monoamine Transporter
VNC	Ventral Nerve Cord

Abstract

Neurotransmitter release from presynaptic terminals can be regulated by altering transmitter load per synaptic vesicle (SV) and/or through the probability of vesicle release. The vesicular acetylcholine transporter (*VAChT*) loads acetylcholine (ACh) into SVs at cholinergic synapses. This project presents three major aims; to investigate the physiological implications of (i) *VAChT* activity modulation in central cholinergic physiology (ii) insecticide resistance through *VAChT* mutagenesis of known resistance mutations and (iii) SV loading through structural manipulation of the *VAChT* C-terminal polyQ region. Chapter 2 of this thesis investigates how pharmacological blockade (5Cl-CASPP exposure) and transgenic up-regulation of *VAChT* affects SV content and release frequency at central synapses in *Drosophila melanogaster* and provides strong evidence that vesicle loading follows a set point model. Chapter 3 examines cholinergic dysfunction in two 5Cl-CASPP resistant genetic backgrounds (*VAChT*^{Y49N} and *VAChT* up-regulation). Both resistance modalities increase spontaneous release frequency suggesting release frequency appears deterministic of CASPP activity. However, the *VAChT*^{Y49N} mutation additionally disrupts action potential-evoked cholinergic release and fictive locomotor patterning through depletion of releasable synaptic vesicles indicative of a functional trade-off. Chapter 4 investigates loading disruption through direct mutagenesis of the *VAChT* polyQ region. Truncation of the polyQ region, by one glutamine residue, results in increased SV loading kinetics whereas polyQ extension is sufficient to reduce loading. Deletion of the polyQ region has no obvious effect on spontaneous release, but evoked synaptic currents show increased duration. Thus the polyQ region of the insect *VAChT* is required for correct vesicle transmitter loading.

Declaration and Copyright Statement

No portion of the work referred to in the thesis has been submitted in support of an application for another degree or qualification of this or any other university or other institute of learning.

i. The author of this thesis (including any appendices and/or schedules to this thesis) owns certain copyright or related rights in it (the “Copyright”) and s/he has given The University of Manchester certain rights to use such Copyright, including for administrative purposes.

ii. Copies of this thesis, either in full or in extracts and whether in hard or electronic copy, may be made only in accordance with the Copyright, Designs and Patents Act 1988 (as amended) and regulations issued under it or, where appropriate, in accordance with licensing agreements which the University has from time to time. This page must form part of any such copies made.

iii. The ownership of certain Copyright, patents, designs, trademarks and other intellectual property (the “Intellectual Property”) and any reproductions of copyright works in the thesis, for example graphs and tables (“Reproductions”), which may be described in this thesis, may not be owned by the author and may be owned by third parties. Such Intellectual Property and Reproductions cannot and must not be made available for use without the prior written permission of the owner(s) of the relevant Intellectual Property and/or Reproductions.

iv. Further information on the conditions under which disclosure, publication and commercialisation of this thesis, the Copyright and any Intellectual Property and/or Reproductions described in it may take place is available in the University IP Policy (see

Acknowledgements

I would like to thank Richard Baines for his support and supervision throughout this project from the unfortunately common mediocracies of administrative tasks to data collection, interpretation and manuscript preparation. Richard has never been too busy to provide advice to myself and others. This ideology emanates throughout all lab members which greatly facilitated a warm, welcoming and enjoyable lab which was a genuine pleasure to be a part of for the past 4 years.

I would also like to thank Jim Goodchild for his support and supervision throughout the project from an industrial angle. Jim hosted me during my industrial placement at Syngenta which was a fantastic experience and allowed me to appreciate the science done within industry. Jim and his team, notably Lucy Firth and Jenny Willis, were incredibly welcoming. Jim never failed to provide refreshing insights into fundamental questions throughout my project.

Of course, supervision is notoriously difficult to conduct effectively when there is no work to supervise. I am therefore, indebted to Richard, Carlo Giachello and Francesca Cash whom not only taught me all manner of physiology techniques, from patching neurons to extracellular muscle recordings in larvae and adults, but who also greatly facilitated my understanding of synaptic physiology through frequent discussions both in the lab and in the pub. Wei-Hsiang Lin was heavily utilised as my personal molecular biology oracle throughout my project, but who also tirelessly taught me countless molecular techniques from cloning, cell culture, transfection, PCR/RT-qPCR and western blotting to name but a few. Wei-Hsiang's help and advice were pivotal in my understanding and implementation of the several successful CRISPR projects

throughout my PhD which, being conducted at the very beginning of our understanding of CRISPR gene editing in *Drosophila,* were a pleasant surprise to say the least.

Once I was considered competent I was allowed to teach newcomers to the lab. Benjamin Castle, Lucia de Andres Bragado, Anna Munro and Adam Bradlaugh were all endowed with my teachings of *Drosophila* electrophysiology…. for which I profusely apologise. I would also like to give my sincerest gratitude to Fiona He and Carol Fan who work tirelessly to keep the lab running at such a high level and give my best of luck to the new PhD starters Fred Mulroe, Jurga Mituzaite and Anna Munro for the rest of their projects.

I would like to thank my family for their support over the last 4 years with special mention to my Mother- Jackie, Twin - Kerry, and soon to be born niece - Mya. Katie Ashcroft deserves a particular thank you for putting up with me over the last year. For some unknown reason you have trusted me enough to introduce me to Matilda and welcome me into your family with open arms for which I am incredibly grateful. Finally, I would also like to thank my friends with a special mention to Tom Pooler, Paddy Pooler and Patrick Garner and to the entirety of my Rugby Team “The Pistol Shrimps” for their “guidance”, admittedly guidance back home from the pub but guidance nonetheless.

General Introduction

1.0 The Synapse

The synapse is the fundamental unit of communication between two cells. At its core, it is no more than a structure that facilitates information transfer within close proximity. This is reflected in the etymology of the word itself from the Greek "syn-" ("together") and "haptein" ("to clasp"). The first synapses are thought to have appeared in conjunction with the first identifiable neural networks over 500 million years ago in the Cambrian seas, in the Phylum *Cnidaria* consisting of ancestral jellyfish and hydras (Miljkovic-Licina et al., 2004). These simple networks consisted of sensory cells in contact with the environment leading to effector cells governing locomotion allowing an individual to adapt and respond to environmental stimuli. The evolutionary success of this system resonates to today when considering almost all modern multicellular life has at least a rudimentary nervous system reminiscent of their ancestral counterparts (with the exception of *Porifera*: the sponges). The adult human brain is estimated to contain 100-500 trillion synapses (Drachman, 2005). This dwarfs even the most controversial estimates of stars in our own galaxy at roughly 100-200 billion (Kornreich, 2017). Thus, the brain is complex and although evolution has vastly diversified the structure and complexity of nervous systems throughout the animal kingdom, the fundamental unit of communication, the synapse, remains remarkably conserved.

Chemical synapses refer specifically to those synapses that utilise neurotransmitter to convey information. Briefly, neurotransmitter is synthesised and loaded into synaptic vesicles where they are stored before release into the synaptic cleft. Here, the chemical signal is identified through a specific receptor type on the neighbouring postsynaptic membrane before being recycled. Unlike vertebrates, which use glutamate, the insect

CNS utilises acetylcholine as its major excitatory neurotransmitter. I will therefore utilise the cholinergic system in order to describe current knowledge of the mature nervous system with a specific focus on nerve terminal vesicle kinetics and cholinergic synapses.

1.1 Synaptic Vesicles and Vesicle Pooling

Nerve terminals can be thought of as computational secretory units whereby fast, sustained release is controlled via both intra and intercellular signalling. Synaptic vesicles (SVs) are abundant components of all chemical presynaptic nerve terminals. In contrast to other types of vesicle (vacuoles, lysosomes etc.), SVs are specialised for uptake, storage and release of neurotransmitters. The composition of SVs is well conserved between humans and invertebrates with a protein to lipid ratio of approximately 1:3 (Südhof, 2004). Despite their unremarkable appearance, SVs are essential for synaptic functioning and contain a variety of proteins necessary for vesicle loading and exocytosis.

1.1.1 Vesicle Pools

Three major vesicle pools have been identified from the rate of neurotransmitter release under differing stimulation conditions; the readily releasable pool, recycling pool and reserve pool (Südhof, 2004, Rizzoli and Betz, 2005). The readily releasable pool (RRP) consists of docked and primed vesicles at the active site that are releasable immediately, typically constituting 1% of the total pool size (Rizzoli and Betz, 2005). The RRP rapidly decreases under initial stimulation followed by a prolonged period of slow release, sustained by the recycling pool (RyP) (Südhof, 2004, Rizzoli and Betz, 2005). The RyP constitutes between 10% - 20% of total pool size and is replenished by newly recycled vesicles (Rizzoli and Betz, 2005). The final characterisation of vesicle pools is

the reserve pool (ResP), this pool constitutes 80%-90% total pool size and is reportedly only triggered under intense stimulation; 30Hz at the *Drosophila* neuromuscular junction (NMJ) (Kuromi and Kidokoro, 2000). The exact mechanism between what modulates the activation of the ResP is unclear. However, the ResP is only mobilised once the RyP has been depleted (Kuromi and Kidokoro, 1998). See Fig. 1.1 for schematic of each pool characterisation.

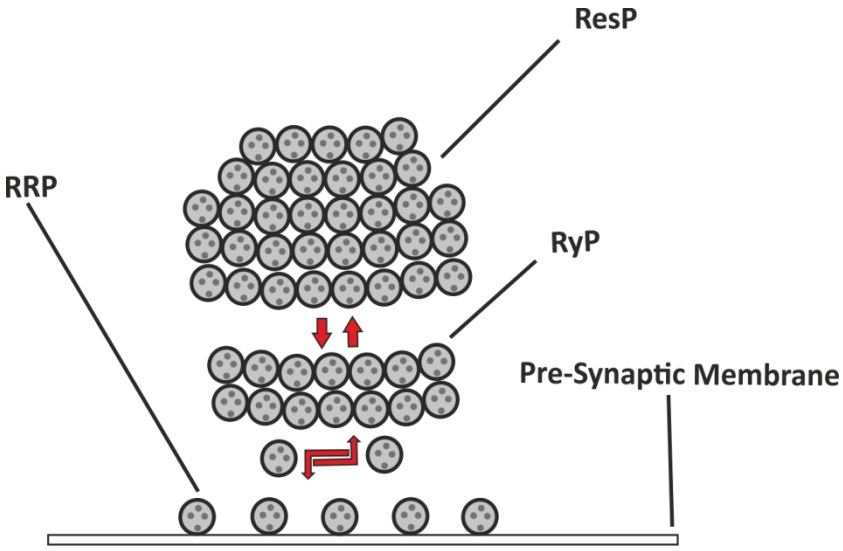

Figure 1.1: Major characterisations of currently identified presynaptic vesicle pools. The readily releasable pool (RRP) consists of only vesicles primed and docked at the presynaptic membrane. The recycling pool (RyP) consists of a larger pool containing what could be considered a backup for the RRP. Together, the RRP and RyP are commonly engaged during physiologically "normal conditions". The reserve pool (ResP) was discovered only under tetanic stimulation and is estimated to make up the vast majority of vesicles at a nerve terminal. Although, in this figure, these pools are shown as morphologically separate it is likely these pools undergo mixing to a large extent (red arrows).

Despite the above characterisation, the number of vesicles in each pool is not consistent between neurons and/or species. Using a combination of electron/fluorescence microscopy and electrophysiology it has been found that in the

goldfish retinal bipolar cell, the reserve pool consists of ~99% of vesicles, with only ~0.17% in the RRP and ~0.6% in the RyP (Rizzoli and Betz, 2005), whereas, at the neuromuscular junction in larval *Drosophila* preparations, 80% of total vesicles are in the ResP, ~14%-19% in the RyP and ~0.4% in the RRP (Rizzoli and Betz, 2005). This suggests a potential problem with the above characterisation. Indeed, a general consensus from major reviews of this area appear to agree that these pools should not be considered morphologically separate and mixing of pools may be more frequent than initially proposed (Südhof, 2004, Rizzoli and Betz, 2005).

1.1.2 The Vesicle Cycle

Synaptic vesicle components are initially trafficked to the synapse using members of the kinesin motor family (Pack-Chung et al., 2007). Once at the synaptic terminal, vesicles are loaded with neurotransmitter. This requires a neurotransmitter transporter and a v-ATPase pump that provides a pH and electrochemical gradient (Maxson and Grinstein, 2014). These transporters are selective for different classes of transmitters. Both loading and transporters will be considered in more detail in Section 1.4.

Once loaded, vesicular exocytosis is mediated by a convergence of three principal proteins forming what is termed a SNARE (soluble N-ethylmaleimide-sensitive factor attachment protein receptor) complex. A vesicle-associated protein (Synaptobrevin) and two proteins situated on the presynaptic membrane (Syntaxin 1 and SNAP-25) make up this complex (Südhof, 2004). Each protein contains at least one homologous sequence called a SNARE motif. Motifs R from Synaptobrevin, Qa from Syntaxin-1 and Qb and Qc from SNAP-25 form a stable SNARE complex (Südhof, 2004). Once stable, SVs are considered docked and primed, ready for Ca^{2+} triggered fusion.

The Ca^{2+} transient develops at the peak of an incoming action potential, ending before repolarization (Südhof, 2004). Synaptotagmin 1 and 2 are the primary Ca^{2+} sensors required to trigger release and are known to interact with the SNARE complex and presynaptic membrane during Ca^{2+} influx.

Post-fusion, vesicles are recycled following several proposed mechanisms. Initially, a 'kiss and stay' route was described whereby SVs are refilled locally, without undocking from the presynaptic membrane (Barker et al., 1972, Südhof, 2004). Further studies predicted that SVs are released before being refilled, after which SVs are docked and primed, referred to as 'kiss and run' (Ceccarelli et al., 1973, Südhof, 2004). Finally, a third route termed 'endosomal recycling' was observed following high stimulation of the nerve terminal whereby SVs are released from the presynaptic membrane and reconstructed via clatherin coated pits, loaded and docked (Heuser and Reese, 1973, Südhof, 2004). A model of the exact mechanism of SV recycling is yet to be proposed. However, these pathways are not necessarily mutually exclusive.

1.2 Acetylcholine Synthesis, Function and Catalysis in the Insect CNS

Acetylcholine was first identified in human heart and vagus nerve by Sir Henry Hallett Dale and Otto Loewi. Their following work studying the transmission of nerve impulses earned them a Nobel Prize in 1936. Acetylcholine is now known as a ubiquitous neurotransmitter found in the vast majority of organisms. The biosynthetic enzyme choline acetyltransferase (*ChAT*) has been found in mammals, insects, fungi, plants and bacteria suggesting the molecule is evolutionarily highly conserved (Horiuchi et al., 2003). In insects ACh is considered the major excitatory neurotransmitter in the CNS (Dupuis et al., 2012).

Choline acetyltransferase facilitates the reversible synthesis of ACh from an acetyl group (from acetyl-coenzyme A) and choline at cholinergic nerve terminals (Soreq and Seidman, 2001); see Fig. 1.2. *ChAT* is initially produced in the soma of cholinergic neurons and transported to the nerve terminal where its concentration is typically at its highest (Mallet et al., 1998). Therefore, the speed at which transfer occurs, rate of production and presence of endogenous substrate are important factors governing the concentration of ACh in cholinergic neurons.

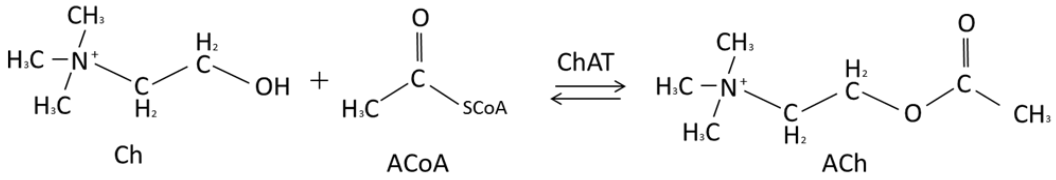

Figure 1.2: The Biosynthesis of Acetylcholine. Chemical structure of reversible cholineacetyletransferase (ChAT) catalysed reaction representing the synthesis of Acetylcholine (ACh) from Acetyl-CoA (ACoA) and Choline (Ch).

Due to its importance in cholinergic neurons, *ChAT* has been considered a particularly reliable biochemical marker. For example, *ChAT* mRNA and activity is first identified 6-7 hours after egg laying (AEL) in *Drosophila* (Carbini et al., 1990), approximately 7-8 hours prior to the first detectable ACh mediated currents (Baines and Bate, 1998). This time delay between expression and function may be explained by non-vesicular ACh roles associated with developmental neural pathfinding (Yang and Kunes, 2004).

Fig. 1.3 shows that *ChAT* mRNA and enzyme activity steadily increase throughout the larval stages of development to reach a maximum in 3rd instar *Drosophila* larvae. *ChAT*

activity then decreases through pupation and reaches a second peak at late pupation/early adult stages (Carbini et al., 1990).

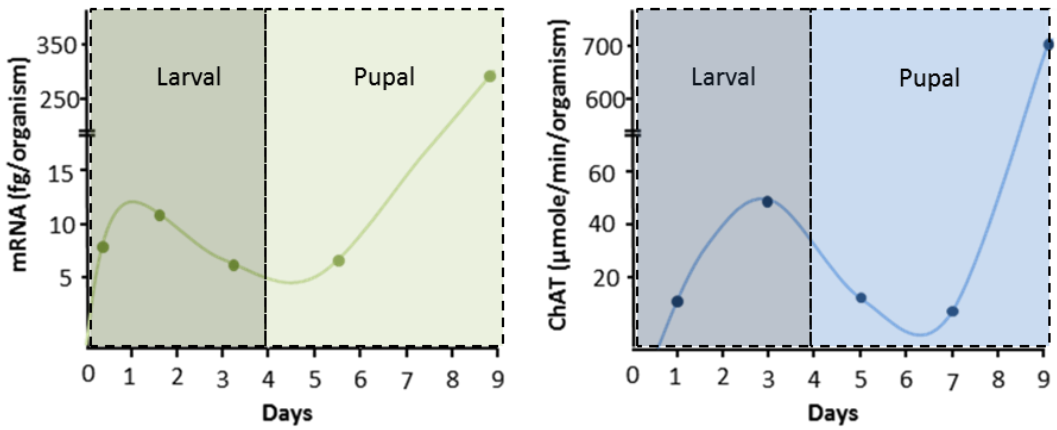

Figure 1.3: Cholinergic machinery expression peak in late larvae and pupae stages. Graphs display the relationship between (a) *ChAT* mRNA expression levels (b) *ChAT* enzyme activity with age displayed in days. Adapted from Carbini et al (1990).

Once released, acetylcholinesterase (*AChE*) inactivates ACh by hydrolysing ACh into acetate and choline (Soreq and Seidman, 2001). *AChE* is known to have an extraordinarily high rate of catalysis; approximately 25,000 molecules per second (Taylor and Radic, 1994). This is unusual as the enzyme catalytic site is similar to other serine hydrolases, having serine, histidine and an acidic residue (glutamate for *AChE*) constituting the catalytic triad, situated centrally within the active site (Soreq and Seidman, 2001). The mechanism for such high turnover is still to be discovered but is thought to be related to the enzyme's unusually strong electric field (Soreq and Seidman, 2001). See Fig. 1.4 for chemical representation of catalysis.

Subsequent to catalysis, selective uptake of choline via the choline transporter protein (*ChT*) situated on the presynaptic terminal replenishes presynaptic stores for the

production of ACh via *ChAT* (Okuda et al., 2000). Cholinergic neurons have been found to increase choline uptake in proportion to ACh demand. This system is believed to be one of the rate limiting steps in ACh synthesis (Yamamura and Snyder, 1972, Kuhar and Murrin, 1978, Okuda et al., 2000).

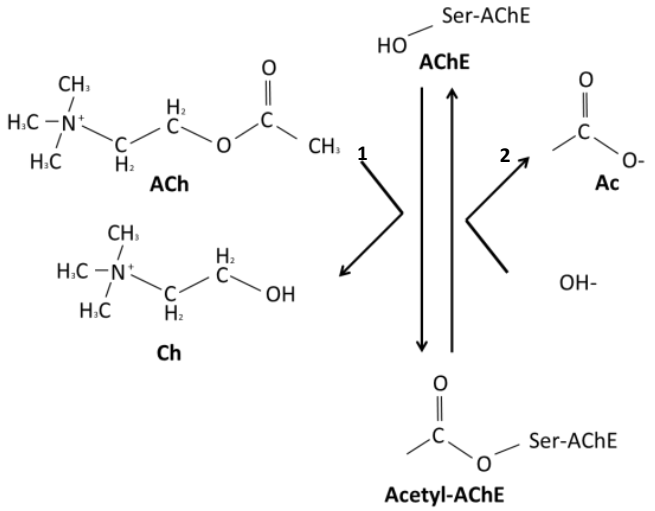

Figure 1.4: Catalysis of Acetylcholine. Hydrolysis of Acetylcholine (ACh) into choline (Ch) and an acetyl-AChE intermediate is catalysed by Acetylecholinesterase (*AChE*) (1). The subsequent hydrolyses of acetyl-AChE releases an Acetate and OH^- (2). Choline is then transported into the nerve terminal where *ChAT* catalyses ACh synthesis. Figure adapted from (Soreq and Seidman, 2001).

1.3 Vesicular Transporters and the *VAChT*

Simply synthesising a biologically active neurotransmitter does not allow controlled release at a synapse. Therefore, neurotransmitter needs to be packaged into synaptic vesicles for storage before release. Transporters known to localise to SVs transport glutamate through vesicular glutamate vesicular transporters (*VGLUTs*) 1-3 (Takamori et al., 2000, Takamori et al., 2001), glycine through VGLYT1 (with *VGLYT2* yet to be shown to localise to SVs) (Núñez et al., 2009, Cubelos et al., 2014), GABA and Glycine

are co-transported through *VGAT* also referred to as *VIAAT* (McIntire et al., 1997, Sagné et al., 1997, Aubrey, 2016) and ACh through the Vesicular Acetylcholine Transporter (*VAChT*) (Erickson et al., 1994). Transfection of *VGLUT1* into GABAergic neurons *in vitro* causes these neurons to became both glutamatergic and GABAergic (Takamori et al., 2000) suggesting that the expression of a particular transporter is indicative of the type of neurotransmitter produced in a given neuron.

VAChT null mutant mice die soon after birth (De Castro et al., 2009) and VAChT null *Drosophila* mutants are embryonic lethal (Kitamoto et al., 1998). In mice *VAChT* knockdown causes memory and social recognition deficits (Prado et al., 2006) whereas *VAChT* up-regulation causes accelerated neuromuscular aging (Naves et al., 2016) as well as influencing gross cholinergic morphology (Janickova et al., 2017). These physiological features echo original findings in *Drosophila* at the glutamatergic neuromuscular junction under *VGLUT* up-regulation (Daniels et al., 2004, Daniels et al., 2011). It is therefore unsurprising that transporter abnormalities including the *VAChT* are synonymous with many neurodegenerative diseases such as Alzheimer's (Ferreira-Vieira et al., 2016), Huntington's (Suzuki et al., 2001) and Parkinson's disease (Mazere et al., 2009).

The *VAChT* is classified within the SLC18 group of the Major Facilitator Superfamily (Lawal and Krantz, 2013), specifically, subclassified within the H^+ Antiporter-1 Family (DHA1, TCID 2.A.1.2) (See Transporter Classification Database (http://www.tcbd.org). Both invertebrates and mammals express a single *VAChT* isoform (*SLC18A3*) (Lawal and Krantz, 2013). This has been shown to be expressed in all cholinergic neurons in the mammalian (Fei and Krantz, 2009) and insect CNS (Kitamoto et al., 1998)

Computational modelling predictions suggest that the *VAChT* contains 12 transmembrane (TM) domains with a large luminal loop between TM1 and TM2 (Usdin et al., 1995, Fei and Krantz, 2009; Fig. 1.5). Unfortunately, a crystalline structure for *VAChT* is unavailable. However, site directed mutagenesis has identified typtophan (W), alanine (A) and phenylalanine (F) residues in TM8 and a cysteine (C) in TM10 as potentially important for ACh affinity. Further regions in TM10 containing an aspartate (D) are believed to be involved in proton exchange and glycine/proline (G/P) is thought to be involved in transport activity on TM5 and TM11 (Lawal and Krantz, 2013) (see Fig. 1.5 for schematic).

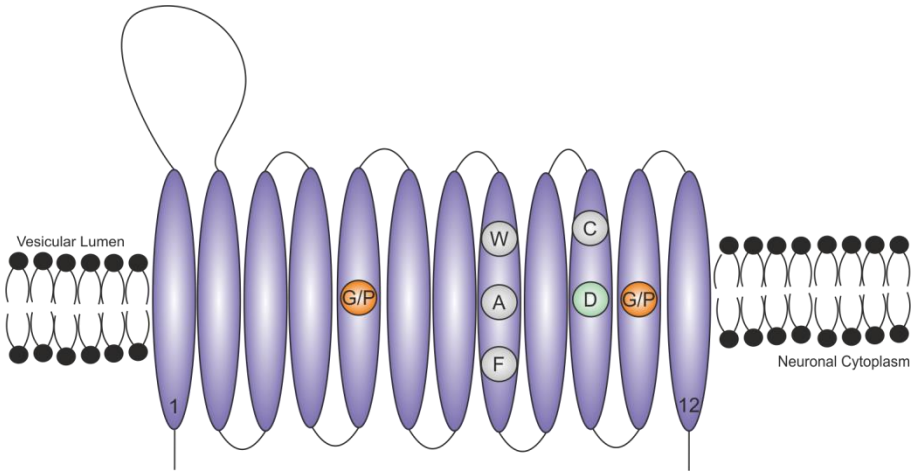

Figure 1.5: Proposed structure of the *VAChT* protein. The *VAChT* contains 12 transmembrane domains (TM1-12: Violet). A glycine and or proline (G/P) on TMs 5 & 11 are thought to be involved in transport activity (orange). Site directed mutagenesis studies have suggested that amino acids typtophan (W), alanine (A) and phenylalanine (F) in TM8 and a cysteine (C) in TM10 are thought to be important in ACh affinity (grey). Whereas, an aspartate (D) on TM10 is thought to be involved in proton exchange (green). Amino acid locations do not reflect their relative positions within the protein. Adapted from (Lawal and Krantz, 2013).

In *Drosophila*, the gene encoding *VAChT* is 7.2 kb and situated within the first intron of the *ChAT* gene; both genes make up what is termed the cholinergic locus (Kitamoto et al., 1998). The use of specific cDNA probes in *Drosophila* suggests both genes are transcribed in the same direction and are likely under similar transcriptional control (Usdin et al., 1995, Kitamoto et al., 1998). This unusual arrangement has been likened to an operon in which multiple genes are under control of a single promoter (Usdin et al., 1995). However, *ChAT* is expressed proportionally more than *VAChT* in the body of adult flies (Kitamoto et al., 1998), whereas, in the head, *ChAT* and *VAChT* are expressed in similar proportions suggesting that post transcriptional control may also be an important determinant of expression (Kitamoto et al., 1998). Expressional regulators of the cholinergic locus are yet to be conclusively identified. However, in recent mammalian models, the chemokine *CXCL12* has been shown to influence expression of the cholinergic locus and the choline transporter (*ChT1*) through downstream Akt signalling (Yan et al., 2016). These signalling molecules are expressed ubiquitously throughout the body and are thought to be mainly involved in cell survival, growth, proliferation and migration through multiple intracellular phosphorylation targets and hence are heavily studied in the cancer field (Liang et al., 2007, Domanska et al., 2013, Guo et al., 2016a). However, a direct and specific interaction between cholinergic machinery and this pathway remains to be specifically identified.

The *Drosophila VAChT* gene has unusually long 5' and 3' UTRs making it much larger in size than its mammalian homologs (~3-4kb) (Mallet et al., 1998). The 5' region contains three potential initiation codons (ATG) followed by multiple termination codons. Conventionally, the ribosome binds to the 5' end of the mRNA, progressively reading until it reaches the first start codon. However, the *VAChT* configuration does not appear to be appropriate for this mechanism. Instead, internal ribosome entry site

(IRES) translation, common in viruses (Tsukiyama-Kohara et al., 1992, Licursi et al., 2011) and reported in eukaryotic mRNA (Pain, 1996), has been proposed whereby ribosomes directly bind to an internal sequence, with translation occurring at the first start codon downstream of the IRES sequence (Kitamoto et al., 1998).

1.4 Vesicle Loading

Vesicular loading requires initial acidification which generates both a pH gradient (ΔpH) and a voltage gradient (Δψ). The ratio of these two components is heavily influenced by the type of neurotransmitter being transported and the activity of other vesicle specific machinery (Takamori, 2016). This is displayed utilising the cholinergic system in Fig. 1.6. This section will discuss the most heavily researched components of vesicle loading.

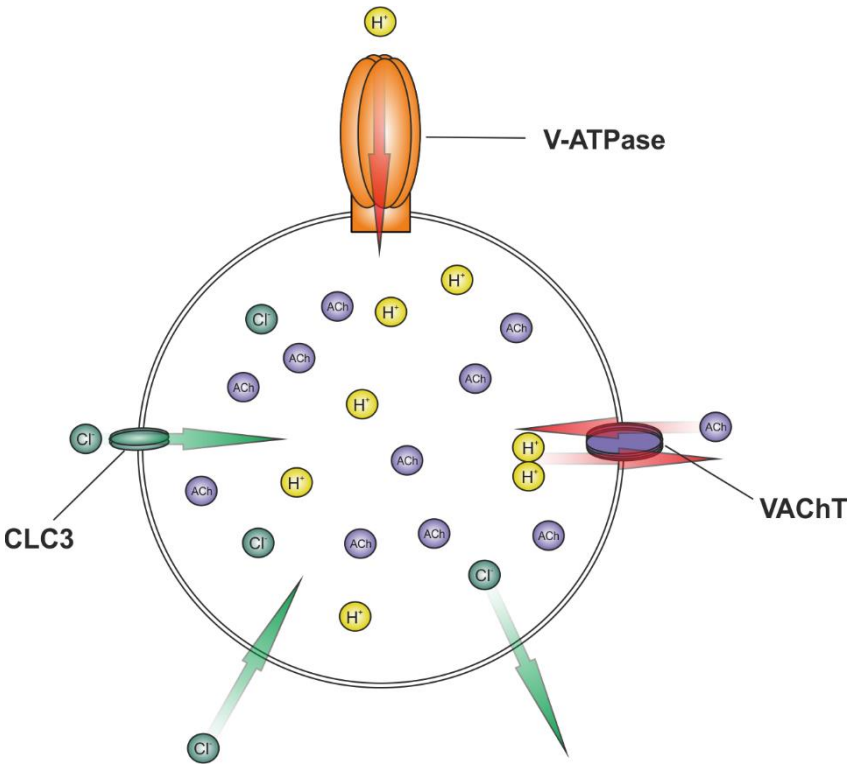

Figure 1.6: Current model for cholinergic loading kinetics. Synaptic Vesicle (SV) loading is governed by a complex interplay between protons (H^+), neurotransmitter (ACh), and chloride ions (Cl^-). Chloride generates an electrochemical gradient assisting the ATP dependent acidification governed by the Vesicular ATPase pump (V-ATPase). Protons

are then actively transported in an antiporter system via the vesicular acetylcholine transporter (*VAChT*) whereby two protons are exchanged for every one molecule of ACh. Red arrows display active transport whereas green arrows display passive leak diffusion of Cl^- through CLC3.

1.4.1 Transporter Activity

Section 1.3 covers transporter diversity at the nerve terminal. However, vesicle loading differs between transporter type and care should be taken when directly comparing vesicular loading kinetics between systems. Monoamine Transporters (*VMATs*) rely mainly on pH whereas glutamate (*VGLUT*) appears to be mainly driven by electrical potential (El Mestikawy et al., 2011, Van Liefferinge et al., 2013). Interestingly GABA (*VGAT/VIAAT*) and ACh (*VAChT*) appear to be sensitive to both gradients (Takamori, 2016).

Transport of ACh into a vesicle involves the exchange of two protons in an antiporter system using the proton-electrochemical gradient generated by the v-ATPase proton pump described above (Südhof, 2004, Lawal and Krantz, 2013). The current model suggests that one proton is used to transport ACh into the SV lumen and another proton is used to re-orientate the substrate binding site back towards the cytoplasm ($2H^+$ for $1ACh^+$) (Parsons, 2000). *In situ*, acidified vesicles exhibit a pH approximately 1.4 units less than un-acidified vesicles (Parsons, 2000). Through pharmacological reduction of the pH and electrical gradient, it was found that although *VAChT* relies on both pH and electrochemical gradients, *VAChT* primarily uses the pH component of this system to drive uptake (Parsons, 2000). Theoretically, the vesicular lumen is reported to have the potential to reach up to a 100 times greater concentration than that of cytoplasmic (1-4mM) ACh concentrations (Parsons et al., 1993, Parsons, 2000). Varoqui

and Erickson show that actual *VAChT* loading kinetics do not approach anywhere near these figures. Using human *VAChT* cDNA expressed in PC12 cells, *VAChT* was shown to display a Km value of 0.97 ± 0.1 mM and Vmax of 0.58 ± 0.04 nmol/min/mg (Varoqui and Erickson, 1996). ACh uptake was linear for approximately 10 min which approached a maximal steady-state between 30 – 60 minutes. Maximal accumulation of ACh was found to saturate at ~4 mM (Varoqui and Erickson, 1996). Subjectively, a 30-minute time period before maximal loading is achieved appears rather slow for a transporter that mediates millisecond responses to synaptic activity. However, these data may explain why up to 90% of vesicles at a synapse are found in the Reserve Pool ready to localise to the presynaptic membrane (Section 1.1.1). Even the aforementioned initial estimates of 100 fold increases in vesicular ACh concentration relative to cytoplasmic ACh is approximately 3000 times less than the predicted driving force extrapolated from cytoplasmic proton availability *in vivo,* suggesting a rather dramatic limiting factor during loading (Parsons et al., 1993, Parsons, 2000). Parsons argues that without a rate limiting mechanism, ACh concentrations would breach a biologically implausible concentration of 3M which may account for some of this variability and that a greater potential for loading would also buffer loading kinetics against variable ACh concentrations at the synapse. Whether or not the limiter is dictated by the transporter, substrate availability or both remains unknown but experimentally, measurements of loading kinetics and transporter activity have also been hugely contradictory.

Other insect vesicular transport proteins such as the *Drosophila VGLUT* localised to the NMJ modulate the amount of neurotransmitter per vesicle (quantal size) through the manipulation of vesicle diameter when under transgenic up-regulation (Daniels et al., 2004). Conversely, mouse NMJ models link a decrease in *VAChT* activity with a

corresponding decrease in quantal size (Prado et al., 2006, Lima et al., 2010). Radiolabelling assays further suggest that human *VAChT* expression fills rat SVs vesicles (derived from PC12 Cells) to 20 times that of control cells (Varoqui and Erickson, 1996) and cultured glutamatergic rat hippocampal neurons increase quantal size under modulation of VGLUT1 (Wilson et al., 2005), whereas manipulating *VAChT* activity at snake NMJ shows no effect on quantal size (Parsons et al., 1999), suggestive of a regulatory mechanism governing vesicle loading in these systems.

Variability in loading kinetics has been articulated before and encouraged Williams in 1997 to develop two distinct models of vesicle filling. The Set-Point Model proposes a mechanism restricting the amount of neurotransmitter per vesicle to a fixed maximum, whereas the Steady State Model suggests the amount of neurotransmitter that enters the SV is offset by leakage, but that both are independent variables that can autonomously change to produce SVs with variable levels of filling (Williams, 1997); see Fig. 1.7 for schematic. The Set Point Model is consistent with the snake NMJ (Parsons et al., 1999), i.e. overexpression of the *VAChT* is not associated with increased quantal size, whereas, the Steady State Model better describes loading at the mouse, *Drosophila* and *C. elegans* NMJ, embryonic *Xenopus* motoneurons and rat hippocampal cultures (Daniels et al., 2004, Prado et al., 2006, Lima et al., 2010, De Castro et al., 2009, Song et al., 1997, Wilson et al., 2005). This variability in vesicle loading both between species and between transporter localisation may highlight fundamental differences in transporter function between phylogenetically distinct species, honed by evolution to supplement diverse functional requirements.

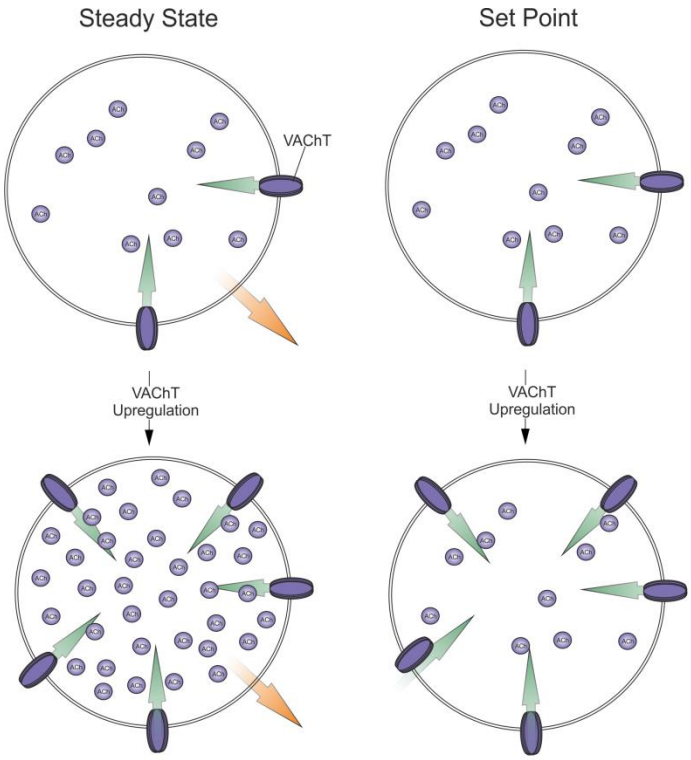

Figure 1.7: Two proposed models of vesicular loading. The 'steady state model' (left) suggests the amount of neurotransmitter that enters the SV is governed between independent variables that can change to produce SVs with variable levels of filling, whereas the 'set-point model' (right) proposes a mechanism restricting the amount of neurotransmitter per vesicle to a fixed maximum. Red arrows indicate passive leakage whereas Green indicates *VAChT* mediated transport.

1.4.2 The v-ATPase Pump

The v-ATPase proton pump sets up the electrochemical gradient for vesicle loading**.** V0 and V1 sections make up the transmembrane and cytosolic domains respectively (Maxson and Grinstein, 2014). V0 is proposed to function mainly for H^+ translocation whereas V1 hydrolyses ATP to support translocation (Maxson and Grinstein, 2014). As a vesicle is released and recycled, its luminal pH changes dramatically and must be dynamically regulated. This is in part achieved by a reversible disassociation of the V0 and V1 domains. The underlying trigger of the disassociation and association is

unknown but appears sensitive to glucose concentration and modulated by microtubules in yeast (Kane, 1995, Xu and Forgac, 2001) raising the possibility for a metabolic sensing function. This mechanism has also been linked to luminal pH in secretory granules whereby association occurs at neutral pH and disassociation occurs at more acidic pH (Poëa-Guyon et al., 2013). A mechanism whereby the α2 subunit of V0 recruits the pH sensitive *Arf* nucleotide exchange factor (ARNO aka CYTH2) suggests luminal pH can be detected at the v-ATPase (Hurtado-Lorenzo et al., 2006, Merkulova et al., 2010). Furthermore, the number of H^+ pumped per ATP (termed coupling efficiency) is known to be variable and has been shown to be between 2 and 4 H^+ per ATP in yeast (Kettner et al., 2003, Cross and Müller, 2004).

In addition to the v-ATPase major role in proton translocation, a secondary role in vesicle fusion has been proposed. Specifically, following vesicle docking and SNARE motif binding, it has been suggested that two adjacent V0 domains can join aiding vesicle fusion (Bayer et al., 2003, Peters et al., 1990)*;* even one V0 domain has been hypothesised to be sufficient to aid vesicle fusion (Baars et al., 2007). However, the precise mechanism for this has not been demonstrated.

1.4.3 Chloride Channels

Small anionic molecules such as Cl^- have classically been ignored when considering vesicular loading as the major contributor to vesicle acidification was thought to be v-ATPase activity. This may be true; however, the v-ATPase is an electrogenic pump and so requires counter-ion flow across the SV membrane for optimal functioning (Moriyama and Nelson, 1987). Indeed, SVs and other small isolated organelles have been recently found to maximally acidify in the presence of Cl^- (Schenck et al., 2009, Takamori, 2016) and so Cl^- may be thought of as a co-requisite to vesicle acidification.

SVs are permeable to Cl^- (Tabb et al., 1992) and one may assume that a slow membrane leak conductance of Cl^- may occur passively given the correct conditions (Takamori, 2016). Mammalian models suggest Cl^- currents have been shown to exist through the *CLC3* channel shown to localise to synaptic vesicles. However, this has been disputed (Schenck et al., 2009). Furthermore, recent evidence is highly suggestive of a Cl^- conductance in the glutamatergic system through the vesicular glutamate transporter (*VGLUT1*) (Schenck et al., 2009). Whereas, Cl^- conductance through *VAChT* is thought to be negligible (Parsons, 2000). As stated above there is evidence that the v-ATPase itself may act as a pH sensor and so one may hypothesise that Cl^- conductance may act as a pre-requisite for the onset of vesicle acidification. Chloride conductance in regard to vesicle loading has been studied in the glutamatergic system (Tabb et al., 1992; Schenck et al., 2009). However, Cl^- contribution to ACh loading remains largely unexplored.

1.4.4 A Limit to Loading?

Williams proposes the set point and steady state model for vesicular loading. However, this assumes vesicles only fuse once full. If steady state loading is accurate, vesicles may fill to variable levels, but what sets this upper limit? Do empty or half-full vesicles not fuse and if so why not?

These types of questions have only just been attempted to be addressed thanks to the development of appropriate optogenetic tools and reporters. Rost et al (2015) generated a light activated proton-pump that localises to synaptic vesicles (pHoenix). Under 546nm stimulation, protons are actively pumped into the vesicle lumen in excess of endogenous v-ATPase activity. pHoenix activation causes a subtle 10% increase in vesicular loading in glutamatergic murine autaptic hippocampal cells in culture

conditions (Rost et al., 2015) suggesting that under normal physiological conditions, vesicles are already nearly at full capacity in this system. Interestingly the authors also noted that full vesicles had a much higher likelihood of release probability than half full vesicles, suggesting vesicles can release when partially loaded but with a lower release probability. The authors suggest this preferential release of full vesicles may allow a more reliable synaptic weighting under repeated bouts of synchronous release. Further, in *Drosophila* and murine dopaminergic neurons, KCl induced synaptic terminal depolarisation causes a hyper-acidification of dopaminergic synaptic vesicles which assists the loading of dopamine into synaptic vesicles through VMAT visualised through dVMAT-pHluorin reporters (Aguilar et al., 2017). The authors were able to visualise pH changes in these vesicles without release by co-expressing the release inhibitor tetanus toxin light chain (TeTxLC). By this method, acidification was found to be mediated by VGLUT activity suggesting not only that neurons may utilise multiple transporters to maximise loading but that neuronal activity itself may be influential in setting loading kinetics, which may be more dynamic than originally postulated (Aguilar et al., 2017).

It appears vesicular loading is an important, conserved and innately highly variable process which differs between neurons, species and possibly activity level. There is substantial information accumulated, over many years, regarding individual components of vesicular loading. However, there remains a gap in how these components synergise into a fully functioning system *in vivo*. The open questions that emerge from this uncertainty are; (i) is vesicular loading innately variable and if so why? (ii) can this variability be explained by common physiological mechanisms? And (iii) what are the main contributory factors governing the limit at which vesicles fill?

1.5. Molecular Characterisation of Fusion Models

Section 1.1 briefly describes the importance of synaptic vesicle fusion within the realms of neurotransmission. However, over the last few decades the underlying mechanisms of synaptic vesicle trafficking and the orchestration of controlled synchronous release have gained much attention. This none more so demonstrated by the 2013 Nobel Prize for Physiology or Medicine being jointly awarded to James E. Rothman, Randy W. Schekman and Thomas C. Südhof for their roles in investigating these phenomena. Given the wealth of knowledge on this literature and relevance to this project, current knowledge of vesicle fusion mechanics will be discussed in further detail in regard to the three recognised modes of fusion in neurons; synchronous, asynchronous and spontaneous vesicle fusion.

Synaptic release was first visualised by Heuser and colleagues (1979) by freezing nerve terminals immediately after evoked SV release (Heuser et al., 1979). Importantly, these observations suggested vesicle release is orchestrated in a highly controlled fashion, localised in parallel with what the authors guessed were calcium channels (which was later proved to be correct). Figure 1.8 shows an image taken directly from this paper and displays what is accepted as one of the first visualisations of synaptic vesicle exocytosis (Heuser et al., 1979).

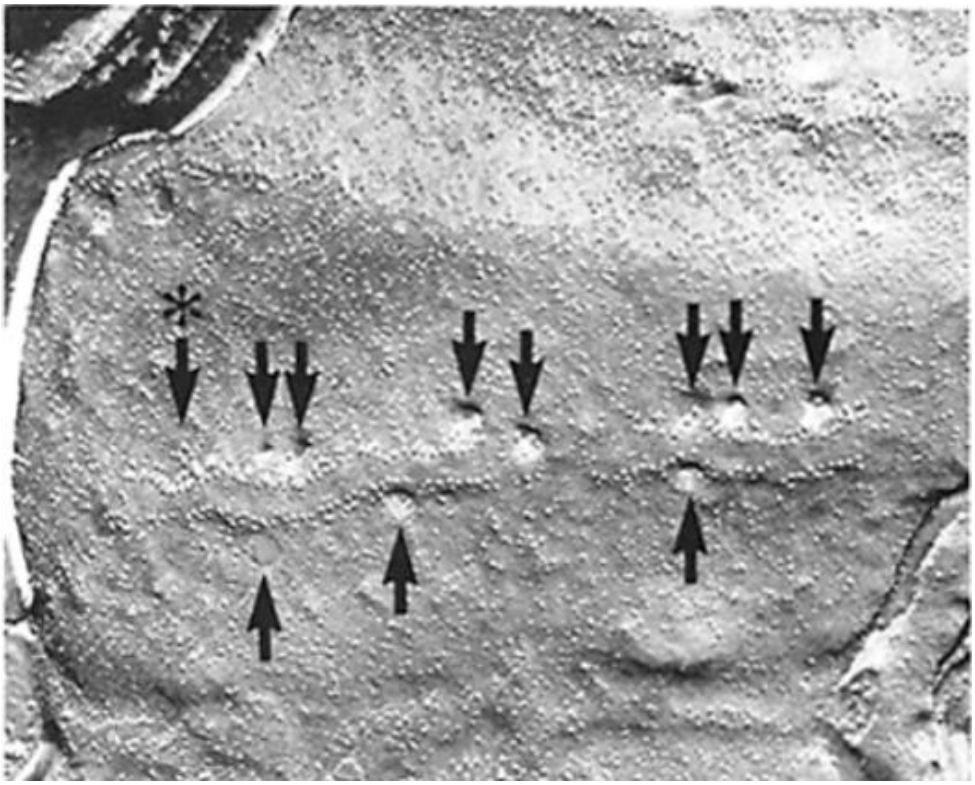

Figure 1.8: First recorded images of synaptic vesicle exocytosis. Frog motoneurons were stimulated in the presence of 1mM 4-AP, 5-6ms before quick freezing. Solid black arrows represent vesicle opening events whereas arrows with an asterisk represent collapsed vesicles. Image taken from (Heuser et al., 1979).

1.5.1 Synchronous Release

To date, the most highly characterised mode of fusion is that derived from the synchronous control of evoked neurotransmitter release or "Synchronous Fusion". In this case, vesicle release is directly linked to an initial Ca^{2+} influx and a consequential mobilisation of complex protein-protein and protein-lipid interactions, all tightly mediated by initial action potential dependent stimulation (Südhof, 2013, Kaeser and Regehr, 2014) (see Fig. 1.9). Release itself is governed primarily by Ca^{2+} sensors (synaptotagmin), SNARE proteins consisting of the vesicle bound synaptobrevin and

two presynaptic bound proteins, syntaxin-1 and SNAP-25 together with SNARE associated Munc (18 and 13) complexes and vesicle bound RAB3 proteins with the small cytosolic protein, complexin, being know to halt vesicle fusion in the absence of Ca^{2+} (Südhof, 2004, Südhof and Rothman, 2009, Li and Kavalali, 2017, Huntwork and Littleton, 2007).

As can be seen in Figure 1.9, there are but milliseconds from peak Ca^{2+} entry till vesicle release and so for controlled release, fusion machinery must work rapidly to initiate fusion but also inactivate rapidly following voltage gated Ca^{2+} channel inactivation and dissipation of local Ca^{2+} concentrations. As a result, Ca^{2+} channel localisation (as postulated by Heuser and colleagues) is tightly localised to release machinery. Ca^{2+} channel localisation has since been found to be orchestrated by RIM proteins and RIM binding protein (RBP) together with Munc-18 complexes (Ma et al., 2013, Mittelstaedt et al., 2010).

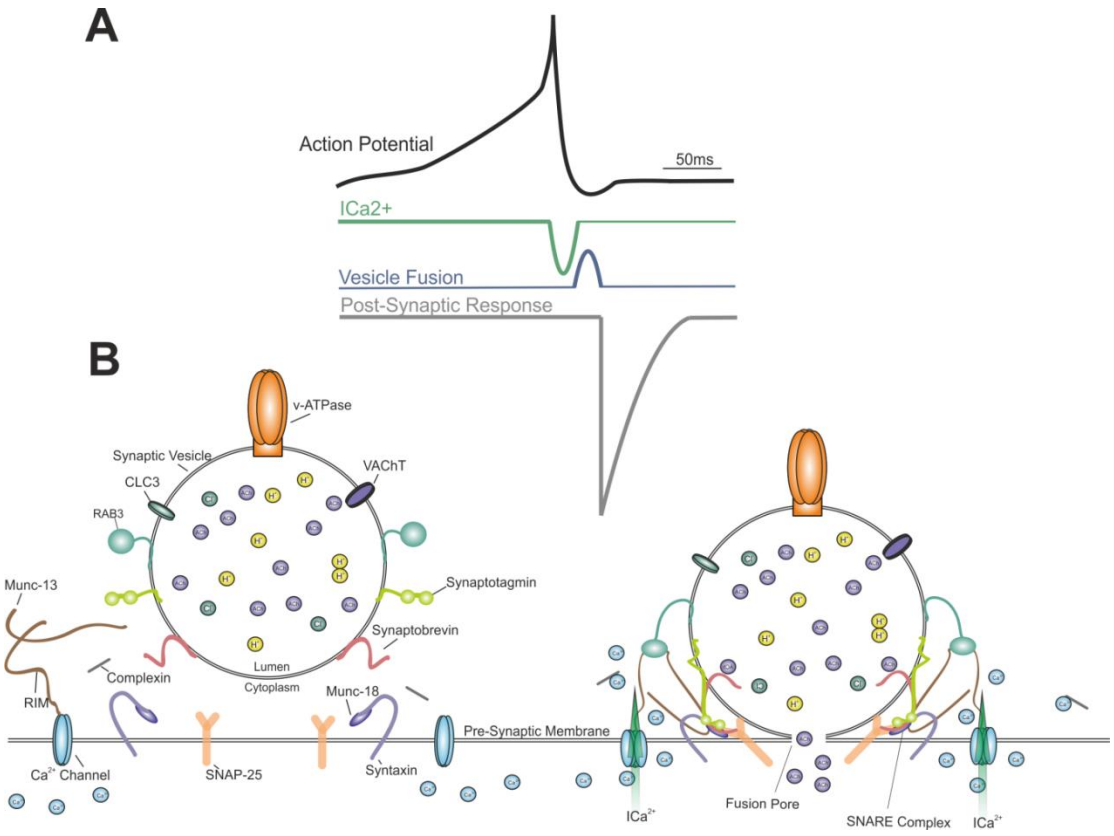

Figure 1.9: Molecular basis for synchronous fusion. (A) Time frame for synchronous fusion relies heavily on precise timing of Ca^{2+} entry into the pre-synaptic terminal. Schematic shows action potential (black) followed by calcium entry (green) leading to fusion of vesicles (blue) with the pre-synaptic membrane and finally the associated post-synaptic response (grey). (B) Currently accepted molecular basis of synchronous fusion. Synaptic vesicles initially localised at active zone, following priming and docking, voltage dependent calcium entry enhances SNARE protein assembly and complexin disassociation facilitating fusion pore opening and neurotransmitter release. Figure adapted from (Kaeser and Regehr, 2014).

Synaptotagmins function as the first step in Ca^{2+} sensing and SNARE assemblage. In the absence of Ca^{2+}, synaptotagmin forms a tripartite structure with the SNARE complex and complexin (Zhou et al., 2017). Once the vesicle is docked, complexins are known to bind to already assembled SNARE complexes and are believed to act as an inhibitor or "fusion clamp" to vesicle release (Huntwork and Littleton, 2007). This is demonstrated

in the *Drosophila* complexin null mutant (*cpx*^{SH1}) which dramatically increases vesicle release through an inability of neurons to control vesicle fusion (Huntwork and Littleton, 2007).

Upon Ca^{2+} entry to the nerve terminal, Synaptotagmin binds Ca^{2+} which unzips complexin, and promotes synaptotagmin affinity for syntaxin-1 and SNAP-25 initiating vesicle fusion (Zhou et al., 2017). Munc-18 proteins are known to interact with syntaxin-1 to regulate SNARE complex assembly and further facilitate SV fusion (Rizo and Südhof, 2012). Munc-13 proteins further bind Munc-18, SNAP-25, syntaxin1, RIM and RAB3 proteins and are further considered vital for normal release (Ma et al., 2013, Richmond et al., 2001, Mittelstaedt et al., 2010, Camacho et al., 2017). The SNARE proteins themselves are key in bringing together the vesicular membrane and presynaptic membrane zippering of the α-helical motifs of all the SNARE proteins allows membrane fusion.

1.5.2 Asynchronous Release

Although synchronous release is thought to dominate the majority of chemical transmission between neurons, neurotransmitter release is not necessarily time locked to stimulation. Asynchronous Fusion is a molecularly distinct and less understood mode of fusion whereby an intracellular build-up of Ca^{2+} following stimulation results in the heightened probability of mass vesicle exocytosis without the need for initial action potential mediated release (Goda and Stevens, 1994, Wen et al., 2010, Kaeser and Regehr, 2014). At excitatory glutamatergic synapses, in the otherwise silent mammalian magnocellular neurosecretory cells located in the paraventricular nucleus of the hypothalamus, a single evoked EPSP initiates multiple bouts of calcium dependent glutamate release for approximately 50ms following an initial stimulation,

which was further shown to prolong postsynaptic spiking (Iremonger and Bains, 2016). Furthermore, in the cholinergic system, retrograde regulation of asynchronous release by synapse-associated protein 97 was found to act through the cell adhesion protein, N-cadherin to enhance specifically asynchronous release and not synchronous release (Neff et al., 2009). Although the molecular mechanisms governing asynchronous release are currently an active area of research, asynchronous release may be thought of as a form of short-term neuronal plasticity to aid the control of neuronal excitability underpinned by separate molecular fusion mechanics.

1.5.3 Spontaneous Release

A third type of fusion termed "Spontaneous Fusion" was originally thought to occur due to unpredictable changes in vesicle fusion machinery resulting in accidental release of single SVs and, at the time, considered unremarkable. Indeed, one paper in a series in which the investigators, Paul Fatt and Bernard Katz, who are accredited for the discovery of spontaneous fusion was serendipitously titled *"Some observations on biological noise"* (Fatt and Katz, 1950, Fatt and Katz, 1952). However, recent evidence suggests spontaneous release has predefined molecular pathways, physiologically separate from those governing synchronous and asynchronous release (Kavalali, 2015). Interestingly, spontaneous release is maintained in the absence of the vesicle associated SNARE protein synaptobrevin, whereas synchronous release is halted (Schoch et al., 2001). Further, there remain structurally very similar proteins expressed on synaptic vesicles that may replace synaptobrevin in spontaneous release which are differentially expressed in different SV pools e.g. VAMPs 4, 7 and VTI1A (Hua et al., 2011, Ramirez et al., 2012). This may suggest that multiple fusion complexes are made which are physiologically separate and dependent on the modality of release. Further evidence suggests regulators of the SNARE complex may be different in synchronous

release. Zhou et al find that at the *C. elegans* NMJ, Munc-13 can affect the spatial localisation of asynchronous and synchronous release but has no effect on spontaneous release (Zhou et al., 2013), again suggestive that separate release modalities may have their own modulatory mechanisms. Interestingly, in *C. elegans,* a glycine to arginine substitution (G342R) in the *VAChT* is reported to disrupt an interaction with synaptobrevin (Sandoval et al., 2006). This phenotype is rescued by a complimentary substitution of an isoleucine to an aspartate in synaptobrevin (Sandoval et al., 2006) suggesting that the *VAChT* itself may play a part in release kinetics.

1.6 Insect Acetylcholine Receptors

Neurotransmitter release from the presynaptic terminal would be rendered mute without the appropriate postsynaptic receptor for signal transduction. In the case of ACh, two major classes of receptor exist: ionotropic nicotinic acetylcholine receptors (*nAChR*) and metabotropic G-protein-coupled muscarinic receptors (*mAChRs*).

1.6.1 Nicotinic Acetylcholine Receptors (*nAChRs*)

Nicotinic acetylcholine receptors mediate the reception of fast cholinergic transmission. *Drosophila* has 10 genes encoding nAChR subunits, 7 alpha subunits (Dα 1-7) and three beta subunits (Dβ 1-3) (Grauso et al., 2002). The *Drosophila* genome has been utilised to characterise insect *nAChR* subunits due to the high sequence homology between species (Dupuis et al., 2012).

The stoichiometry of the *Drosophila nAChRs* is yet to be fully characterised but basic properties are extrapolated from mammalian *nAChRs*. Each *nAChR* consists of five subunits; α, β, δ, ε and γ. The major differentiation between subunit types involves the presence of two adjacent cysteine residues referred to as α subunits, those without these adjacent cysteine residues are termed β or non-α subunits (Corringer et al.,

2000). Each subunit contains an extracellular domain on the N-terminal containing a cysteine loop (found in all ligand gated ion channels) and 4 transmembrane domains (M1-4) with the ligand binding site located between subunits as can be seen Fig. 1.10 (Corringer et al., 2000, Sattelle et al., 2005).

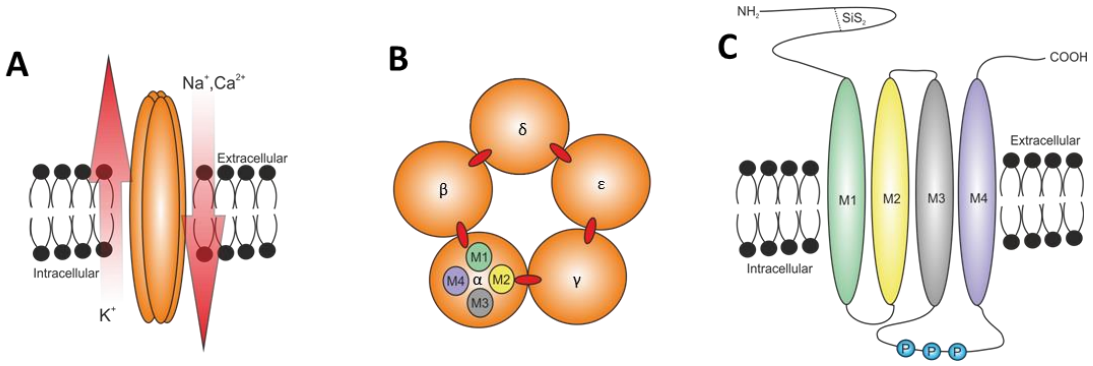

Figure 1.10. nAChR localization and structure. (A) Schematic representation of a *nAChR* within the postsynaptic membrane (B) orientation of transmembrane domains (M1-4) with M2 constituting the channel pore and hence the gating properties together with proposed ligand binding sites (L) with the 5 subunits labelled as appropriate (α, β, δ, ε and γ). (C) Schematic of an individual *nAChR* subunit showing transmembrane domains (M1-4), a large phosphorylation site between M3 and M4 (P) and the presence of a large N-terminal extracellular domain containing a disulfide bond (SiS_2) between two cysteine residues.

At least 2 α-subunits are essential for receptor functioning, the presence of other subunits serving to alter various physiological/pharmacological properties of the receptor (Sattelle et al., 2005). The proportion of α to β-subunits is not uniform. Heterologous expression in *Xenopus* oocytes shows that Dα2 forms functional homomeric receptors (Sawruk et al., 1990), whereas more recent studies have shown functional *nAChRs* can be generated under co-expression of insect α-subunits and vertebrate β-subunits (Dederer et al., 2011). These non-uniform constructs make *nAChR* characterisation difficult. However, three possible receptor complexes have

been suggested through immunoprecipitation studies; a combination of Dβ1 and Dα3, a combination of Dα1, Dα2 and Dβ2 and a final complex based on Dβ1 and Dβ2, association (Sattelle et al., 2005, Chamaon et al., 2002). It is evident that these suggested characterisations are incomplete and further work is required to differentiate *nAChR* subunit composition.

Insect *nAChR* diversity is further complicated by several post transcriptional mechanisms: namely, alternative splicing and RNA editing. The former arises from reorganisation of pre-mRNA exons during splicing. This can also involve the insertion or deletion of a sequence generating long and short isoforms (Sattelle et al., 2005). This process affects primary gene transcripts and in insects, has been observed in the α4 (exon 4 and 4' variants) and α6 (exons 3 and 8) subunits (Dupuis et al., 2012, Sattelle et al., 2005). These splice variants may influence channel functioning. For example, in *A. melifera* the α6-subunit (exon 8) variant influences residues between M3 and M4 which are involved in agonist binding (Jones et al., 2006); one might expect this would influence ACh affinity and thus receptor sensitivity.

RNA editing results from the targeted mutation of an RNA sequence resulting in the synthesis of a protein not initially encoded in the genome (Dupuis et al., 2012). In *Drosophila* Dα5-7 and Dβ1-2 display RNA editing (Dupuis et al., 2012). The α6-subunit has received the most attention as edited transcripts can be found amongst other insects (*D. melanogaster, A. gambiae, B. mori, T. castaneum* and *A. mellifera)* (Dupuis et al., 2012).

The edited RNA sequence involves the modification of individual bases in an enzymatic process whereby an adenosine is transformed to an inosine via an adenosine deaminases enzyme, known as A-I editing (Jin et al., 2007). The inosine acts as a

guanosine during translation, thus conferring a possible change in protein function. It is important to note that this mechanism is not seen in all species. For example *A. gambiae* displays extraordinarily short flanking intronic sequences on the same α6 subunit and no A-I editing (Jin et al., 2007).

1.6.2 Muscarinic Acetylcholine Receptors (*mAChRs*)

Muscarinic receptors are G-protein-coupled receptors and are found on both the pre- and postsynaptic terminals that mediate a response to ACh. The G-protein consists of three major subunits (α, β and γ). Upon agonist binding to the *mAChR*, G-protein disassociation allows interaction with molecules in the cytosol (see Fig. 1.11). The effects are varied and poorly characterised in insects in comparison to those of mammalian studies in which they are localised in parasympathetic nerves.

All *mAChR* subtypes display 7 transmembrane regions (Thiele, 2013). Prior to ACh-binding, the G-protein binds a GDP molecule and is considered inactive. Upon agonist binding, the GDP is exchanged for a GTP, allowing the disassociation of the α-subunit (Thiele, 2013). The α-subunit then interacts with various cytosolic molecules in one of many potential cascade mechanisms (see Fig. 1.11).

Up until recently, there was only one identified *mAChR* in *Drosophila* (Type A). Type A (*CG4356*) corresponds with the classical interpretation of *mAChR* pharmacology, being activated by low concentrations of ACh ($EC_{50,}$ 5 x 10^{-8}M) and inhibited by atropine (Collin et al., 2013), whereas the newly identified Type B (*CG7918*) is also activated by ACh, but has a 1000-fold lower sensitivity to muscarinic blockers. In a follow-up paper the authors (Ren et al., 2015) find that Type A receptors are linked to Gq/11 signalling pathway responsible for intracellular Ca^{2+} release from ER via the PIP2 pathway, whereas Type B are linked with the Gi/0 pathway responsible for cAMP/PKA messaging

long been associated with many effects including voltage gated K^+ channel modulation (Chung and Kaczmarek, 1995).

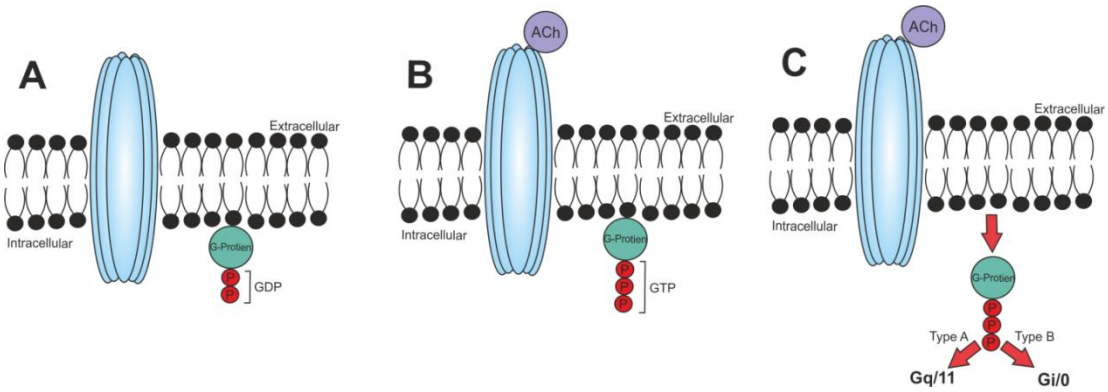

Figure 1.11: mAChR localization and structure. Schematic representation of *mAChRs* activity following ACh binding displaying 7 putative transmembrane regions (blue) with associated G-protein (green). (A) G-protein binding a two phosphates molecule (red) in its inactive state (GDP). (B) under ACh binding to *mAChR* (grey), a GDP is exchanged for a GTP. (C) G-protein disassociation then acts through one of two pathways based on *mAChR* subtype.

There is much room for development in our current understanding of the insect cholinergic system. An explicit understanding of the insect cholinergic system is important when developing insecticides that target the system for the progression of safer, more effective pesticides.

1.7 Insect Control and Current Use

Insects act as vectors for some of the most medically and economically important diseases in the modern world. Life threatening diseases from malaria, dengue fever, leishmaniasis and chagas disease to the more common *Salmonella* and *E. coli* food poisonings can all be vectored by insects. Preventative measures and treatment for these diseases have been costly at a global scale both throughout recent history and through to the modern day. Using African countries as an example, In 1980-1995

malaria alone cost 31 African countries $73.6 billion US dollars in economic growth (theoretical cost to GDP, adjusted for inflation) (Sachs and Malaney, 2002). The most recent estimates from the centre for disease control and prevention (CDCP) suggest that African nations are annually spending $12 billion on preventative measures and treatment (http://www.cdc.gov/malaria/malaria_worldwide/impact.html).

Additionally, insects act as major agricultural pests. In Brazil, insect pests annually cause approximately 25 million tons of damage to food, fibre, and biofuels, equating to a total annual economic loss of $17.7 billion US dollars every year (Oliveira et al., 2014). Furthermore, estimates of global rice production between 2001 and 2003 predict a potential loss of yield of up to 24.7% due to animal pests (including but not exclusive to insects), equivalent to 230 million tonnes (Oerke, 2006). Actual global loss of rice production equated to ~15% of total potential yield. These predictions suggest 90 million tonnes of rice were saved during this three year period. These figures are attributable to improved food security measures, including the use of insecticides (Oerke, 2006).

Since the introduction of dichlorodiphenyltrichloroethane (DDT) and polychlorocycloalkanes (PCCAs) in the 1940s, yield per hectare of almost all arable crops has increased dramatically (Casida and Durkin, 2013, Goulson, 2013). Current rice production has increased from 220 million tonnes in 1961 to approximately 740 million tonnes in 2013 (FAO: http://faostat3.fao.org/download/Q/QC/E). Although not exclusively attributable to pesticide development given the improvement of fertilizers (Sakamoto, 2006) and introduction and increased use of GMOs (Owen, 2000), there remains little doubt that insecticides have made a sizable contribution to yield.

1.7.1 Insecticides as Neurotoxins

Most insecticides are neurotoxins. There are several reasons why the majority of successful insecticides at present target the CNS. They initially have a fast onset and a prolonged effect due to poor detoxification mechanisms in insects (Casida and Durkin, 2013). Furthermore, the nervous system has many potential targets, small disruptions in which are potentially lethal.

As might be predicted, the use of insecticides shows a clear pattern with the development of resistance. Fig. 1.12 shows a decrease in the use of organophosphates and methylcarbonates and an increase in neonicotinoids between 1997 and 2010 (Casida and Durkin, 2013). In recent years, the development of resistance and worries of the impact on non-target organisms (in particular bees) has also governed a decrease in the use of neonicotinoids (Blacquiere et al., 2012). In the absence of effective alternative control methods in order to sustain supply needs, the development of new insecticides via the identification of new target sites currently remains one of the only ways to counteract the effects of resistance.

There are currently 4 major neural insecticide targets: acetylcholinesterase (*AChE*) for organophosphates and methylcarbonates, which block *AChE* leading to saturation at cholinergic synapses resulting in excitotoxicity and ultimately cell death; nicotinic acetylcholine receptors (*nAChRs*) for neonicotinoids working through a similar excitotoxic mechanism by holding receptor gating open; voltage gated sodium channels for pyrethroids work by shutting down the ability of neurons to generate action potentials; and chloride channel blockers (including GABA receptors) for fiproles which shut down the ability of the CNS to modulate excitatory input (Casida and Durkin, 2013). However, many more compounds have been recently developed targeting

Ryanodine receptors (Diamides), Octopamine pathways (Amitrazs), TRPV channels (Pymetrozines), Glutamate-gated chloride channels (Avermectins) together with a whole host of multi-site non-specific inhibitors (Borates, Fluorides and Alkyl Halides. See http://www.irac-online.org/modes-of-action/ for more information). This increase in "other" compounds is demonstrated in global insecticide sales seen in Fig 1.12.

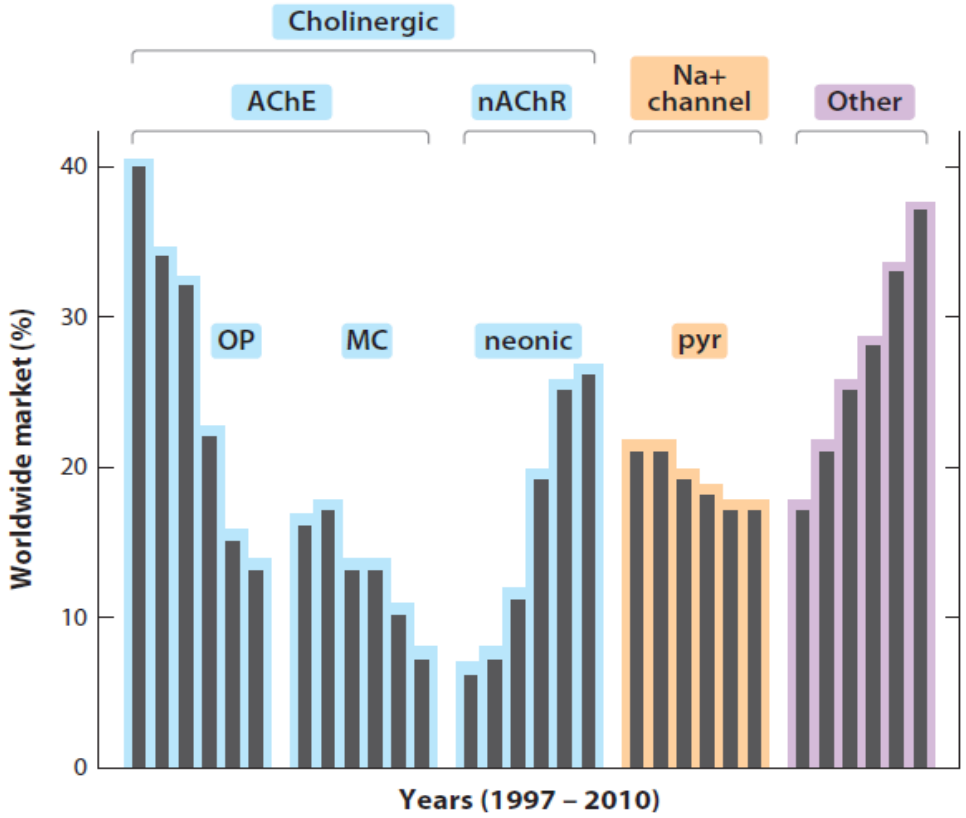

Figure 1.12: Worldwide market trends in the use of different insecticide classes from 1997-2010. (OP = organophosphates, MP = methylcarbonates, neonic = neonicotinoids, pyr = pyrethriods). Taken from (Casida and Durkin, 2013).

1.7.2 The *VAChT* as a Target for Insecticides

CASPP compounds are a potential new class of potent neuroactive insecticide specifically targeting the *VAChT* developed by Syngenta; see 1.12 for structure of two

major neuroactive compounds (SYN351 and SYN876) (Sluder et al., 2012). Initially, CASPP compounds were shown to suppress the effects of *AChE* inhibitors (Aldicarb) in *C. elegans* suggesting the compound is important at cholinergic synapses (Sluder et al., 2012). A forward genetic screen using *C. elegans* selecting against CASPP lethality identified 7 mutations that mapped to the *unc-17* locus coding for *VAChT* (Sluder et al., 2012). This finding was verified in *Drosophila* where up-regulation of both the wild type *VAChT* and the resistant point mutation *VAChT*^{Y49N} gave 3 fold and 10 fold higher resistance respectively compared to genetic controls (Sluder et al., 2012). Although multiple CASPP compounds have been generated 5Cl-CASPP (aka SYN351 or (5-chloro-1=-[(E)-3-(4-chlorophenyl)allyl]spiro[indoline-3,4=-piperidine]-1-yl}-(2-chloro-4-pyridyl)) is considered the most potent.

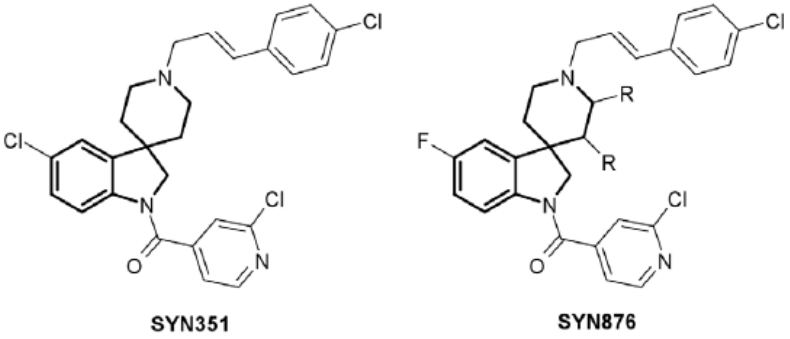

Figure 1.13: Chemical structures for CASPP compounds SYN351 and SYN876 labelled accordingly: taken from Sluder et al (2012).

1.7.3 Insecticide Resistance

The generation of new insecticides to combat resistance has been tried and tested over centuries but is irrefutably flawed by basic laws of natural selection. The consequence of such a strategy is the development of resistance to the predominant classes of

insecticides a position we find ourselves in today. At this point one may ask themselves "what happens when there are no more targets?"

In fact multi-drug resistant phenotypes (or "cross resistance") have been identified since initial discoveries of DDT resistance in *Musca domestica* (Hoyer and Plapp Jr, 1966). Through time, *M. domestica* populations have attained resistant alleles for the majority of pesticide classes including but not limited to organophosphates, carbamates, pyrethroids, neonicotinoids and non-neuronal insecticides such as insect growth regulators (IGRs) with some levels of resistance reportedly >18,000 times higher than in susceptible insects (Bass et al., 2015, Shono et al., 2002, Naqqash et al., 2016). Notably, similar levels and breadth of resistance occur in *Aedes, Anopheles* and *Culix spp* of mosquito carriers of dengue fever, malaria and West Nile virus respectively. The same is true for sand flies, black flies, tsetse flies, blowflies and cockroaches (Naqqash et al., 2016).

For these reasons a large global effort to characterise these mutations has been conducted. IR Mapper is an online tool developed in an attempt to pool global records of currently identified cases of insecticide resistance throughout history and across multiple species (Coleman et al., 2017). Fig. 1.14 shows a clear increase in the number and range of resistance cases in *Anopheles* mosquitos spanning all major classes of insecticide between 1982-2000 and 2000-2018 respectively (http://anopheles.irmapper.com/). Whether, in this case, this difference is due to availability of data remains to be seen. However, it is clear that resistance is rapidly becoming a much larger global problem.

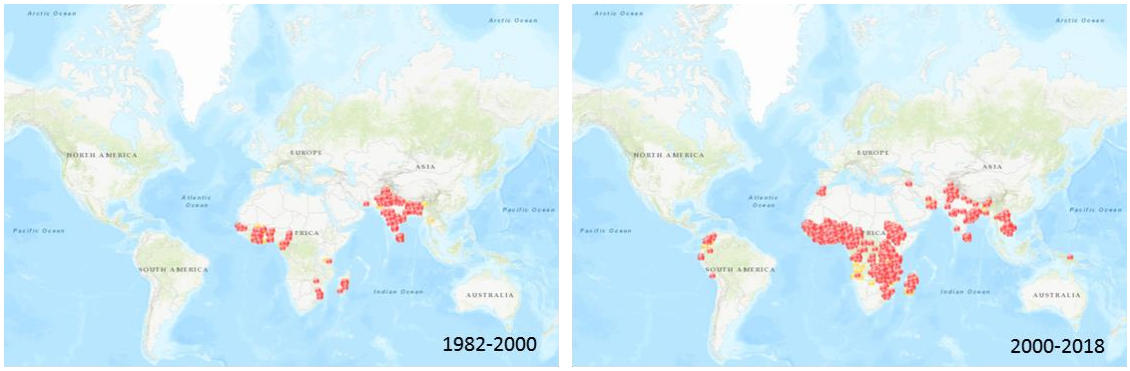

Figure 1.14: Resistance to modern insecticides is increasing rapidly. Results from two Search results from IR mapper for *Anopheles* mosquitos between 1982-2000 and 2000-2018 show an obvious increase in the number of confirmed cases of resistance (red) and possible resistance (orange). Note a particular increase in African countries and a recent spread to South America and Indonesia (http://anopheles.irmapper.com/).

In an effort to address the spread of resistance, industrial companies are now incorporating the likelihood of resistance while developing new insecticides. However, molecular characterisation of these mutations and their presence or not in the field is unfortunately where our knowledge regarding resistance mechanisms ends, with little to no information pertaining to the physiological implications of these types of mutation to neural functioning. Using CASPP insecticides as an example, transgenic up-regulation of both the *VAChT* and of a specific point mutation (*VAChT*^{Y49N}) have been shown to generate high levels of resistance to these insecticides (Sluder et al., 2012). Chapter 3 of this thesis aims to unpick the functional implications of these modes of resistance in order to gain a better understanding of how resistance influences central cholinergic physiology to guide a more informed approach for managing resistance in the future.

1.8 *Drosophila melanogaster* as a Model Organism

Since the discovery of the white eyed mutant by Thomas Hunt Morgan in the early 1900s, a century of *Drosophila* research has been at the forefront of identifying and untangling some of the most fundamental biological processes such as chromosomal inheritance, gene mapping, recombination and mutagenesis. In addition to its milestones in modern genetics, in the last 30 years *Drosophila* has proved a useful tool in vision (Pak, 1995), cancer research (Potter et al., 2000), learning and memory (McGuire et al., 2005), cell communication (Mumm and Kopan, 2000) and drug discovery (Nichols, 2006) and has been specifically identified as a good model for the study of various other systems, for example: mitochondrial diseases (Foriel et al., 2015), gut homeostasis (Guo et al., 2016b) and the study of transport proteins (Martin and Krantz, 2014).

Drosophila has caught the attention of many research fields for several reasons; fruit flies are cheap and easily reared allowing high throughput of experiments. Generation times are short at ~10 days at 25°C and progeny can be easily monitored. After fertilisation and oviposition, embryos develop through 20 distinct stages over 24 hours (Hartenstein and Wodarz, 2013). Hatching precedes 5 days of larval development through 3 stages (L1-3) following which a further 5 days of pupal stage occurs in which a reorganisation of the nervous system occurs and where adult organs develop through imaginal disks. Adults live 3-4 weeks in optimal conditions. The genome is small, containing only 4 chromosomes (in comparison to 23 in humans) and displays low functional redundancy, whereas higher organisms tend to display paralogous genes, which can complicate loss of function analyses (Zhang, 2003).

In addition to the fly's practical advantages, the modern molecular genetics era combined with the availability of the complete sequence of the fly genome has transformed the fly from a simple high throughput insect model to an experimenter's so called "swiss army knife" (Duffy, 2002).

1.8.1 *Drosophila* – Getting into the Rhythm

The ability of an organism to find a reproductive mate, avoid potential predators and find and consume food, all come with obvious and advantageous selective value. Evolutionary tick boxes such as these are dictated by the ability of an animal to navigate its environment and thus locomotion has been heavily studied by physiologists for decades. Thomas Brown proposed the current model of locomotor circuitry in 1911, the details of which are still not in full clarity despite 100 years of research. Brown suggested that rhythmic locomotion, or "the act of progression" as he terms it, is produced centrally in the absence of sensory stimulation and is dictated by musculature working as pairs and driven by antagonistic inhibition, what is now known as "reciprocal inhibition" (Brown, 1911). This itself assumes a network of neurons specifically evolved to generate this rhythmic pattern of synaptic input or a "Central Pattern Generator Network" (CPG).

CPGs have long been identified in both invertebrates and vertebrates (Cohen and Wallén, 1980, Grillner, 1985, Delvolvé et al., 1999, Wilson, 1961, Marder and Bucher, 2007). They regulate breathing, swimming, walking, swallowing and, in *Drosophila* larvae, crawling. One of the most convincing ways to confirm the presence of a CPG is to remove the brain from the animal and place it in physiological saline and examine the presence of a so called "fictive motor pattern". However, this approach can be muddied in systems where the CPG system controls multiple behaviours, for example,

the same musculature is used for coughing, gasping, sighing and breathing and so attributing these behaviours to one physiological output may be convoluted (Marder and Bucher, 2001). Where CNS extraction has been successful in outlining the CPG network, different types of CPG have been termed "oscillators". The rawest form of reciprocal inhibition can be found where two neurons directly inhibit each other, termed half-centre oscillators (Sharp et al., 1996, Marder and Bucher, 2001). These neurons do not show innate patterns of bursting when isolated and so exhibit rhythmic bursting only when paired. This is true in the gastric mill of the Jonah crab, *Cancer borealis* (Sharp et al., 1996), the heart of the medical leech, *Hirudo medicinalis* (Arbas and Calabrese, 1987) and tadpole locomotion (Roberts et al., 1998). These smaller oscillators are thought to govern much larger movements particularly in segmented organisms by which multiple oscillators are coordinated via ascending and descending pathways (Marder and Bucher, 2001). This hypothesis has remained speculative until recently where *Drosophila's* genetic tractability combined with modern methodologies and associated connectome projects of the locomotor system are all beginning to pick apart exactly how complex motor progression is conducted.

Behaviourally, forward larval locomotion is dictated by waves of muscular contractions from posterior to anterior, and the reciprocal for backwards locomotion (Heckscher et al., 2012). Waves of fictive locomotion are segmentally interconnected in the larval VNC and can be visualised as waves of activity in the downstream motoneurons under calcium imaging (Streit et al., 2016, Lemon et al., 2015, Pulver et al., 2015). These waves of activity are coupled with rhythmic ACh mediated excitatory synaptic inputs from the CPG network (Cash et al., 2015, Baines et al., 2001, Lee and O'Dowd, 1999, Baines and Bate, 1998). Recently, an excitatory premotoneuron (A27h) and inhibitory premotoneuron (GDL) were identified and shown to localise in segmentally repeatable

patterns of expression being activated during waves of fictive locomotion (Fushiki et al., 2016). In this study, A27h was sufficient for forward locomotion whereas the inhibitory GDLs were needed for both forward and backward locomotion (see Fig. 1.15 for schematic). The authors therefore suggest an underlying coupling mechanism and, by their own words, are highly suggestive of a reciprocal inhibition model proposed by Brown, 100 years ago.

"Taken together, our findings define a mechanism for wave propagation in which the contraction of one segment is concomitant with the relaxation of the adjacent anterior segment, and the cessation of contraction is in turn coupled with the stimulation of contraction in next anterior segment" (Fushiki et al., 2016).

It would, however, be unrealistic to think that these fictive patterns of locomotion cannot be influenced by sensory stimuli. CPGs and reflex pathways have long been known to share interneurons (Pearson, 1995) and much effort has also gone into mapping out related peripheral circuits that modulate the *Drosophila* CPG. So called "Wave neurons" are downstream of noci/ mechanosensors and thought to initiate anterior and posterior segmental contraction (Takagi et al., 2017). Interestingly, optogenetic activation of more anterior wave neurons initiates backwards locomotion whereas more posterior stimulation initiates forward locomotion. This behavioural output is also shown by calcium imaging and when the associated nociceptor or mechanoreceptor is stimulated. Taken together, these findings suggest that these neurons act to kick-start the CPG under behaviourally aversive conditions (Takagi et al., 2017). Another example targeting neurons not directly related to CPG kinetics are demonstrated in Even-skipped+ (Eve^{+}) interneurons. A subset of these so-called EL-neurons (Eve^{+} neurons driven by the EL-GAL4 driver) directly synapse onto RP2

motoneurons and can modulate excitatory drive (Heckscher et al., 2015) these neurons are believed to form their own a functionally isolated circuit involved in head-turning while still modulating CPG kinetics. Although there will inevitably remain many more neurons involved in the CPG generation, the *Drosophila* larva is set to be the first complex organism to have its complete locomotor circuit mapped.

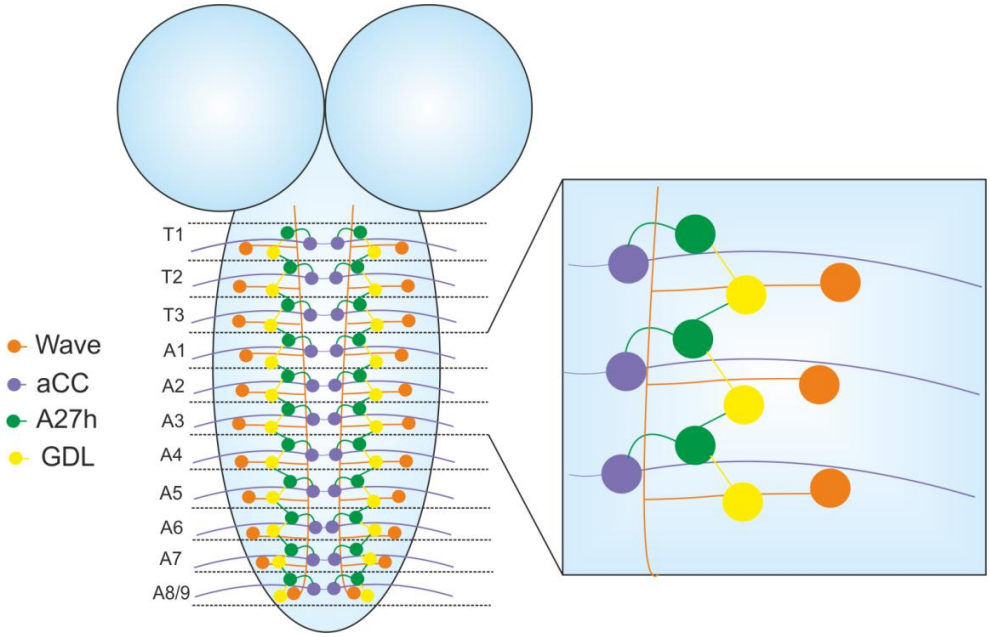

Figure 1.15: Localisation of proposed interneurons involved in CPG innervation. Wave neurons (orange) act to initiate CPG activity. The interaction between A27h (green) and GDL (yellow) are thought to act through local inhibition. Excitatory A27h projects onto both aCC motoneurons (Purple) and into the anterior segment onto the inhibitory GDL neuron and thus inactivating retrograde segmental contraction and precipitating forward locomotion.

1.8.2 The Motoneuron (MN)

Although the examination of fictive locomotor pattern in an isolated CNS is informative it is useful to remember that, in reality, the CNS requires motor targets to convert

neural coded information into kinetic force to drive locomotion. This role is conducted by motoneurons (MNs) (Hecksher et al., 2015).

Larval motoneurons are born in early neuroblast lineages (30 per half segment) and then enter a hierarchical progression towards more derived MN subtypes resulting in a total of 36 MNs per half segment (Landgraf and Thor, 2006). The initial division is thought to be between ventral MNs (vMNs) and dorsally projecting MNs (dMNs) (Landgraf and Thor, 2006). Within the dMNs lie the subclasses RP2 and aCC. Although aCC/RP2 MNs display obvious morphological differences in their dendritic field projections, they have been found to express remarkably similar molecular determinants (*even-skipped, Grain* and *Zfh1*) (Landgraf and Thor, 2006). In a similar fashion, MNs from vMNs subclass all express *Islet, Lim3, Drifter, Nkx6* and *Hb9* yet somehow differentiate into their own individual MN identities (Landgraf and Thor, 2006) suggestive of an early determinant to MN specification.

Even-skipped is known to regulate the netrin receptor *unc-5* known to be important in axonal pathfinding towards the dorsal muscle field and further modulates expression of *grain* and *zfh1* (Labrador et al., 2005). zfh1 also plays a crucial role in neural pathfinding as loss of function mutants show severely retarded axon projection localisation (Layden et al., 2006). It is now well established that these unique signals amongst others such as ROBO-slit in the CNS (Dickson and Gilestro, 2006), assist axonal projection towards their respective target sites.

These developmental molecular determinants guide MN projection through three principal nerves to motor units; the intersegmental nerve (ISN) innervating internal body wall musculature, segmental nerve (SN) and transverse nerves (TN) innervating external musculature (Landgraf and Thor, 2006). RP2 and aCC MNs belong to the ISN

subclass, innervate dorsal muscles DA2 and DA1 respectively and have reliable soma localisation and axonal projections throughout all larval stages allowing the repeatable study of identified neurons possible through all larval life stages (Baines and Bate, 1998, Baines et al., 2001).

Fictive locomotor patterning was found to develop over 13-17h after egg laying (AEL) in aCC/RP2 MNs (Baines and Bate, 1998). Responsiveness to applied ACh is initially seen 13-14h AEL whereas endogenously produced rhythmic activity is first observed 16h AEL with fully formed ACh mediated spontaneous rhythmic currents (SRCs) representative of later stage motoneuron kinetics at 17h AEL (Baines and Bate, 1998) (see figure 1.16). When action potential mediated activity is blocked, spontaneous release of single vesicles remains, termed minis (Fig. 1.16). Motoneurons also hyperpolarise to focal application of GABA and glutamate, reaching reversal potential at -56 ± 3mV and -55 ± 2mV respectively; this was found to be mediated by a Cl^- conductance and blocked by picrotoxin (PTx) (Rohrbough and Broadie, 2002), suggesting that *Drosophila* MNs are receptive to ACh (excitatory), glutamate and GABA (inhibitory).

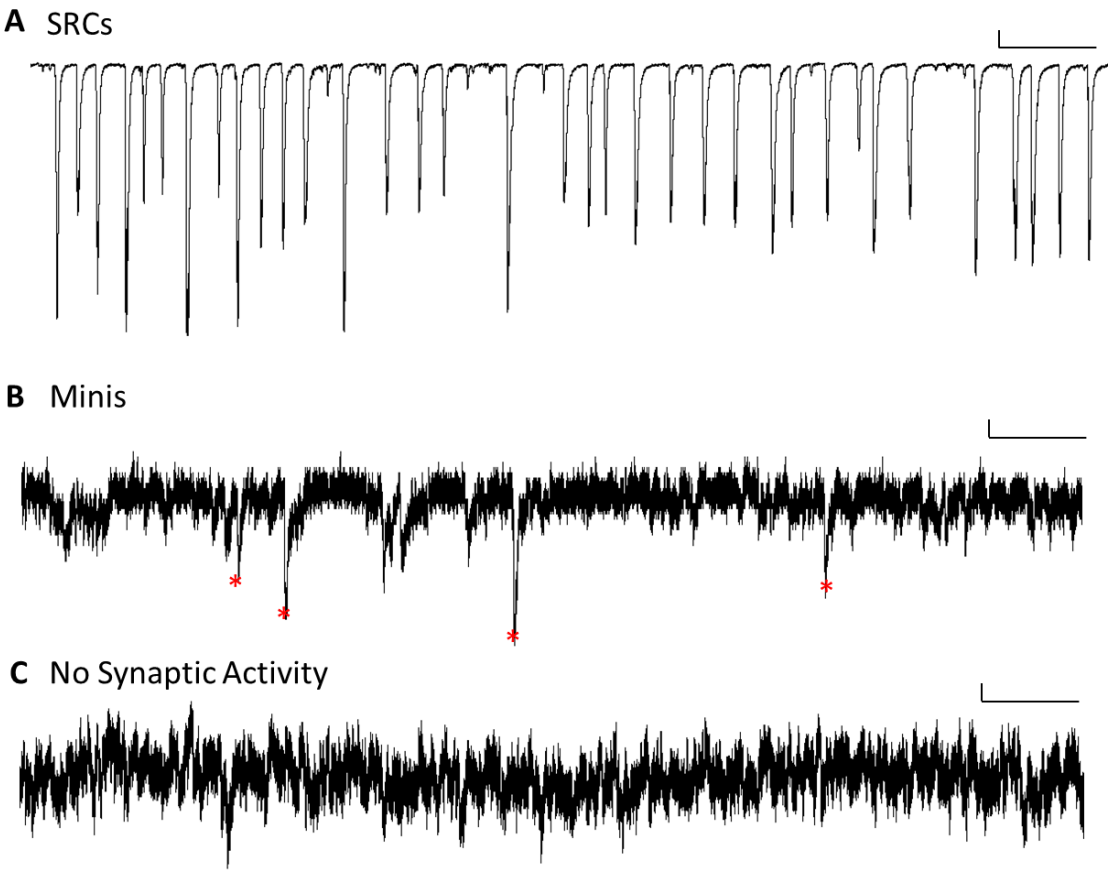

Figure 1.16: Representative traces of excitatory ACh mediated synaptic currents from *Drosophila* aCC MNs (A) Endogenously produced spontaneous rhythmic currents (SRCs) indicative of mass vesicle exocytosis released synchronously in an action potential dependent fashion, indicative of a fictive locomotor pattern. Scale Bar (50pA/3s). (B) The addition of 2µm TTX blocks voltage gated sodium channels and thus presynaptic action potentials allowing the visualisation of small spontaneous cholinergic events representative of individual vesicle release termed minis. Scale Bar (2pA/50ms). (C) A combination of TTX and the nicotinic antagonist mecamylamine results in no observable current change leaving background noise of approximately 5pA. Scale Bar (2pA/50ms).

When excitatory synaptic inputs are blocked with either tetanus light chain toxin (*TeTxLC*) or through use of a restrictive temperature sensitive allele of choline acetyltransferase (Cha^{ts2}), morphological development remains similar (Baines et al., 2001). However, increases in outward K^+ current and increased firing in response to injected current suggests MNs increase excitability when synaptic input is reduced during development (Baines et al., 2001). This effect was reversible by lowering Cha^{ts2} below its restrictive temperature after a 5h period of restrictive development (Cha^{ts2} activation) at 18h AEL and suggests MNs can tune intrinsic excitability following initial development (Baines et al., 2001). Further, hyperpolarisation of aCC through the expression of the potassium channel subunit $Kir_{2.1}$ reduces intrinsic excitability but does not change synaptic inputs in this system suggesting this tuning is strictly presynaptic in nature and not related modification of intrinsic excitability in itself (Baines et al., 2001).

1.9 Thesis outline:

This thesis is split into three result chapters followed by a general discussion in an alternate format. Each result chapter is in the style of a paper either currently published or in the process of submission at the time of thesis submission.

Chapter 2 focuses on the implications to central cholinergic functioning when under transgenic up-regulation and pharmacological blockade of the *VAChT*. Together with the identification of an uncommon polymorphism manifesting in the C-terminal of the *VAChT* as a single amino acid truncation in the *VAChT* poly-Q region that appears to regulate *VAChT* loading kinetics ($VAChT^{12Q}$).

Cash, F., Vernon, S. W., Phelan, P., Goodchild, J., & Baines, R. A. (2016). Central cholinergic synaptic vesicle loading obeys the set-point model in Drosophila. Journal of Neurophysiology, 115(2), 843-850.

Chapter 3 explicitly investigates the physiological implications of the presence of resistance phenotypes to cholinergic physiology and the response of the resistant condition to CASPP challenge under both up-regulation of wild type *VAChT* and a through a CRISPR induced point mutation *VAChT*^{Y49N}.

Vernon, S. W., Goodchild, J., & Baines, R. A. (2018). The VAChT^{Y49N} mutation provides insecticide-resistance but perturbs evoked cholinergic neurotransmission in Drosophila. PLOSOne (in press)

Chapter 4 specifically targets vesicle loading mechanics utilising the previously described UAS-*VAChT*^{12Q} together with CRISPR induced manipulation of the *VAChT* polyQ region. This chapter provides evidence that the c-terminal *VAChT* polyQ region modulated cholinergic synaptic vesicle loading

Vernon, S. W., Goodchild, J., & Baines, R. A. (2018). A poly-glutamine region in the Drosophila vesicular acetylcholine transporter dictates fill-level of cholinergic synaptic vesicles. Journal of Neuroscience (in preparation)

Central cholinergic synaptic vesicle loading obeys the set-point model in *Drosophila.*

Francesca Cash[1], Samuel W Vernon[1], Pauline Phelan[2], Jim Goodchild [3] and Richard A Baines[1]

[1]Faculty of Life Sciences, University of Manchester, Manchester M13 9PT, United Kingdom., [2]School of Biosciences, University of Kent, Kent, CT2 7NZ, United Kingdom., [3]Syngenta Crop Protection Research, Bracknell, Berkshire, United Kingdom

Reference:

Cash, F., Vernon, S. W., Phelan, P., Goodchild, J., & Baines, R. A. (2016). Central cholinergic synaptic vesicle loading obeys the set-point model in Drosophila. *Journal of Neurophysiology*, 115(2), 843-850.

2.0 Statement of Contribution.

SV conducted, analysed and assisted interpretation of Figures 2 and 3. FC conducted, analysed and interpreted Figures 4 and 5. Figure 1 was conducted in tandem between FC and SV. Additional experiments relevant but not included in publication are further presented in Appendix 1. FC wrote manuscript with assistance of RAB, JG and SV. Modifications to the text are made in order to incorporate the further relevant data conducted during this project presented in Appendix 1 (section 2.7) and for stylistic consistency for the purpose of this thesis.

2.1 Abstract

Experimental evidence shows that neurotransmitter release, from presynaptic terminals, can be regulated by altering transmitter load per synaptic vesicle (SV) and/or through change in the probability of vesicle release. The vesicular acetylcholine transporter (*VAChT*) loads acetylcholine (ACh) into SVs at cholinergic synapses. We investigated how the *VAChT* affects SV content and release frequency at central synapses in *Drosophila melanogaster* by using an insecticidal compound, 5Cl-CASPP, to block *VAChT* and by transgenic overexpression of *VAChT* in cholinergic interneurons. Decreasing *VAChT* activity produces a decrease in spontaneous SV release with no change to quantal size and no decrease in number of vesicles at the active zone. This suggests that many vesicles are lacking in neurotransmitter. Overexpression of *VAChT* leads to increased frequency of SV release, but again with no change in quantal size or vesicle number. This indicates that loading of central cholinergic SVs obeys the 'set-point' model, rather than the 'steady-state' model that better describes loading at the vertebrate NMJ. However, we show that expression of a *VAChT* polymorphism lacking one glutamine residue in a C-terminal polyQ domain leads to increased spontaneous SV release and increased quantal size. This effect spotlights the poly-glutamine domain as potentially being important for sensing the level of neurotransmitter in cholinergic SVs.

Key words: acetylcholine, *Drosophila*, central synapse, synaptic vesicle, vesicular transporter

2.2 Introduction

Vesicular transporters load neurotransmitter into SVs. Classes of transporter include the vesicular acetylcholine transporter (*VAChT*), the transporters for glutamate (VGLUT), monoamines (VMAT) and GABA and glycine (VGAT and VIAAT) (Fei and Krantz, 2009). A change in spontaneous quantal release frequency (probability of fusion of single SVs), following change in expression of *VAChT* or VGLUT, suggests these transporters may have a second function in neurotransmitter release (Song et al., 1997, Parsons et al., 1999, Daniels et al., 2004, Lima et al., 2010, Rodrigues et al., 2013, Daniels et al., 2006).

The *VAChT* transports ACh into SVs by exchanging two protons for one molecule of ACh (Usdin et al., 1995, Nguyen et al., 1998). The number of transporters per SV is unknown, but has been estimated to be between one and three (Van der Kloot, 2003). This has led to speculation that even small reductions in *VAChT* expression level may result in SVs devoid of transporter (Prado et al., 2013). Partial knock-down of *VAChT* in mice results in a reduction in both frequency and amplitude of quantal miniature end-plate potentials at the neuromuscular junction (NMJ) (Lima et al., 2010, Rodrigues et al., 2013). Electron microscopy showed no reduction in total SV number but altered SV distribution in the synaptic terminals of the NMJ (Rodrigues et al., 2013). By contrast, over-expression of *VAChT*, in *Xenopus* spinal motoneurons, results in increased quantal size and also frequency at the NMJ (Song et al., 1997). The increase in amplitude has been used to argue for a 'steady-state' model of SV filling, where inflow is balanced by outflow rather than an alternate 'set-point' model (Williams, 1997). Alteration of *VAChT* activity at the NMJ is seemingly sufficient to increase ACh loading into SVs, an effect that is not countered by a compensatory change in outflow. The consequence is

increased ACh per SV. However, whether this model applies to central cholinergic synapses has yet to be determined.

Here we show that overexpression of *VAChT* (d*VAChT*), in *Drosophila* cholinergic premotor interneurons, is sufficient to increase frequency of spontaneous miniature events (minis) recorded in motoneurons but does not increase their amplitude. Action potential-dependent synaptic currents are not affected. These changes mirror the proposed roles for *VAChT* in mammalian CNS with respect to facilitating SV release but, importantly, provide evidence to support the 'set-point' model for SV loading. We identify a poly-glutamine region in d*VAChT* that is seemingly important for SV-filling. Expression of a d*VAChT* polymorphism missing one glutamine (from thirteen in wildtype) results in minis that are increased in both amplitude and frequency. Ultrastructural analysis shows no change to SV size. Determination of quantal content of action potential-evoked synaptic release also shows no change indicating that this variant raises the set-point of filling or alternatively switches loading to obey the 'steady-state' model. The d*VAChT* poly-glutamine region is unique to some insect species and may offer an exploitable target for insecticide design.

2.3 Methods

2.3.1 Fly stocks and 5Cl-CASPP application

Flies were maintained under standard conditions at 25°C. Cha^{B19}-GAL4 (termed *cha*) was used to express UAS-*VAChT* in cholinergic neurons (Salvaterra and Kitamoto, 2001). The wildtype UAS-*VAChT* transgene was made during the course of this study. The UAS-$VAChT^{12Q}$ transgene was made by Syngenta. Sequencing confirmed that this was the only change to the amino acid sequence. The control used for 5Cl-CASPP ([5-chloro-1'-[(E)-3-(4-chlorophenyl)allyl]spiro[indoline-3,4'-piperidine]-1-yl]-(2-chloro-4-

pyridyl)methanone, made by Syngenta) was RRa-GAL4:CD8-GFP (termed RRa) which expresses in just the aCC/RP2 motoneurons in wall-climbing third instar larvae (Lin et al., 2014) and shows no differences in synaptic excitation to true wildtype strains. UAS-Dα7 (Bloomington #39692) was rebalanced over a TM3::GFP balancer. Controls for transgenic flies were parental and are indicated in the text. 5Cl-CASPP (0.5 µg) (5 µl of 100 µl/ml CASPP solution) was dissolved in acetone (5 µl) and added to the surface of a grape-agar plate (50 mm) in 1 ml of aqueous dried yeast extract (5% Merck, Darmstadt, Germany). After being left to dry overnight at room temperature, second instar larvae were allowed to feed for 24 h.

2.3.2 qRT-PCR

CNSs were collected from third-instar wall-climbing larvae. After RNA extraction (QIAGEN RNeasy Micro kit), cDNA was synthesized using the Fermentas Reverse Aid H minus First strand cDNA synthesis kit. Twenty CNSs were collected for each sample. qRT-PCR was performed using a Roche LightCycler480 II (Roche) with SYBRG Master reaction mix. The thermal profile used was 5 min at 95°C followed by 45 cycles of 10 s at 95°C, followed by 10 s at 60°C, and finally 10 s at 72°C. Results were analysed by the Δ/Δ C_t method and are expressed as relative RNA expression. C_t values used were the means of three or five independent repeats. Control gene was rp49. Primers were as follows: rp49 primers CCAGTCGGATCGATCGATATGCTA and ACGTTGTGCACCAGGAA; *VAChT* primers CTCATCCTCGTGATTGTA and ACGGGTATGATCTTTCC; ChAT primers ATCACACCGAGCGATACA and TATAGTCGGCCATCGTTTCA.

2.3.3 Electrophysiology

Recordings were performed at room temperature (20°C to 22°C). Third-instar larvae were dissected in saline (135 mM NaCl, 5 mM KCl, 4 mM $MgCl_2 \cdot 6H_2O$, 2

mM $CaCl_2 \cdot 2H_2O$, 5 mM N-Tris [hydroxymethyl]methyl-2-aminoethanesulfonic acid (TES), 36 mM sucrose, pH 7.15) to remove the CNS. The CNS was secured to a Sylgard (Dow-Corning, USA) coated coverslip using tissue glue (GLUture, WPI, Florida, USA). The neurolemma surrounding the CNS was partially removed using protease (1% type XIV; Sigma, Dorset, UK) contained in a wide-bore (~15 µm) patch pipette.

Whole-cell recording were carried out using borosilicate glass electrodes (GC100TF-10; Harvard Apparatus, Edenbridge, UK), fire-polished to resistances of between 8 – 12.5 MΩ. The aCC/RP2 motoneurons were identified either by the presence of GFP (RRa-GAL4; CD8-GFP) or by position within the ventral nerve cord. In non-GFP larvae, cell identity was confirmed after recording by filling with 0.1% Alexa Fluor 488 hydrazyde sodium salt (Invitrogen), included in the internal patch saline (140 mM K^+ gluconate, 2 mM $MgCl_2 \cdot 6H_2O$, 2 mM EGTA, 5 mM KCl, and 20 mM HEPES, pH 7.4). Tetrodotoxin (TTX, 2 µM) was included in the external saline to block action potential-induced synaptic currents. Recordings were made using an Axopatch-1D amplifier. Cells were held at -60 mV and recordings sampled at 100 kHz and a lowpass filter of 0.5 kHz for minis and sampled at 20 kHz with a lowpass filter of 0.2 kHz for spontaneous rhythmic currents (SRCs), using pClamp 10.4 (Molecular Devices, Sunnyvale, CA). Only neurons with an input resistance >500 MΩ were accepted for analysis. SRC amplitude was normalised to cell capacitance which was measured by integrating the area under the capacity transient resulting from a step protocol from -60mV to -90mV. This is because larger neurons produce bigger SRCs. Mini amplitude is not significantly affected by cell size and is reported as amplitude. SRC area was analyzed using the area function of Clampfit and is reported as pA/msec. MiniAnalysis (Synaptosoft, Decatur, GA) was used to measure amplitude and area of minis.

To measure the response of motoneurons to ACh, the bath was perfused with 0.3 mM ACh (diluted in external saline) for 1 minute before being washed off. TTX was included in the external saline to prevent action-potential dependent synaptic release. Amplitude of response was measured in Clampfit.

BafilomycinA1 was dissolved in 20 µl DMSO before being diluted to 100 µM stock in external saline. BafilomycinA1 was added to the bath to a final concentration of 3 µM (0.4% DMSO). SRCs were recorded for 20 minutes from application. Control recordings were made in the presence of 0.4% DMSO. The threshold search function in Clampfit was used to identify all events >50 pA to avoid the program identifying fluctuations in the baseline as evoked currents.

2.3.4 Electron Microscopy

Third instar wall-climbing larvae were dissected in phosphate buffered saline (PBS; 137 mM NaCl, 2.7 mM KCl, 10 mM Na_2HPO_4, 2 mM KH_2PO_4, pH 7.4) and fixed in 2.5% glutaraldehyde in 100 mM HEPES buffer, pH 7.2 for a minimum of 1 h. Samples were post-fixed in 1% osmium tetroxide and 1.5% potassium ferocyamide in 0.1 M cacodylate buffer for 1 h. Samples were then incubated in 1% theocarbohydrazide for 20 mins at room temperature before transfer to 2% osmium tetroxide for 30 mins. Samples were stained in aqueous 1% uranyl acetate for 1 h, dehydrated in a graded ethanol series and embedded in TAAB Low Viscosity resin (TAAB Laboratories Equipment Ltd). Sections (70-80 nm) were cut from the the ventral nerve cord in the same area as the motoneurons. Images were observed with a FEI Tecnai 12 Biotwin Transmission Electron Microscope. Micrographs were taken at 11,000X and random images were taken at 1,900X magnification to assess number of active zones. 5Cl-CASPP treated larvae had been acutely fed for 24 h prior to dissection.

2.3.5 Image analysis

Images were coded and randomized for blind analysis. Images were analyzed using ImageJ (National Institute of Health, USA). Length of the pre-synaptic membrane, the shortest distance from the center of each vesicle to the membrane and the diameter of each vesicle was measured. Only vesicles within 200 nm of the pre-synaptic membrane were included to avoid inclusion of vesicles closer to a neighboring synapse. In random images, taken at 1,900X magnification, the unbiased frame function was used in ImageJ to create a randomly placed frame of 29.4 μm^2 within the image. The number of active zones within each frame was counted, only frames which had vesicle containing tissue in >50% of their area were included in the analysis.

2.3.6 Statistics

Statistical significance was calculated using a 2-sample unpaired T-test where it was relevant to compare samples to their own parental controls. ANOVA with post hoc Bonferonni's test was used where multiple groups shared the same control. In both tests, confidence intervals of $P \leq 0.05$ (*), $P \leq 0.01$ (**) and $P \leq 0.001$ (***) were used for significance.

2.4 Results

2.4.1 Expression level of *VAChT* affects only frequency of SV release

To determine how changing levels of *VAChT* affect transmitter release at central cholinergic synapses we used two complimentary approaches to alter the activity of this transporter. To down-regulate, we used the insecticidal compound 5Cl-CASPP that specifically inhibits *VAChT* (Sluder et al., 2012). Up-regulation was achieved by expression of a wildtype *VAChT* transgene in all cholinergic neurons. To investigate the consequences for cholinergic synaptic function, we undertook patch clamp recordings

from the well characterised aCC/RP2 motoneurons. These neurons receive identical cholinergic synaptic input (Baines et al., 1999) . We recorded spontaneous release of neurotransmitter (i.e. minis) by blocking all action potential-dependent release with addition of TTX to the extracellular saline (see methods). We also recorded action potential-dependent currents (no TTX present), termed SRCs, to determine the effect on multiple SV release.

Larvae fed 5Cl-CASPP for 24 hours prior to recording showed a marked decrease in the frequency of minis recorded in aCC/RP2 (frequency: 27.5 ± 4.2 vs. 6.9 ± 1.0 per min, P = 0.0007, control vs. 5Cl-CASPP, Fig. 2.1). By contrast, no change in amplitude was observed (amplitude: 6.7 ± 0.6 vs. 6.4 ± 0.3 pA, P = 0.8). Minis were also recorded from *cha^{B19}>VAChT* larvae to examine the effect of increased levels of *VAChT*. Larvae which over-expressed this wildtype form of *VAChT* showed a 50% increase in mini frequency (31.8 ± 6.4 vs. 63.9 ± 6.8 per min, P = 0.03). No significant change was seen in amplitude (Fig. 2.1). The differences in basal values for both mini amplitude and frequency in vehicle-exposed and GAL4/UAS parental stocks (i.e. controls) are most likely due to differences in genetic backgrounds of these respective lines.

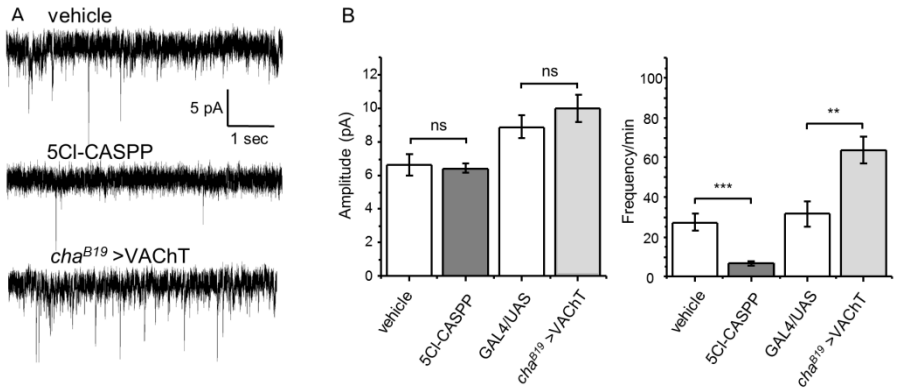

Figure 2.1. *VAChT* regulates mini frequency. (A) Representative traces of minis recorded from aCC motoneurons in *cha^{B19}*/+ third instar larvae exposed to acetone (vehicle), larvae acutely fed 5Cl-CASPP and *cha^{B19}>VAChT* larvae. (B) 5Cl-CASPP has no

effect on mini amplitude, but is sufficient to cause a significant decrease in mini frequency (n ≥ 9). Increased expression of *VAChT* similarly has no effect on mini amplitude but also results in a significant increase in mini frequency (n ≥ 8). Genotype for 5Cl-CASPP fed larvae and its control is RRa-GAL4:CD8-GFP. Control for cha^{B19}>*VAChT* is cha^{B19}/+ and UAS-*VAChT*/+ (denoted GAL4/UAS), which did not differ and have been combined. Values are mean ± sem.

We carried out qRT-PCR to quantify overexpression of *VAChT* compared to controls (cha^{B19}/+) and found a significant up-regulation of transcript (2.8 ± 0.6 fold-change in RNA expression, P = 0.01, n = 3). The *VAChT* and choline acetyltransferase (ChAT) genes share the same first exon and the remainder of the *VAChT* gene is contained within the first intron of ChAT (Kitamoto et al., 1998). For this reason, we also carried out qRT-PCR for the ChAT transcript to ensure that ChAT expression was not inadvertently changed. There was no significant increase in ChAT transcript abundance (0.1 ± 0.2 fold change, P = 1.0 n = 5). Therefore, we conclude that increased mini frequency is due to overexpression of *VAChT* without change to ChAT transcript level.

In the absence of TTX, larger inward synaptic currents can be recorded in *Drosophila* motoneurons. These SRCs are due to action potential-dependent release of multiple SVs (Baines et al., 1999, Rohrbough and Broadie, 2002). SRCs recorded after 5Cl-CASPP treatment were not significantly different to control in amplitude (29.8 ± 3.6 vs. 39.0 ± 6.1 pA/pF control vs. treated, P = 0.2) or duration (506 ± 32 vs. 543 ± 30 ms, P = 0.4, Fig. 2.2A-C). However, SRC frequency was significantly decreased (19.2 ± 4.1 vs. 3.1 ± 1.1 per min, control vs. treated, P= 0.0013, Fig. 2.2D). By contrast, overexpression of *VAChT* did not affect SRC amplitude, duration or frequency (Fig. 2.2B-D). These data are further in agreement with evoked ChR2 mediated SRCs (see Appendix 1, section 2.7.1)

Thus we conclude that manipulating *VAChT* affects only frequency of mini release which, when reduced by blocking activity of *VAChT*, similarly reduces the frequency of evoked release.

The possibility exists that manipulating *VAChT* in presynaptic neurons evokes post-synaptic compensation, specifically change in level of nAChR expression. Such changes, if occurring, might complicate our analysis. To test this possibility, we directly exposed the aCC motoneuron to applied ACh. The amplitude of the response to perfused ACh, under voltage clamp, was not altered in 5Cl-CASPP fed larvae (12.2 ± 1.7 vs. 11.2 ± 2pA/pF, unfed vs. fed, P = 0.7, n = 6 and 7, respectively). ACh response was also unchanged in larvae which over-expressed *VAChT* in cholinergic neurons (8.3 ± 1.2 vs.10.2 ± 2.9 pA/pF, controls vs. cha^{B19}>*VAChT*, P = 0.5, n = 13 and 6, respectively). By contrast, expression of the $nAChR_{D\alpha7}$ subunit in aCC, which has previously been linked to excitability (Ping and Tsunoda, 2012) , was sufficient to increase response to applied ACh (8.8 ± 0.9 vs. 11.8 ± 0.8 pA/pF, control vs. RRa>$nAChR_{D\alpha7}$, P = 0.02, n = 13 and 11, respectively). This confirms that the experiment is sensitive enough to detect post-synaptic changes in nAChR expression that affect response to ACh. We conclude, therefore, that the observed change in mini frequency caused by altering active *VAChT* levels is a primarily presynaptic effect.

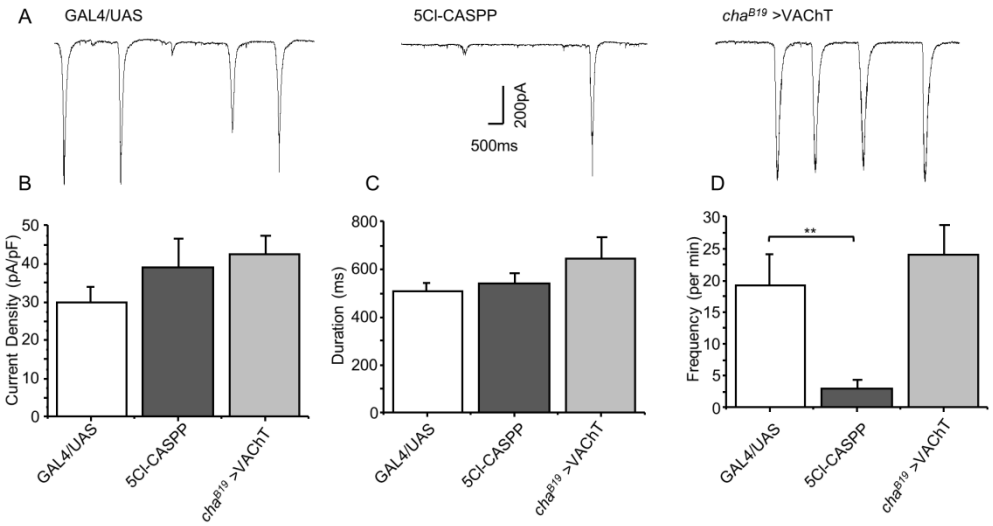

Figure 2.2. Inhibition of *VAChT* decreases SRC frequency. (A) Representative traces of SRCs recorded from aCC motoneurons in control (*cha*^{B19}/+) larvae, larvae acutely fed 5Cl-CASPP and *cha*^{B19}>*VAChT* larvae. (B-D) 5Cl-CASPP causes no significant change to SRC amplitude or duration but is sufficient to significantly decrease frequency. Overexpression of *VAChT* does not affect amplitude, duration or frequency of SRCs. Genotype for 5Cl-CASPP fed larvae and its control (exposed to acetone) is RRa-GAL4:CD8-GFP. Control for *cha*^{B19}>*VAChT* is *cha*^{B19}/+ and UAS-*VAChT*/+ (denoted GAL4/UAS), which did not differ and have been combined. Values are mean ± sem, n = 10

2.4.2 Expression of *VAChT*^{12Q} affects both frequency and amplitude of SV release

Mammalian *VAChT* contains a di-leucine motif within the cytoplasmic C-terminal. This motif is involved in localisation of *VAChT* to membranes and endocytosis after neurotransmitter release (Tan et al., 1998, Barbosa et al., 2002). By comparison, *Drosophila VAChT* lacks a di-leucine motif, but instead has a 13 glutamine polyQ-domain in the C-terminal. Little is known about the normal function of polyQ domains, but functions may include protein-protein interactions, transcriptional regulation and RNA binding and signalling (see discussion). Therefore, the polyQ domain may

substitute the role of the mammalian di-leucine motif. The precise number of glutamines is thought to be important (Schaefer et al., 2012), and to investigate this we overexpressed a known polymorphism which lacks one glutamine at position 549 (termed *VAChT*^{12Q}, (Sluder et al., 2012)).

Expression of *VAChT*^{12Q} in cholinergic neurons increased the frequency of recorded minis (67.5 ± 10.5 vs. 34.5 ± 6.1 per min, *cha*^{B19}>*VAChT*^{12Q} vs. control, P = 0.011, Fig. 2.3A-B) and the amplitude (14.4 ± 1.3 vs. 8.3 ± 0.6 pA, P = 0.0004, Fig. 2.3A, C). In contrast to expression of wildtype *VAChT*, expression of *VAChT*^{12Q} also influenced SRC kinetics. The most notable effect was a significant increase in SRC duration (1117 ± 125 vs. 588 ± 31 ms, P = 0.0003, Fig. 2.3F) and decreased frequency (18.4 ± 1.9 vs. 33.1 ± 2.9 per min, P = 0.00008, Fig. 2.3G). By contrast, SRC amplitude was not significantly changed (41.6 ± 4.6 vs. 33.3 ± 3.0pA/pF, P = 0.15, Fig. 2.3E). Analysis of expression level of transgenic *VAChT*^{12Q} compared to transgenic expression of wildtype *VAChT* show comparable levels (3.1 ± 0.3 vs. 2.8 ± 0.6 fold increase, *VAChT*^{12Q} vs. *VAChT*, P = 0.7, n = 5 and 3), indicating that the different effect of the former was not due to increased levels of expression.

To determine if increased duration of SRCs, produced following expression of *VAChT*^{12Q}, is due to the increased amplitude of minis (i.e. larger quanta) or an increased number of SVs released per action potential, the total number of SVs released over a 20 min time period was measured. This was achieved by blocking SV-recycling using bafilomycin. Bafilomycin inhibits the proton pump, preventing acidification of the SV (Bowman et al., 1988). Rundown of SRCs was recorded for 20 min after addition of bafilomycin (Fig. 2.4A). Total SV number (i.e. number of SVs released during the 20 min period) was calculated by dividing combined area of SRCs by mean mini area.

Combined area of SRCs is representative of total ACh release and was found to be increased following over-expression of *VAChT*^{12Q} compared to control (1.0 x10^7 ± 0.1 x10^7 vs. 2.38 x10^7 ± 0.4 x10^7 pA/msec, P = 0.01, Fig. 2.4B). Mean mini area was also increased under these conditions (52.9 ± 6.2 vs. 141.0 ± 11.8pA/msec, P = 0.00001, Fig. 2.4C), indicating that each SV released more ACh. Analysis of released quanta (SRC area / mean mini area) shows that the number of SVs released was not significantly different between *cha*^{B19}>*VAChT*^{12Q} and control (2.0 x 10^5 ± 0.2 x 10^5 vs. 1.9 x 10^5 ± 0.3 x 10^5 quanta, P = 0.8, Fig. 2.4D). The number of quanta per SRC was also not altered (707.3 ± 117.0 vs. 584.8 ± 116.1 quanta per SRC, P = 0.5, Fig. 2.4E). We conclude that longer duration SRCs, due to expression of *VAChT*^{12Q}, likely results from increased SV transmitter content, rather than increased number of SVs released.

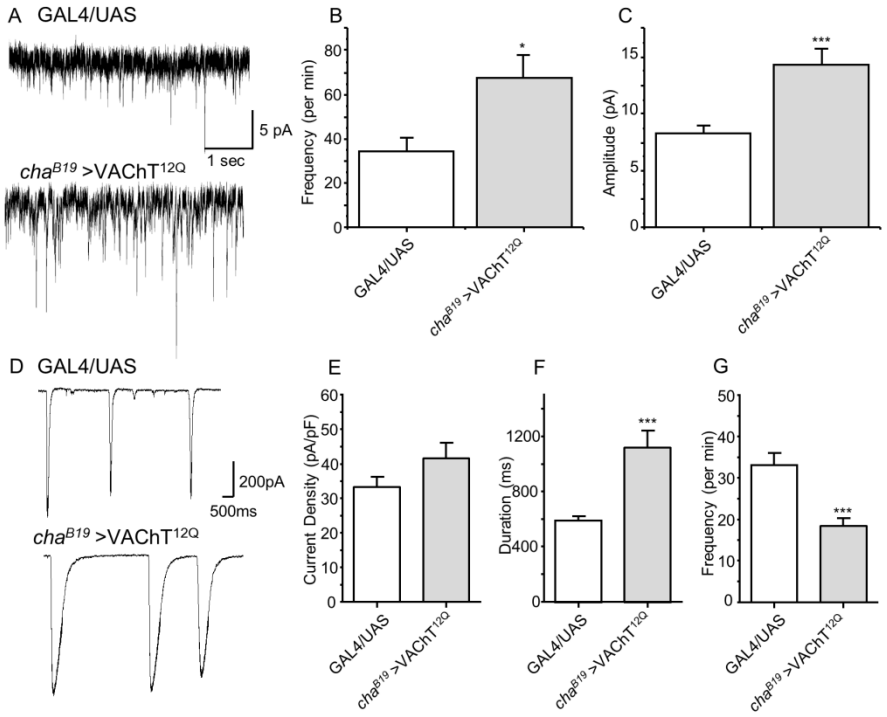

Figure 2.3. *VAChT*^{12Q} regulates mini amplitude and SRC duration. (A) Representative traces of minis recorded from aCC in *cha*^{B19}/+ (GAL4/UAS) and *cha*^{B19}>*VAChT*^{12Q}. (B-C)

Expression of the *VAChT*^{12Q} polymorphism is sufficient to increase mini frequency and amplitude compared to parental controls (n = 10 and 7, respectively). (D) Representative traces of SRCs recorded form aCC in UAS/+ (GAL4/UAS) and *cha*^{B19}>*VAChT*^{12Q}. (E-G) Expression of *VAChT*^{12Q} increases SRC duration, and decreases frequency, compared to parental controls (GAL4/UAS). SRC amplitude is not significantly different. Controls are *cha*^{B19}/+ and UAS-*VAChT*^{12Q}/+ which did not differ and have been combined. Values are mean ± sem, n = 25 and 28, respectively.

We also tested the effect of 5Cl-CASPP, which was sufficient to reduce mini frequency without change to amplitude (see Fig. 2.1). Exposure to this inhibitor significantly reduced the combined SRC area ($1.3 \times 10^7 \pm 0.3 \times 10^7$ vs. $0.2 \times 10^7 \pm 0.09 \times 10^7$ pA/msec, P = 0.008, Fig. 2.4B) whilst mean mini area showed no difference to controls (34.4 ± 3.1 vs. 50.4 ± 10.1 pA/msec, P = 0.2, Fig. 2.4C). Calculation of number of released SVs showed a significant reduction ($2.5 \times 10^5 \pm 0.6 \times 10^5$ vs. $0.5 \times 10^5 \pm 0.2 \times 10^5$ total quanta, P = 0.01, Fig 2.4D). However, the number of quanta released per SRC was unchanged (955.2 ± 208.5 vs. 674.27 ± 234.02 quanta per SRC, P = 0.4, Fig. 2.4E). Collectively, these data indicate that 5Cl-CASPP prevents filling of SVs which, in turn, limits the frequency of SRCs that can be supported.

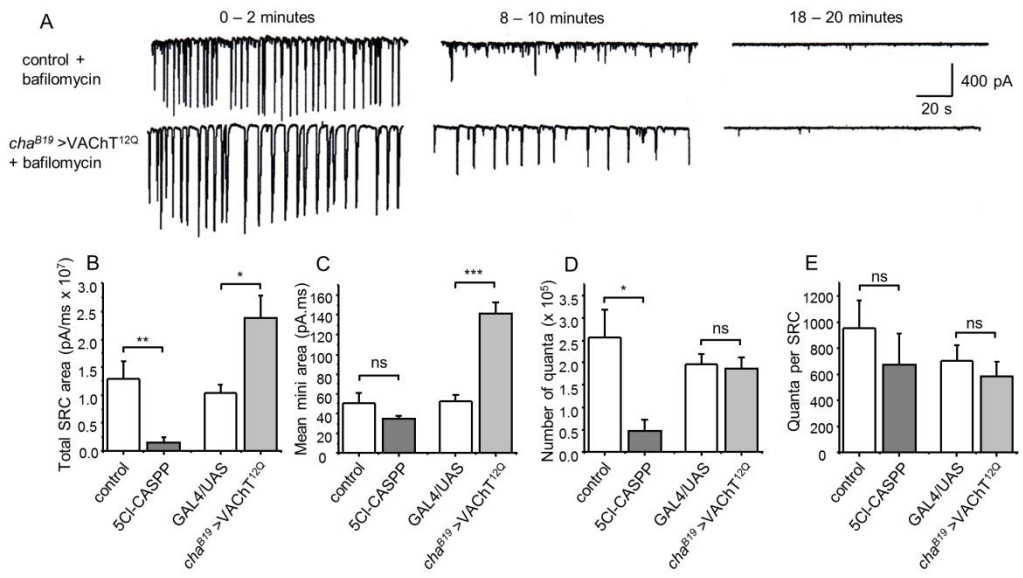

Figure 2.4. *VAChT*^{12Q} increases ACh release. (A) Representative traces of SRC rundown in control (*cha*^{B19}/+) + bafilomycin and *cha*^{B19}>*VAChT*^{12Q} + bafilomycin over a 20 min period. (B) Total area of all SRCs recorded over the 20 minute period is significantly reduced in 5Cl-CASPP-fed larvae and significantly increased in *cha*^{B19}>*VAChT*^{12Q} larvae. (C) Mean mini area is not significantly different in larvae acutely fed 5Cl-CASPP but is significantly increased in *cha*^{B19}>*VAChT*^{12Q} larvae. (D) Number of quanta (ACh-containing SVs) released over 20 minutes is significantly decreased in larvae acutely fed 5Cl-CASPP but is not different in *cha*^{B19}>*VAChT*^{12Q} larvae. (E) Quanta per SRC is not significantly reduced in either 5Cl-CASPP fed larvae or *cha*^{B19}>*VAChT*^{12Q}. Control for 5Cl-CASPP is vehicle-fed only. Control for *cha*^{B19}>*VAChT*^{12Q} is *cha*^{B19}/+ and UAS-*VAChT*^{12Q}/+ (which did not differ). Values are mean ± sem, n ≥ 6.

2.4.3 Altering levels of *VAChT* or exposure to 5Cl-CASPP does not affect SV size

We show that expression of *VAChT*^{12Q} is sufficient to increase frequency and amplitude of minis recorded in the aCC/RP2 motoneurons. Both effects are indicative of a change in SV volume and/or an increase in number of releasable SVs (i.e. quanta), the latter possibly due to an increase in number of active zones.

We analysed putative cholinergic synapses at the ultrastructural level in third-instar CNS (sections were taken from the approximate area that electrophysiological recordings were made, see methods). We took advantage of the fact that the majority of central neurons in *Drosophila* are cholinergic and thus, the majority of synapses in the dorsal motor neuropil will be those of cholinergic premotor interneurons (Gorczyca and Hall, 1987, Yasuyama and Salvaterra, 1999). Controls (cha^{B19}) were compared to CNS derived from both 5Cl-CASPP-fed larvae and from cha^{B19}>$VAChT^{12Q}$ transgenic larvae. Measurement of SV size, distribution with respect to the active zone and active zone length did not differ between control, cha^{B19}>$VAChT^{12Q}$ and WT larvae fed 5Cl-CASPP (Fig. 2.5). This suggests that, in cha^{B19}>$VAChT^{12Q}$ larvae, SVs are normal in size and supports the finding that altered release of ACh is not due to an altered number of SVs at the active zone. That minis have larger amplitude in cha^{B19}>$VAChT^{12Q}$, is perhaps consistent with SVs containing more ACh under these conditions. However, whether this is the case remains to be determined particularly given that overexpression of wildtype *VAChT* does not change mini amplitude. We must also test the possibility that expression of $VAChT^{12Q}$, similar to its wildtype counterpart, does not evoke postsynaptic compensation. To address number of active zones, we analysed random images taken at a lower magnification. Again, there was no apparent change in active zone number across the three conditions (Fig. 2.5B). This indicates that the change in frequency observed in minis is not likely due to a change in the number of active zones, but rather an increased release probability.

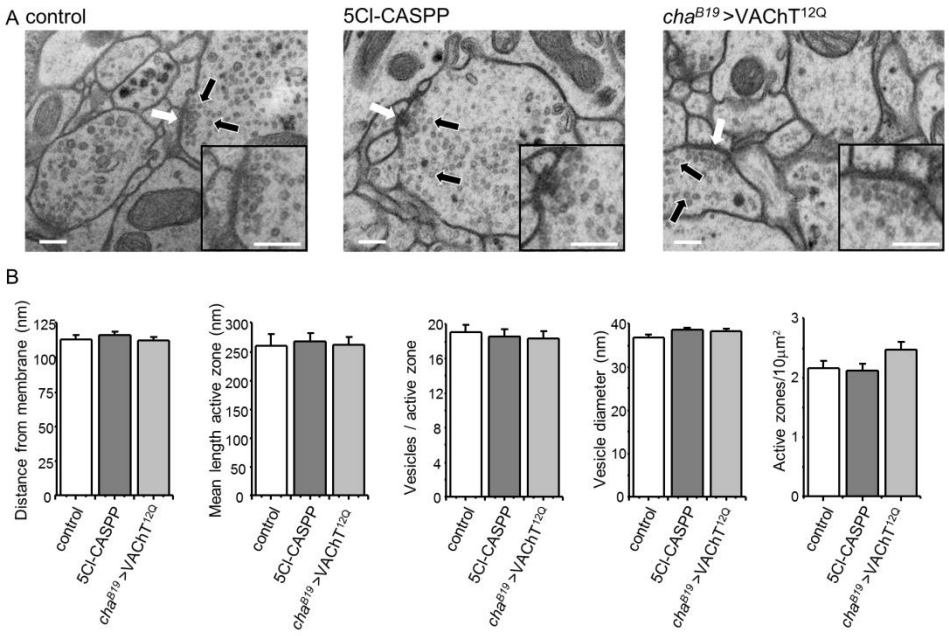

Figure 2.5. *VAChT* does not influence active zone morphology. (A) Representative micrographs showing active zones in control, larvae fed 5Cl-CASPP and *cha*^{B19}>*VAChT*^{12Q}. Black arrows indicate vesicles, white arrows indicate active zones. (B) Changing *VAChT* activity (by chemical block or transgene overexpression) has no effect on distribution of SVs at the active zone, length of active zone, SV number or diameter. Number of active zones is also not affected. Values are mean ± SEM. n ≥ 29, referring to number of active zones analysed and n ≥ 41 for active zone image analysis. Control is *cha*^{B19}/+, Scale is 200 nm.

2.5 Discussion

Using a *Drosophila* central synapse, we have investigated *in vivo* how *VAChT* regulates cholinergic transmission. We demonstrate that decreased *VAChT* activity leads to decreased spontaneous quantal release frequency. Increased *VAChT* activity, by contrast, leads to increased frequency of spontaneous release with no change to amplitude or number of SVs at the active zone, suggestive of an increased probability of SV release.

Decreased functional *VAChT* causes a reduction in spontaneous quantal release frequency but not quantal size. This is in agreement with studies at *Drosophila* and snake NMJs, where decreased vesicular transporter results in decreased frequency but not amplitude of miniature excitatory junctional potentials (Parsons et al., 1999, Daniels et al., 2006). However, many studies in mice and rat also link decreased *VAChT* with decreased transmitter load (Wilson et al., 2005, Prado et al., 2006, Lima et al., 2010, Rodrigues et al., 2013). A possible explanation for this apparent difference is that *Drosophila* cholinergic SVs usually contain only one *VAChT* and so each SV is either loaded with ACh or empty if the *VAChT* is blocked by 5Cl-CASPP. We report no change in vesicle number or size at the active zone which suggests that there may be empty vesicles which undergo recycling, as has been previously reported (Parsons et al., 1999). This is supported by a decrease in total quanta released after bafilomycin treatment.

When *VAChT* activity is increased, we see a clear increase in frequency with no change in amplitude of spontaneous quantal release. An increase in mini frequency with increased *VAChT* is in good agreement with a study in *Xenopus* spinal neurons (Song et al., 1997). Moreover, VGLUT overexpression at the *Drosophila* NMJ results in a modest increase in quantal release (Daniels et al., 2004). However, these studies, and another in rat (Wilson et al., 2005), consistently report an increase in transmitter load of the SVs which supports the 'steady-state' model of SV filling. Based on our observations, SV loading of ACh at central synapses in *Drosophila* is consistent with a 'set-point' model which caps the amount of uptake regardless of transporter activity (Williams, 1997). Williams suggests the set point model is achieved through a feedback mechanism. Our observation that following removal of a single glutamine residue from a 13-glutamine polyQ domain, mini amplitude is significantly increased indicates that this region may

be involved in that feedback mechanism. An alternative is that *VAChT*^{12Q}, which is a naturally-occurring polymorphism, obeys the steady state model. Either way, it would seem that our data does not support one clear mechanism, raising the possibility that SV filling may differ between species and, perhaps even within a species where such polymorphisms are expressed.

We further show that increased spontaneous release frequency is not likely caused by an increase in the number of vesicles at the active zone or active zone density. This corroborates previous work that shows *VAChT* plays a second role: facilitating SV mobilisation or fusion. In *C. elegans,* an interaction between *VAChT* and SV release machinery has been reported (Sandoval et al., 2006). A glycine to arginine amino acid change at position 347 disrupts an interaction with synaptobrevin, a vesicle associated membrane protein that is pivotal for exocytosis (Link et al., 1992, Schiavo et al., 1992). The glycine at position 347 is well conserved and is present in *Drosophila VAChT*. However, a glycine to arginine substitution at this position in the *Drosophila VAChT* seemingly results in a non-functional protein that cannot rescue the *VAChT* null (see Appendix 1, section 2.7.2).

Our study presents supporting data for a dual role for *VAChT* in SV filling and release. Moreover, it provides evidence to suggest that the polyQ domain of *Drosophila VAChT* has a role in determining SV transmitter load. Mammals including humans, rats and mice have a di-leucine motif at residues 485-486 within the cytoplasmic C-terminal. This di-leucine motif has been reported to be important for localising *VAChT* to the SV membrane and also to play a role in endocytosis after neurotransmitter release through an interaction with the AP-2 complex (Tan et al., 1998, Barbosa et al., 2002). *Drosophila VAChT* does not have a di-leucine motif but, unlike the mammalian *VAChT*

sequences mentioned, has a 13 residue polyQ domain at the C-terminal. Extended polyQ domains are associated with diseases such as Huntington's and spinocerebellar ataxia (Lievens et al., 2005; Sokolov et al., 2006). Little is known about the normal function of polyQ domains, but functions may include protein-protein interactions, transcriptional regulation and RNA binding and signalling (Schaefer et al., 2012). This poses the possibility that the polyQ domain may be responsible for *VAChT* localisation and endocytosis in *Drosophila*. It has been suggested that the number of glutamines may be of importance (Schaefer et al., 2012). It is possible, therefore, that *VAChT*^{12Q} may be transported more efficiently to the SV membrane. In *Drosophila melanogaster* the *VAChT*$^{-Q}$ tested in this study is a naturally occurring polymorphism identified during cloning of the *Drosophila VAChT* by Sluder et al (2012, supplementary text) and subsequently confirmed by sequencing PCR products from cDNA libraries.

A BLAST search for similar amino acid sequences and predicted sequences of *VAChT* found that many *Drosophila* species contain polyQ domains in the same region as *D. melanogaster*, but that the length varied from 15 in *D. pseudoobscura* to 5 in *D. grimshawi*. Other insects that also have a polyQ domain in the same region include the housefly *Musca domestica,* which has a 9 residue polyQ domain, and three *Anopheles* mosquitoes: *A. sinensis*, *A. gambiae and A. darlingi* with 7, 10 and 7 glutamines respectively. Ant, moth, bee and butterfly species found during the search did not contain a polyQ of more than 2 glutamines in the same region. The presence of the polyQ domain in three malaria transmitting mosquito species but not other insects identifies this region as a possible target for insecticides to control these disease carrying insects.

2.6 Acknowledgements

We are grateful to Marcus Allen who originated this project. We thank members of the Baines group for their help and advice during the course of this work. We also thank Dr Aleksandr Mironov (University of Manchester Electron Microscopy Unit) for assistance and advice with TEM sample preparation and imaging. This work was supported by a Biotechnology and Biological Sciences Research Council (BBSRC) CASE studentship to FC and by a BBSRC project grant to RAB (BB/J005002/1). Work on this project benefited from the Manchester Fly Facility, established through funds from University and the Wellcome Trust (087742/Z/08/Z). The funders had no role in study design, data collection and analysis, decision to publish, or preparation of the manuscript.

2.7 Appendix 1

2.7.1 *VAChT* up-regulation decreases synaptic variability

SRCs were further studied where cholinergic input to *Drosophila* motoneurons can be tightly controlled using Channel Rhodopsin (ChR2) expressed in cholinergic pre-synaptic interneurons (cha^{B19}). ChR2 evoked SRCs were stimulated using 100 ms pulses of blue light (λ470 nm, 100ms, light intensity 9.65 mW/cm^2) either at 1Hz or 0.3Hz and recordings carried out from RP2 motoneurons as described in 2.2.3. The amplitude of each event was recorded and the relationship between the first and consecutive SRC was obtained termed the Paired-Pulse Ratio (PPR). ChR2 activation requires a retinol co-factor for channel activation. As such, flies were additionally fed 100 µl/vial of 0.1 M all trans-retinal (Sigma, #R2500) in 100% EtOH applied to the surface of standard media and raised in blackout vials in order to prevent ChR2 activation throughout larval development.

Consistent with recordings of spontaneous SRC release (Fig. 2.2), ChR2 evoked SRCs do not differ in amplitude between cha^{B19}>ChR2 or cha^{B19}>ChR2 ; *VAChT* (26.40 ± 2.53 vs. 29.04 ± 2.39pA/pF, cha^{B19}>ChR2 vs. cha^{B19}>ChR2; *VAChT* respectively, P = 0.49, Fig. 2.6A-B), following a 1 Hz time interval (23.16 ± 3.67 vs. 29.91 ± 2.93pA/pF, P = 0.21) or after 0.3Hz time interval (25.84 ± 2.61 vs. 28.66 ± 2.57, P = 0.48). Furthermore, PPR did not differ at 1Hz (0.75 ± 0.21 vs. 0.87 ± 0.07pA/pF cha^{B19}>ChR2 vs. cha^{B19}>ChR2; *VAChT* respectively, P = 0.19, Fig. 2.6C) or after 0.3Hz (0.85 ± 0.04 vs. 0.86 ± 0.05pA/pF, P = 0.86), suggesting up-regulation of *VAChT* does not influence the ability of cholinergic pre-motoneurons to release ACh, despite an up-regulation of spontaneous vesicle release (Fig. 2.1).

Surprisingly, a clear reduction in variability between the first and second SRC at 1Hz (Std Dev: 0.21 vs. 0.06, *cha*^{B19}>ChR2 and *cha*^{B19}>ChR2 ; *VAChT* respectively, P = 0.02, Fig 2.6D) was observed between recordings, an effect which was abolished following a 0.3Hz time delay (0.13 vs. 0.11, P = 0.86), suggesting although increased *VAChT* expression does not influence individual SRC kinetics, loading variability between stimulation is significantly enhanced. This may be explained by enhanced vesicle loading or recycling.

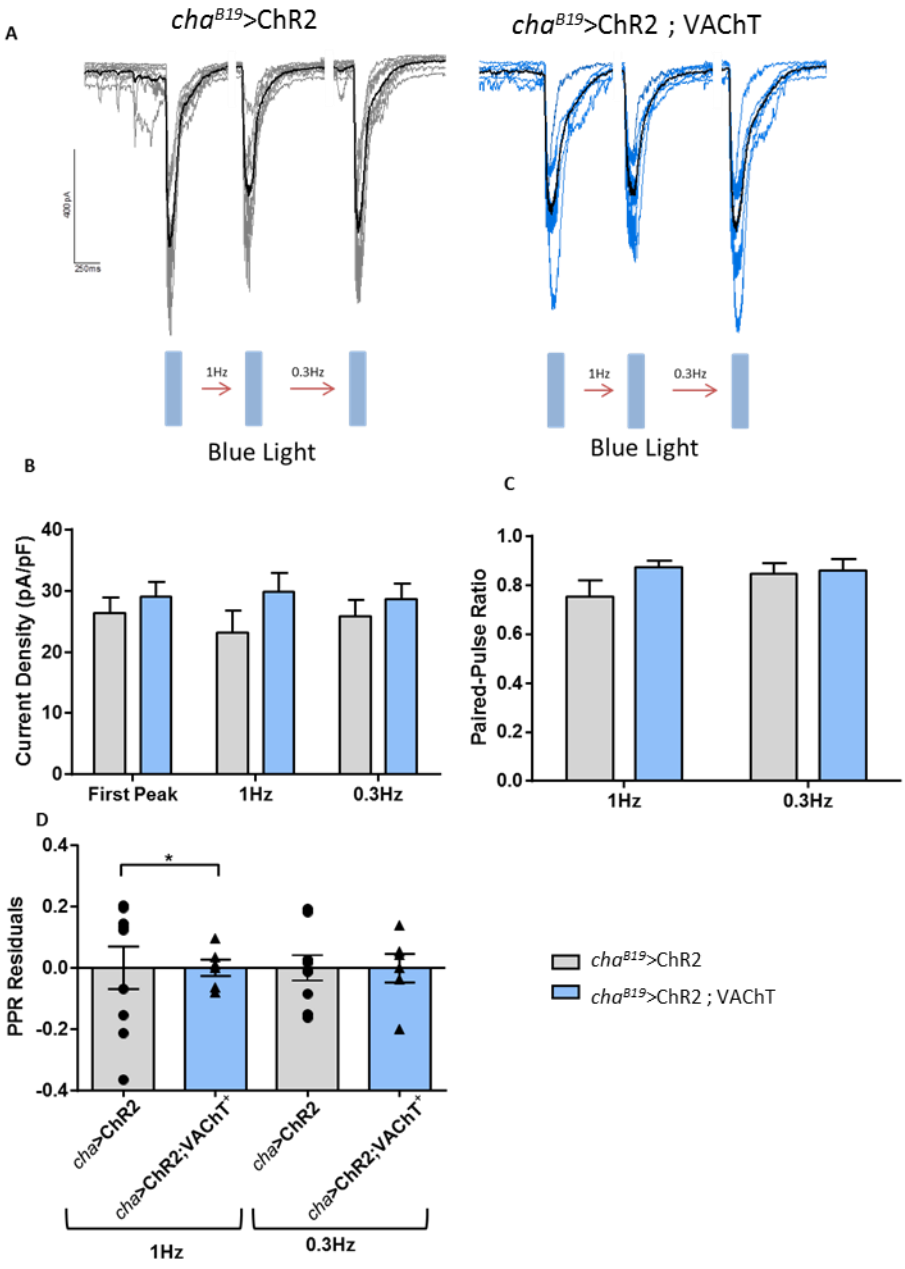

Figure 2.6. Transgenic up-regulation of *VAChT* reduces the variability between evoked SRCs. (A) representative traces of SRCs elicited with a 1Hz and a 0.3Hz time interval recorded from RP2 motoneurons in control larvae overexpressing channel rhodopsin (*cha*^{B19}>ChR2, N = 9) and larvae overexpressing both channel rhodopsin and *VAChT* (*cha*^{B19}>ChR2; *VAChT*, N = 6). (B) *cha*^{B19}>ChR2; *VAChT* causes no significant change to SRC amplitude of the initial evoked SRC (P=0.49), following a 1 Hz time interval (P = 0.21) or after 0.3Hz time interval (P = 0.48). (C) Although increased, *cha*^{B19}>ChR2; *VAChT* causes no significant change to the relationship between initial stimulation and 1 Hz evoked SRCs (0.75 ± 0.21 vs. 0.87 ± 0.07pA/pF, P = 0.19) or after 0.3Hz (P = 0.86). (D) *cha*^{B19}>ChR2; *VAChT* decreases the variability in amplitude between the first and second stimulation after 1Hz (P = 0.02), an effect which is abolished following a 0.3Hz time delay (P = 0.86).

2.7.2 Rescue of *VAChT*^{null} utilising GAL4 expression of *VAChT*

The *VAChT*^{G342R} mutation represents a point mutation causing a disruption in binding between *VAChT* and the vesicle bound SNARE protein, synaptobrevin (Sandoval et al., 2006). To ascertain whether UAS-*VAChT*^{G342R} and UAS-*VAChT* can rescue *VAChT*^{null}, the respective transgenes were crossed into a homozygous null mutant (*VAChT*^{null}) previously characterised (Kitomoto et al., 1996). *VAChT*^{null} mutants are embryonic lethal due to an inability to load and release full cholinergic synaptic vesicles. Figure 2.7 displays schematic of the cross-used for creation of rescue lines.

Rescue of *VAChT*^{null} is not only dependent on the level of transcript expression but also the period in which expression occurs, both of which differ between GAL4 lines. These may have unforeseen consequences for the successful rescue of the *VAChT*^{null} phenotype. In an attempt to alleviate these potential pitfalls, three different GAL4 drivers were utilised. *cha*^{B19} is specific to cholinergic neurons. However, it activates at a later stage in embryonic development (~13-15 hours AEL) (Salvaterra and Kitamoto,

2001). GAL4-*1407* expression persists through all larval stages and activates early in development (9 hours AEL). However, it is indiscriminately expressed in all neurons (Sweeney et al., 1995). *Scabrous* (*sca*) activates at a much earlier time period (~3 hours AEL). However, is also expressed in all neurons, with expression diminishing at late L1 (Mlodzik et al., 1990).

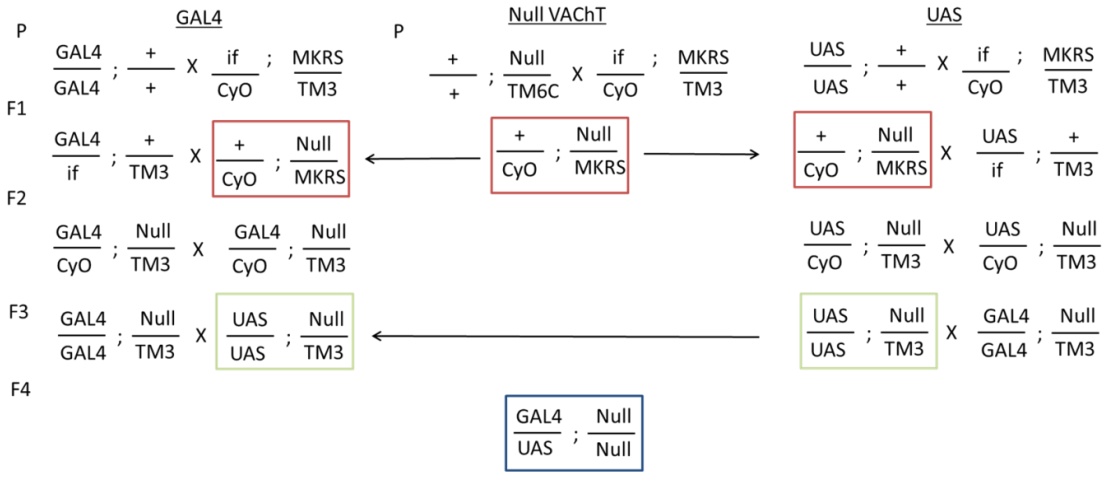

Figure 2.7. Crossing scheme utilised to create *VAChT* Rescue lines. GAL4 is indicative of one of the three GAL4 drivers used for expression (*cha*^{B19}*, 1407 or sca*) whereas UAS refers to *VAChT* and *VAChT*^{G342R}. Null refers to the embryonic lethal *VAChT*^{null} mutation. Balancer chromosomes used where CyO::GFP and TM3::GFP, markers were if and MKRS. The use of GFP allowed the identification of larval genotype throughout crossing and for identification purposes when assessing rescue. The heterozygous null mutants were crossed in at F1 (red box), F2 cross allows the attainment of homozygous GAL4 or UAS respectively in combination with a heterozygous *VAChT*^{null}. F3 (green box) allows the inclusion of both GAL4 and UAS on the second chromosome together with *VAChT*^{null} and were kept as stable lines following confirmation of GAL4 homozygosity through crossing with + ; + ; UAS-CD8::GFP. The final F4 generation were selected for against the presence of GFP present on TM3 only (Blue Box).

As shown in the above crossing scheme, F3 generation flies can be differentiated from the desired F4 generation via the absence of GFP. Flies were allowed to lay for 24 hours following which embryos were left for a further 24 hours and screened for hatched GFP negative larvae. All F4 lines were confirmed to express the correct GAL4 driver through crossing with + ; + ; UAS-CD8::GFP which show 100% of embryo/larvae expressing GFP with the correct pattern of expression.

Figure 2.8 shows that *cha*^{B19} elicits zero viable offspring through either *VAChT* or *VAChT*^{G342R} expression (n = 200 per genotype). This was surprising as *cha*^{B19} follows the expression pattern of the cholinergic locus which encompasses both *ChAT* and *VAChT* and suggests either that *cha*^{B19} does not accurately mimic endogenous *VAChT* timings or levels which have important consequences for cholinergic development or both *VAChT* constructs generate a non-viable protein. This was not the case as both *1407* and *sca* rescued the *VAChT*^{null} phenotype, 93% of *1407>VAChT* and 88.5% of *sca>VAChT* produced viable offspring. However, *VAChT*^{G342R} produced 100% embryonic mortality using either *1407* or *sca*. Failure to rescue *VAChT*^{null} with *VAChT*^{G342R} whereas its rescue with wildtype VAChT suggests the G342R mutation generates a non-functional protein in agreement with previous literature (Sandoval et al., 2006). Due to relevance to this thesis and ectopic nature of rescue, this line of questioning was not followed up further.

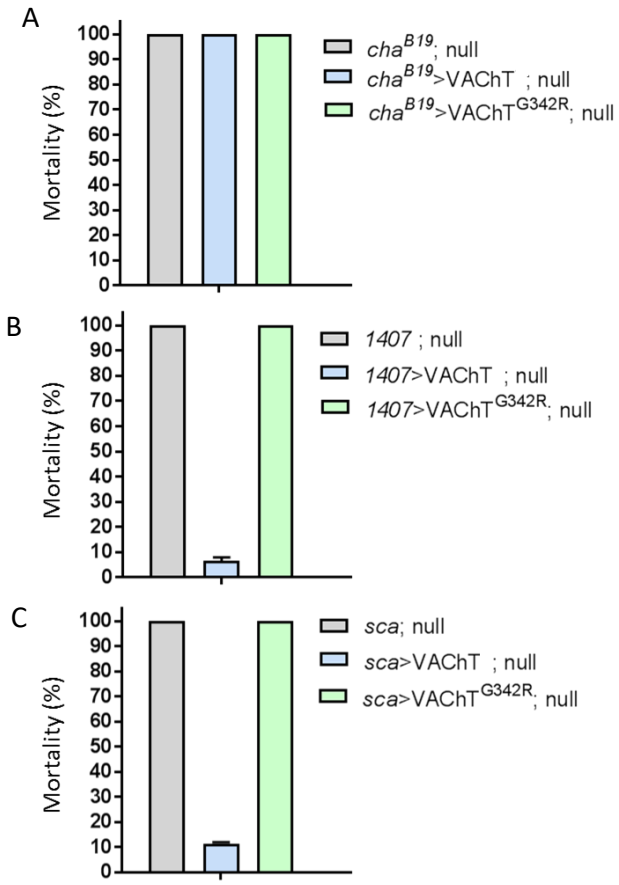

Figure 2.8. *VAChT not VAChT^{G342R} rescues VAChT^{null}. (A) cha^{B19}* does not produce any viable offspring when driving either *VAChT* construct suggesting that this GAL4 does not mimic endogenous levels and/or timings important for cholinergic development. (B) 1407 produces 93% viable offspring for *VAChT*. However, no viable offspring are produced through *VAChT*^{G342R} expression and (C) in a similar fashion *sca* expression produces 88.5% viable offspring for *VAChT*. However, no viable offspring are produced through *VAChT*^{G342R} expression. n = 200 per genotype.

The *VAChT*^{Y49N} mutation provides insecticide-resistance but perturbs evoked cholinergic neurotransmission in *Drosophila*

Samuel W. Vernon[1], Jim Goodchild[2] and Richard A. Baines[1*]

[1]Division of Neuroscience and Experimental Psychology, School of Biological Sciences, Faculty of Biology, Medicine and Health, University of Manchester, Manchester Academic Health Science Centre, Manchester, M13 9PL, UK. [2]Syngenta Crop Protection Research, Bracknell, Berkshire, UK.

Reference

Vernon, S. W., Goodchild, J., & Baines, R. A. (2018). The *VAChT*^{Y49N} mutation provides insecticide-resistance but perturbs evoked cholinergic neurotransmission in *Drosophila*. *PLOSOne* (in press)

3.0 Statement of Contribution.

SV conducted, analysed and interpreted all figures. SV wrote manuscript with assistance of RAB and JG. Modifications to the text is made in order to incorporate the further relevant data conducted during this project presented in Appendix 2 (section 3.7) and for stylistic consistency for the purpose of this thesis.

3.1 Abstract

Global agriculture and the control of insect disease vectors have developed with a heavy reliance on insecticides. The increasing incidence of resistance, for virtually all insecticides, threatens both food supply and effective control of insect borne disease. CASPP ((5-chloro-1'-[(E)-3-(4-chlorophenyl)allyl]spiro[indoline-3,4'-piperidine]-1-yl}-(2-chloro-4-pyridyl)methanone)) compounds are a potential new class of neuroactive insecticide specifically targeting the Vesicular Acetylcholine Transporter (*VAChT*). Resistance to CASPP, under laboratory conditions, has been reported following either up-regulation of wildtype *VAChT* expression or the presence of a specific point mutation ($VAChT^{Y49N}$). However, the underlying mechanism of CASPP-resistance, together with the consequence to insect viability of achieving resistance, is unknown. In this study, we use electrophysiological characterisation of cholinergic release at *Drosophila* larval interneuron→motoneuron synapses to investigate the physiological implications of these two identified modes of CASPP resistance. We show that both *VAChT* up-regulation or the expression of $VAChT^{Y49N}$ increases miniature (mini) release frequency. Mini frequency appears deterministic of CASPP activity. However, maintenance of SV release is not indicative of resistance in all cases. This is evidenced through expression of syntaxin or complexin mutants ($sytx^{3\text{-}61}/cpx^{SH1}$) that show similarly high mini release frequency but are not resistant to CASPP. The $VAChT^{Y49N}$ mutation additionally disrupts action potential-evoked cholinergic release and fictive locomotor patterning through depletion of releasable synaptic vesicles. This observation suggests a functional trade-off for this point mutation, which is not seen when wildtype *VAChT* is up-regulated.

3.2 Introduction

Vesicular transporters load neurotransmitter into synaptic vesicles (SV) for storage before release. Transporter localisation dictates loading substrate and differs between vesicle classification (Takamori, 2016). Small clear SVs mostly store fast-acting neurotransmitters. Transporters known to localise to small clear SVs include the vesicular glutamate transporters *VGLUTs 1-3* (Takamori et al., 2000, Takamori et al., 2001, Fremeau et al., 2002), the glycine transporter *VGLYT1* (Núñez et al., 2009, Cubelos et al., 2014), the vesicular GABA and Glycine co-transporter *VGAT/VIAAT* (McIntire et al., 1997, Sagné et al., 1997, Aubrey, 2016), *VAChT* (Erickson et al., 1994) and vesicular monoamine transporters (*VMATs*) (German et al., 2015). The insect CNS and to a lesser, but still significant, extent the mammalian CNS relies on ACh and *VAChT* for excitatory synaptic signalling. *Drosophila VAChT* null mutants die during embryogenesis (Kitamoto et al., 2000) whilst mammalian *VAChT* null mutants are lethal soon after birth (De Castro et al., 2009). *VAChT* knockdown also results in memory deficits in both mice and insects (Prado et al., 2006, Barnstedt et al., 2016). By contrast, *VAChT* up-regulation causes accelerated neuromuscular aging (Sugita et al., 2016) and disrupted central cholinergic morphological development (Janickova et al., 2017). Altered physiological and morphological phenotypes are also reported in *Drosophila* at the glutamatergic neuromuscular junction (NMJ) following *VGLUT* up-regulation (Daniels et al., 2011). It is, perhaps, unsurprising that transporter abnormalities are associated with many neurodegenerative diseases including Alzheimer's (Ferreira-Vieira et al., 2016), Huntington's (Suzuki et al., 2001) and Parkinson's disease (Mazere et al., 2009).

Cholinergic central interneurons form a central pattern generator that drives *Drosophila* motoneurons and are pivotal in governing the control of larval peristalsis (Baines et al., 2001). Normal cholinergic function is essential for survival and, as a result, the cholinergic system is a major target for insecticide development (Casida and Durkin, 2013). CASPP compounds specifically bind to, and inhibit the function of, *VAChT* (Cassayre et al., 2010, Sluder et al., 2012, Maienfisch et al., 2011b, Cassayre et al., 2011, Maienfisch et al., 2011a, Maienfisch et al., 2011c). CASPP mortality is associated with an inability of central neurons to release ACh (Cash et al., 2015). However, transgenic up-regulation of *VAChT* significantly reduces CASPP lethality in adult *Drosophila* (Sluder et al., 2012) and, moreover, greatly increases spontaneous mini release of ACh from larval *Drosophila* central premotor interneurons (Cash et al., 2015). This suggests a causal relationship between up-regulation of target activity and resistance to CASPP. Furthermore, transgenic expression of the $VAChT^{Y49N}$ mutation, in an otherwise wildtype background, provides complete insensitivity to CASPP (Sluder et al., 2012). However, the physiological implications to CNS function of the presence of this resistance allele, and its response to insecticide treatment, have not been described.

Insecticide resistant phenotypes have been formally identified since the initial discovery of DDT resistance in *Musca domestica* in 1966 (Hoyer and Plapp Jr, 1966) and have been characterised into four sub categories; (i) behavioural changes, (ii) altered penetration, (iii) target site modification and (iv) metabolic resistance (Belinato and Martins, 2016). Through these mechanisms, insects have attained resistant alleles for the majority of pesticide classes including but not limited to organophosphates, carbamates, pyrethroids, neonicotinoids and non-neuronal insecticides such as insect growth regulators (IGRs) (Bass et al., 2015, Shono et al., 2002, Naqqash et al., 2016,

Metcalf, 1989). However, little is known about the physiological implications brought about by resistant genotypes. Here we utilise *Drosophila* as a model to study CASPP resistance generated through transgenic up-regulation of wildtype *VAChT* transcript achieved via the GAL4/UAS system and through the endogenous expression of a CRISPR-induced knock-in of $VAChT^{Y49N}$. Electrophysiological characterisation of cholinergic minis in identified *Drosophila* motoneurons (specifically the anterior corner cell, aCC and Raw Prawn 2, RP2 motoneurons) shows that CASPP resistance is associated with the maintenance of mini release frequency. However, despite trends in enhanced synaptic transmission, we further demonstrate that similarly increased mini release, achieved through up-regulation of mutant membrane bound SNARE protein syntaxin $(sytx^{3-69})$ (Lagow et al., 2007) or the absence of complexin (cpx^{SH1}) (Huntwork and Littleton, 2007), does not lead to CASPP-resistance. This suggests that resistance to this class of insecticide cannot be fully explained by enhanced mini release at cholinergic synapses. Perturbation of evoked release (i.e. action-potential dependent) associated with $VAChT^{Y49N}$ additionally disrupts the ability of the cholinergic locomotor system to maintain sustained activity attributed by an apparent change in SV release. These deficits translate into fitness costs observed through abnormalities in locomotion and adult longevity.

3.3 Materials and methods

3.3.1 Fly stocks

Flies were maintained under standard conditions at 25°C. GAL4 drivers used to recapitulate expression of the cholinergic locus were cha^{B19} (Salvaterra and Kitamoto, 2001) and *ChAT-BAC* (gifted by Dr. Steve Stowers: Montana State University). These lines were used to drive expression of UAS-*VAChT*, UAS-$sytx^{3-69}$ (syntaxin mutant

generously provide by Dr. Bing Zhang, University of Missouri) or UAS-*ChR2*^{ChETA} (Bloomington 36354) (Gunaydin et al., 2010) . The complexin mutant (*cpx*^{SH1}) was generously provided by Dr. Troy Littleton (Massachusetts Institute of Technology). The wild-type UAS-*VAChT* is described in (Cash et al., 2015). CRISPR constructs were prepared as described below and injected into c*as9*-expressing embryos (*yw*; attP40 *nos-cas9* /*CyO*;*+*) by BestGene Inc., (Chino Hills, CA, USA). Control lines were Canton-S and the CRISPR-injected line lacking construct insertion (*yw*; attP40 *nos-cas9* ;*+*).

3.3.2 gRNA and insert design, template oligo and plasmid construction

The CRISPR Optimal Target Finder tool (http://tools.flycrispr.molbio.wisc.edu/targetFinder/) was used to specify target cut sequence specificity (GATTACCGCTATCAGGTACC). Two guide RNA constructs were made to generate cuts in 5'- and 3'-UTR of *VAChT*, respectively. The gRNA oligonucleotides (5' to 3') are: 5'-UTR: CTTCGAGAGGAAGTCCCAAAGAAAC and AAACGTTTCTTTGGGACTTCCTCTC; 3'-UTR: CTTCGTATTATTACTATAGACATAT and AAACATATGTCTATAGTAATAATAC, sense and antisense, respectively). 100 pmol of each 5' phosphorylated sense and antisense gRNA oligonucleotides were mixed, denatured at 95^{o}C and then reduced to 25^{o}C at a rate of -0.1^{o}C/sec and ligated to the guide RNA expression plasmid, pU6-BbsI-chiRNA (plasmid #45946, addgene). A *VAChT*^{Y49N}, containing 5' and 3' PAM site mutations, that prevent cas9 cleavage, was cloned to pHD-DsRed vector (plasmid #51434, addgene) as a dsDNA donor template for CRISPR/Cas9-mediated homology-directed repair (HDR). Oligos used to generate PAM site mutations are depicted in Table 3.1. Briefly, for 5' PAM site mutagenesis, PCR of primers a+b and c+d (containing TGG to TGC point mutations) were run against

Drosophila genomic DNA (PCR1). Following purification, PCR products (a+b and c+d) were used as templates for a second PCR using the most 5' and 3' primers of PCR1 (primers a and d, Table 3.1). This process was repeated for 3' PAM site mutagenesis utilising primers (e+f and g+h). Full UTR sequence with PAM mutations were purified, sequenced and mobilised to pHD-DsRed using restriction digests (5' = AscI & BssSI), 3' = SpeI & XhoI). *VAChT*^{Y49N} ORF was generously provided by Syngenta and cloned into pHD-DsRed vector using restriction enzymes (EcoR1 and Nde1). Sequence confirmation was confirmed by Sanger sequencing at the Manchester Sequencing Facility.

Table 3.1. Primers used for creation of *Drosophila VAChT* UTR with modified PAM sites (5': a,b,c,d and 3': e,f,g,h).

Sequence	Use
ATCGGGCGCGCCGAATTCATGCTTGGGTCGACTTAAGCTC	a
ACAAAGTTCTGATGCAGTTTCTTTGG	b
CCAAAGAAACTGCATCAGAACTTTGT	c
CTTAAATAGTCGGGTATAATCGGTACTA	d
GTACACTAGTTCGTGTTCTTTTGCACACCTCC	e
ACGTACCACTTGGCTATATGTCTATA	f
TATAGACATATAGCCAAGTGGTACGT	g
GCTACTCGAGAAGTCCGCCACAATGACAACC	h

3.3.3 Identification of positive progeny

Positive progeny were identified by the expression of DsRed in larvae following the 3xP3 expression pattern. Single adult males were selected and individually balanced using *CyO* and *TM3*. Fully balanced lines were sequenced for the *VAChT*^{Y49N} sequence. DsRed was removed using a Cre-recombinase line (y^1w^{67c23} *P Crey 1b*; D^**/TM3,* Sb^1, flybase ID: FBst0000851). Lines were then homozygosed using (w^- ; *if/CyO* ; *MKRS/TM3*) and cleaned generating a final stock of w^- ; *+* ; *VAChT*^{Y49N}.

3.3.4 Mortality and 5Cl-CASPP application

5Cl-CASPP (also termed Syn351), made by Syngenta (Sluder et al., 2012), was added to food vials containing standard cornmeal medium. 5Cl-CASPP was solubilized in acetone (which was added alone as vehicle control). CASPP solution (50 µl) was added to each vial and blunt forceps were used to break up the food surface to aid penetrance. A total of 60 first instar larvae were assayed per drug concentration, 20 larvae per vial. Larvae were reared at 25°C for 7 days (in a humid incubator). Mortality rate was measured as the proportion of larvae developing to pupae, against those that did not. For use in electrophysiology assays, 5Cl-CASPP (10 µg/ml) was added to the surface of grape-agar plates (50 mm diameter) in 1 ml of aqueous dried yeast extract (5%; Merck, Darmstadt, Germany). After being left to dry overnight at room temperature, second instar larvae were allowed to feed for 24 h before recording.

3.3.5 Larval whole-cell patch-clamp recordings

Recordings were performed at room temperature (20-22°C). Third-instar larvae were dissected in external saline (in mM: 135 NaCl, 5 KCl, 4 $MgCl_2 \cdot 6H_2O$, 2 $CaCl_2 \cdot 2H_2O$, 5 N-Tris[hydroxymethyl]methyl-2-aminoethanesulfonic acid, and 36 sucrose, pH 7.15). The CNS was removed and secured to a Sylgard (Dow-Corning, Midland, Michigan, USA)-coated cover slip using tissue glue (GLUture; WPI, Hitchin, UK). The glia surrounding the CNS was partially removed using protease (1% type XIV; Sigma, Dorset, UK) contained in a wide-bore (15 µm) patch pipette. Whole cell recordings were carried out using borosilicate glass electrodes (GC100TF-10; Harvard Apparatus, Edenbridge, UK), fire-polished to resistances of between 8-12 MΩ. The aCC/RP2 motoneurons were identified by soma position within the ventral nerve cord. When needed, cell identity was confirmed after recording by filling with 0.1% Alexa Fluor 488 hydrazyde sodium salt (Invitrogen, Carlsbad, California, USA), included in the internal patch saline (in mM:

140 potassium gluconate, 2 $MgCl_2 \cdot 6H_2O$, 2 EGTA, 5 KCl, and 20 HEPES, pH 7.4). Tetrodotoxin (TTX, 2 µM, Alomone Labs, Hadassah Ein Kerem, Israel) was included in the external saline to block action potential-induced SV release. Recordings were made using a MultiClamp 700B amplifier. Cells were held at -60 mV and recordings were sampled at 100 kHz and lowpass filtered at 0.5 kHz, using pClamp 10.6 (Molecular Devices, Sunnyvale, CA). Only neurons with an input resistance of ≥ 500 MΩ were accepted for analysis.

Evoked vesicle exocytosis, mimicking action potential mediated spontaneous rhythmic

currents (SRCs), was elicited through driving UAS-ChR2^{Cheta} (λ470 nm, 10 ms, 1 Hz/10 Hz) using the cholinergic driver ChAT-BAC in the background of the wild type *VAChT* or mutant *VAChT*^{Y49N}. Stimulations were carried out for up to 1 hour. As is true for other cholinergic drivers (e.g. *cha*^{B19}-GAL4), ChAT-BAC shows weak expression in aCC (our unpublished observations). Recordings conducted in the presence of the nAChR antagonist, mecamylamine, reveal a small ~20 pA inward depolarising current in unison with stimulating light pulses (i.e. due to this weak expression). Therefore, events ≤ 20 pA, measured using the Clampfit threshold search function, were considered a failed event and thus the point at which the vesicle pool had been depleted.

3.3.6 Larval extracellular recordings

Bursts of spiking driven by cholinergic synaptic input in aCC/RP2 motoneurons were investigated using loose patch extracellular recordings. Recordings were conducted using a 1.3 MΩ recording electrode filled with extracellular solution allowing a loose seal on the soma when applying gentle suction. Recordings, sampled at 20 KHz, were made for 3 minutes with the second minute of each recording taken for analysis. The number of activity bursts within this second minute of recording, together with the

number of spikes per burst (for the first 10 bursts) were quantified and averaged for each recording. Bursts were defined as a minimum of three events within 25 ms.

3.3.7 Adult giant fibre recordings

Flies were sedated on ice for 5 mins before being mounted in dental wax (Kemdent, UK). Appendages, wings and proboscis were secured into the wax with thorax being positioned at a 45° angle aiding penetration of recording electrodes. Two sharpened tungsten wires (0.2 mm) were inserted into the CNS through each compound eye whereas the third was positioned into the abdomen. Stimulation was conducted with a SIU5A stimulus isolation unit (Grass Technologies, USA) controlled via a S88 stimulator (Grass Technologies, USA). Positioning of both stimulating and earth electrodes was confirmed with a pulse (50 V, 0.02 ms) through observation of wing twitching (DLM stimulation) and tergotrochanteral muscle contraction (TTM stimulation). Intracellular recording electrodes (20 – 30 MΩ) (GC100FS-10; Harvard Apparatus, WPI, USA) were filled with 3M KCl for recording. Glass recording electrodes were inserted into DLM 45a and the TTM, identified by position of the bristles on the thorax. Recordings were performed using an Axoclamp-2A amplifier (Axon instruments, USA) controlled by pClamp 10.4 and a Digidata 1440A (Molecular Devices, USA). The responsiveness of the respective muscle (DLM and TTM) to a train of 10 stimuli at 100 Hz, termed “Following Frequency”, was recorded.

3.3.8 Larval crawling

Single larvae were placed on a 55 x 34 mm, 2% nutrient free agarose island surrounded by 5 M NaCl to prevent escape. Recordings were conducted for 3 minutes using EthoVision XT (Version 11, Noldus, Wayeningen, Netherlands) in a Daniovision Behavioural Chamber (Noldus, Wayeningen, Netherlands), using a Basler GenIcam

(Basler acA1300-60, Resolution: 1280 x 960, Frame Rate: 15 Hz). Background was adjusted for using the inbuilt dynamic subtraction function, and a smoothing function of 10 was applied (each data point was a function of 10 data points averaged). Larvae were considered moving when breaching a 0.30 mm distance threshold. Recordings were discarded if sample detection threshold was ≤15% of total recording. Mean velocity (mm/s) and total distance covered (mm) within each 3 minute recording were taken for analysis.

3.3.9 Oviposition and longevity

Number of eggs laid per mated female was taken as one measure of overall fitness. 10-20 virgin females were allowed to mate for 48 hours under standard rearing conditions before being transferred to egg laying chambers mounted on a grape-agar plate (50 mm) supplemented with yeast paste. Following a 24 hour period, total number of embryos per plate was quantified. Following oviposition, single mated females from each genotype were added to single vials and allowed to lay for 5 days. The presence of viable larvae was considered proof the female had been mated. Total life span was further taken as a measure of general fitness. Newly eclosed male flies were added to standard rearing vials at a density of 10 flies per vial per replicate. Flies were transferred to fresh medium three times per week and deaths recorded, as per (Grandison et al., 2009).

3.3.10 Quantitative RT-PCR (qRT-PCR)

Ten CNSs were collected from third-instar wall-climbing larvae. RNA was extracted using the RNeasy micro kit (QIAGEN, Manchester, UK). Single strand cDNA was synthesized using the Revert Aid^{TM} H minus First strand cDNA synthesis kit (Fermentas, Massachusetts, USA). qRT-PCR was performed using a LightCycler480 II (Roche, Basel,

Switzerland) with SYBR Green I Master reaction mix (Roche, Basel, Switzerland). The thermal profile used was 10 min at 95°C followed by 45 cycles of 10 s at 95°C, followed by 10 s at 60°C, and finally 10 s at 72°C. Single-product amplification was confirmed by post-reaction dissociation analysis. PCR primers were designed with the aid of LightCycler Probe Design Software 2.0 (v1.0) (Roche, Basel, Switzerland). Results were analysed by the $2^{-\Delta Ct}$ method where ΔCt was determined by subtracting the average *rp49* Ct value from that of *VAChT*. Ct values used were the means of four to five independent repeats of 10 CNS per sample. Control gene was *rp49*. Primers (5' to 3') were as follows: *rp49*, CCAGTCGGATCGATCGATATGCTA and ACGTTGTGCACCAGGAA; *VAChT*, CTCATCCTCGTGATTGTA and ACGGGTATGATCTTTCC.

3.3.11 Statistics

LD_{50} values were calculated by fitting a regression analysis to the relationship between % mortality and log[dose] using the following equation: $Response = \frac{100}{1+10^{(LogLD_{50}-X)}}$. Statistical significance between group means was assessed using either a Student's t-test (where a single experimental group is compared to a single control group), a one-way ANOVA followed by Bonferroni's post-hoc test (multiple experimental groups) or a Chi-Square test. In all tests, confidence intervals of $*P \leq 0.05$, $**P \leq 0.01$, and $***P \leq 0.001$ and **** $P < 0.0001$ were used for significance. Data shown are mean ± s.e.m.

3.4 Results

3.4.1 Increased *VAChT* or the presence of $VAChT^{Y49N}$ infers resistance to 5Cl-CASPP

Transgenic up-regulation (using GAL4/UAS) of either *VAChT* or $VAChT^{Y49N}$, in a wildtype background, is sufficient to provide resistance to 5Cl-CASPP (Sluder et al., 2012). To validate the previously published observation of 5Cl-CASPP resistance when *VAChT* is

up-regulated, and to ascertain resistance associated with endogenously expressed *VAChT*^{Y49N}, mortality assays were conducted in larvae where *VAChT* was up-regulated in all cholinergic neurons (*cha*^{B19}>*VAChT*) or expression of *VAChT*^{Y49N} achieved through CRISPR knock-in (*VAChT*$^{Y49N/Y49N}$ and *VAChT*$^{Y49N/+}$).

In agreement with previously published data (Sluder et al., 2012), transgenic over-expression of wildtype *VAChT* significantly reduced 5Cl-CASPP toxicity compared with parental controls (GAL4/+ and UAS/+). The observed LD_{50} values were: 4.2 ± 0.2, 3.3 ± 0.1 vs. 10.7 ± 1.0 µg/ml, +/*cha*^{B19}, +/*VAChT* and *cha*^{B19}>*VAChT* respectively, ($P = 1 \times 10^{-4}$, Fig. 3.1A). Previously published work shows GAL4-mediated expression increases *VAChT* transcript abundance by ~ 2.8 fold (Cash et al., 2015). Similarly, the presence of a single copy of *VAChT*^{Y49N}, achieved by CRISPR-mediated gene replacement, provides resistance to 5Cl-CASPP. Fig. 3.1B shows heterozygous *VAChT*$^{Y49N/+}$ larvae have significantly reduced mortality compared with CS (LD_{50}: 3.9 ± 0.2 vs. 10.1 ± 1.0 µg/ml, CS vs. *VAChT*$^{Y49N/+}$ respectively, $P = 1 \times 10^{-4}$). Remarkably, homozygous *VAChT*^{Y49N} mutants display a complete insensitivity to 5Cl-CASPP at all concentrations tested (10ug/ml being the maximal practicable dose). QRT-PCR measurement of *VAChT*^{Y49N} transcript abundance shows that expression level does not differ from *VAChT* in control lines (1.3 ± 1.1 fold change, *VAChT*$^{Y49N/Y49N}$ vs. combined control CS + CRISPR control, P = 0.37). It is noteworthy that the CRISPR control differs from CS in resistance to CASPP (LD_{50}: 3.9 ± 0.2 vs. 4.8 ± 0.3, CS vs. CRISPR control, P = 0.02). However, *VAChT* transcript does not differ in level between CS and CRISPR control (P = 0.29), suggesting this additional resistance is likely due to differences in genetic background (which have not been controlled for). This difference does not, however, obscure the main observation that the presence of *VAChT*^{Y49N}, at endogenous expression levels, provides complete resistance to 5Cl-CASPP.

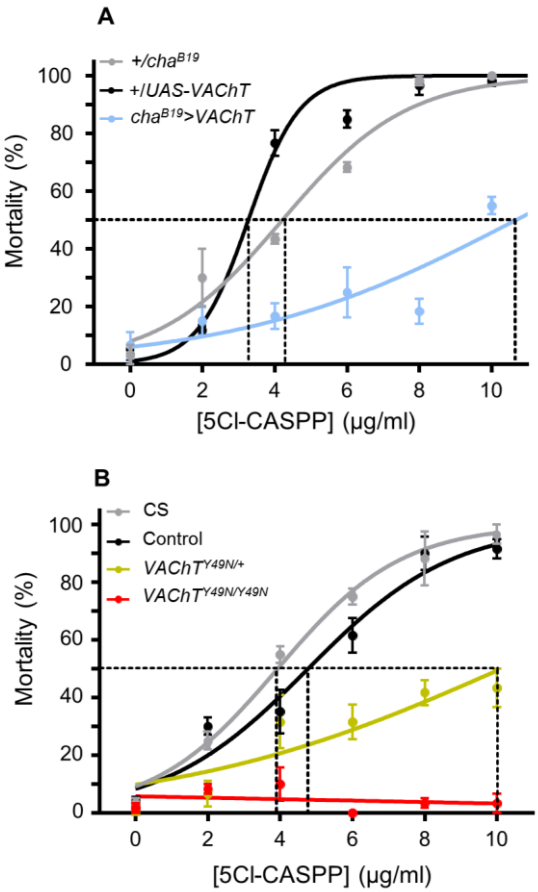

Figure 3.1. *VAChT* up-regulation or endogenous *VAChT*^{Y49N} provides resistance to 5Cl-CASPP. (A) Mortality curves for +/UAS-*VAChT* (black), +/ *cha*^{B19} (grey) and *cha*^{B19}>*VAChT* genotype larvae (blue) exposed to 5Cl-CASPP (0-10 µg/ml). Transgenic expression of *VAChT* significantly (P = 1 x 10^{-4}) reduced 5Cl-CASPP toxicity compared with parental controls (LD_{50}: 4.2 ± 0.2, 3.3 ± 0.1 vs. 10.7 ± 1.0 µg/ml, +/*cha*^{B19}, +/*VAChT* and *cha*^{B19}>*VAChT*, respectively). (B) Heterozygous *VAChT*^{Y49N} mutants (*VAChT*$^{Y49N/+}$; yellow) show significantly reduced mortality to 5Cl-CASPP compared with CS (grey) (LD_{50}: 3.9 ± 0.2 vs. 10.1 ± 1.0 µg/ml, CS vs. *VAChT*$^{Y49N/+}$ respectively, P = 1 x 10^{-4}) and the CRISPR control genotype (black) (LD_{50}: 4.8 ± 0.3, P = 1 x 10^{-4}). Homozygous *VAChT*^{Y49N} mutants (red) display complete insensitivity to 5Cl-CASPP at all concentrations tested. All data points are mean ± sem, n = 60 larvae tested at each concentration. Dotted lines represent LD_{50}.

3.4.2 Elevated *VAChT* increases frequency of spontaneous release events

To investigate the consequence for cholinergic synaptic function associated with observed 5Cl-CASPP resistance, we undertook patch-clamp recordings from well-characterized aCC/RP2 motoneurons. These neurons receive identical cholinergic synaptic input (Baines et al., 1999). We recorded spontaneous minis, achieved by blocking action potential-dependent activity with TTX. We have previously shown that exposure to 5Cl-CASPP significantly reduces mini frequency, but does not affect mini amplitude (Cash et al., 2015). In order to validate these data, and to provide a baseline for comparison with the experiments conducted as part of this study, we repeated this analysis. We observed the same results. 5Cl-CASPP (10 µg/ml) mediated inhibition of *VAChT* results in a significant reduction in mini frequency (38.8 ± 5.6 vs. 13.2 ± 2.9 per min, vehicle vs. 5Cl-CASPP respectively, $P = 2 \times 10^{-3}$, Fig. 3.2A-B) but no effect on mini amplitude (P = 0.91, Fig. 3.2A-B). By contrast, up-regulation of wildtype *VAChT* is sufficient to increase mini frequency, without change to amplitude (Cash et al., 2015). Exposure of this genotype (cha^{B19}>*VAChT*) to 5Cl-CASPP also results in a significant reduction in mini frequency (86.8 ± 19.3 vs. 31.0 ± 6.3 per min, vehicle vs. 5Cl-CASPP respectively, P = 0.01) and no change to amplitude (P = 0.94, Fig. 3.2A-B). However, the reduction in absolute level of mini frequency, observed following exposure to CASPP, is to a degree that is not significantly different to untreated CS (treated with vehicle, P = 0.99).

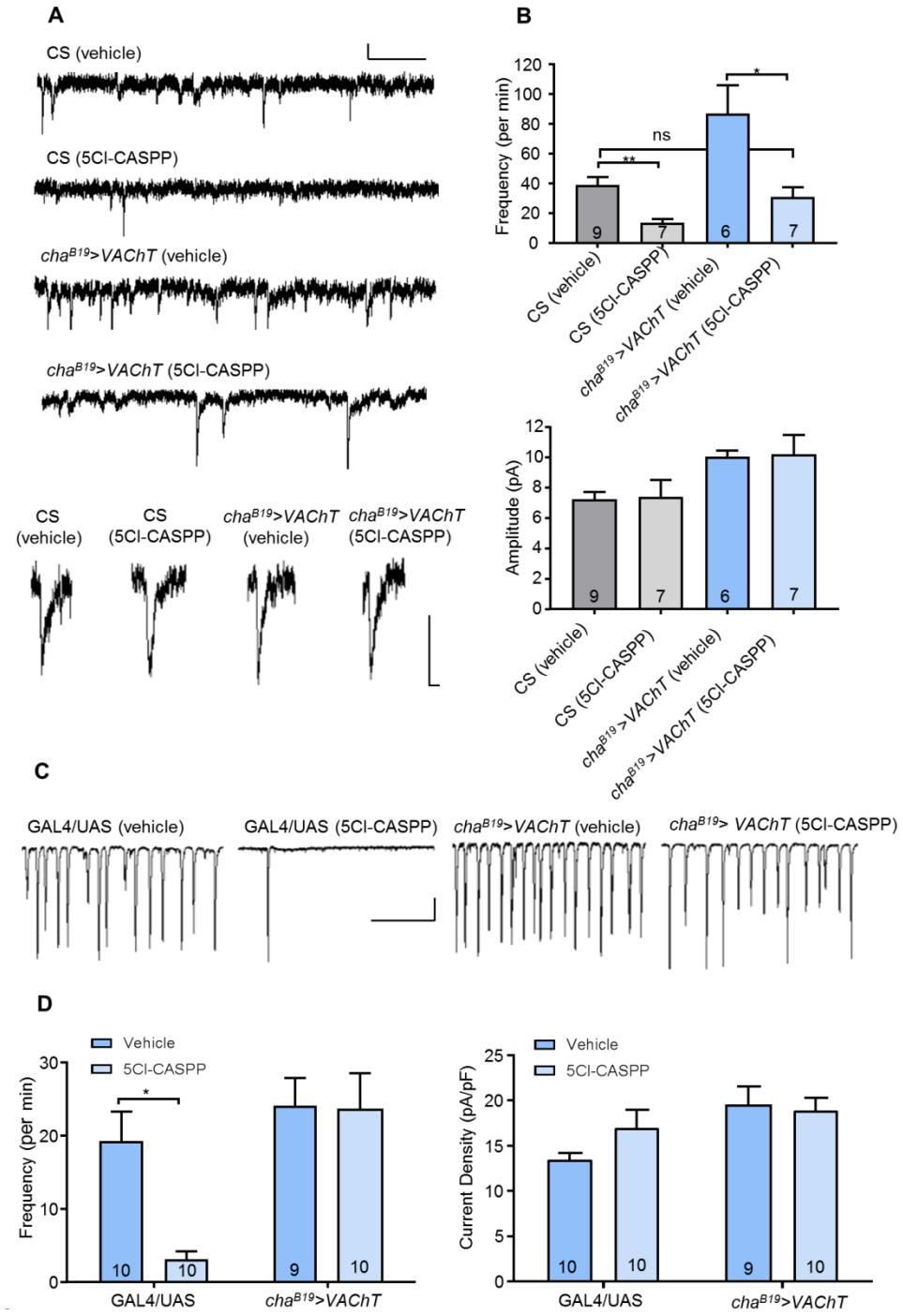

Figure 3.2. *VAChT* level modulates frequency of spontaneous release events. (A) Representative traces of minis recorded from L3 aCC/RP2 in either CS or *cha^{B19}>VAChT* (fed acetone or 10 µg/ml 5Cl-CASPP). Scale Bars (full trace: 10 pA/20 sec, single mini: 5 pA/5 ms) (B) 5Cl-CASPP-dependent down-regulation of *VAChT* activity in CS (grey bars) results in a reduction in mini frequency (38.8 ± 5.6 vs. 13.2 ± 2.9 per minute, vehicle vs. 5Cl-CASPP respectively, P = 2 x 10^{-3}) with no effect on amplitude (P = 0.91). Exposure of a resistant background (blue bars, achieved by up-regulation of *VAChT*: *cha^{B19}>VAChT*)

to 5Cl-CASPP also causes a significant reduction in mini frequency (86.8 ± 19.3 vs. 31.0 ± 6.3 per minute, vehicle vs. 5Cl-CASPP respectively, P = 0.01). However, the reduction in absolute level of mini frequency is to a level not significantly different to CS (treated with vehicle). Exposure of the resistant background to 5Cl-CASPP had no effect on mini amplitude (P = 0.94) (C) Representative traces of SRCs recorded from L3 aCC/RP2 in GAL4/+ and UAS/+ parental stocks and *cha*^{B19}>*VAChT* (fed acetone or 10 µg/ml 5Cl-CASPP). Scale Bar (400pA/20sec). (D) 5Cl-CASPP dramatically reduces SRC frequency in parental controls (19.2 ± 4.1 vs. 3.1 ± 1.1 per min, vehicle vs. 5Cl-CASPP respectively, P = 0.03) but with no effect to amplitude (P = 0.58). The effect of 5Cl-CASPP on SRC frequency is rescued following up-regulation of *VAChT* (24.1 ± 3.8 vs. 23.5 ± 4.9, vehicle vs. 5Cl-CASPP respectively, P = 1) with no obvious effect to amplitude (P = 1). All data points are mean ± sem, n stated in each bar.

Exposure to 5Cl-CASPP also dramatically reduces the frequency of spontaneous rhythmic currents (SRCs), representative of action potential-dependent mass vesicle exocytosis (19.2 ± 4.1 vs. 3.1 ± 1.1 per min, vehicle vs. 5Cl-CASPP respectively, P = 0.03) with no effect on SRC amplitude (P = 0.58, Fig. 3.2C-D). This is suggestive of an inability of the cholinergic premotor interneurons to maintain wildtype evoked SVs release in the presence of 5Cl-CASPP. The lack of effect on SRC amplitude, moreover, suggests that the premotor terminals release a relatively fixed number of SVs per release event: if the required number of 'full' SVs is not available, no evoked release seemingly occurs. The reduction in SRC frequency is rescued by the up-regulation of wildtype *VAChT* (24.1 ± 3.8 vs. 23.5 ± 4.9, vehicle vs. 5Cl-CASPP respectively, P = 1), again with no obvious effect on SRC amplitude (P = 1). Taken together, these data suggest that up-regulation of *VAChT* is sufficient to confer CASPP-resistance through maintenance of cholinergic SV release above a threshold level (approximately equal to that observed in CS/CRISPR control lines).

3.4.3 Expression of *VAChT*^{Y49N} provides resistance to 5Cl-CASPP through heightened SV release

Genomic replacement of *VAChT*^{49Y} by *VAChT*^{49N} increases mini frequency (41.2 ± 6.8 vs. 95.2 ± 19.1 vs. 87.2 ± 13.3 per min, control (CS + CRISPR control combined), *VAChT*$^{Y49N/+}$, *VAChT*$^{Y49N/Y49N}$, respectively, P = 0.02 and 0.04, Fig. 3.3A-B). By contrast, no effect on mini amplitude was observed, either for heterozygous or homozygous *VAChT*^{Y49N} (Fig. 3.3B). The observed resistance to 5Cl-CASPP induced by expression of *VAChT*^{Y49N} may thus be due to the maintenance of cholinergic mini release frequency above a critical threshold value (as described above). To test this, we measured mini frequency and amplitude in the presence of 5Cl-CASPP. As expected, mini frequency was significantly reduced in controls following ingestion of 5Cl-CASPP (10 µg/ml, 38.8 ± 4.2 vs. 14.3 ± 1.8 per min, P = 1 x 10^{-4}, Fig. 3.3C-D). Mini frequency was also significantly reduced in the heterozygous *VAChT*$^{Y49N/+}$ following exposure to 5Cl-CASPP (65.2 ± 10.8 vs. 30.3 ± 4.8 per min, vehicle vs. 5Cl-CASPP respectively, P = 0.01), but to a level that was not significantly different from controls fed vehicle (38.8 ± 4.2 vs. 30.3 ± 4.8 per min, P = 1). Homozygous expression of *VAChT*$^{Y49N/Y49N}$ is, however, sufficient to completely prevent 5Cl-CASPP from reducing mini frequency (69.3 ± 20.5 vs. 61.0 ± 18.1 per min, vehicle vs. 5Cl-CASPP respectively, P = 0.78). No significant change in mini amplitude was observed for any treatment (Fig. 3.3E). These data are consistent with *VAChT*^{Y49N} providing resistance to 5Cl-CASPP through maintenance of a threshold frequency of cholinergic mini release. Moreover, resistance would appear proportional to mini release frequency.

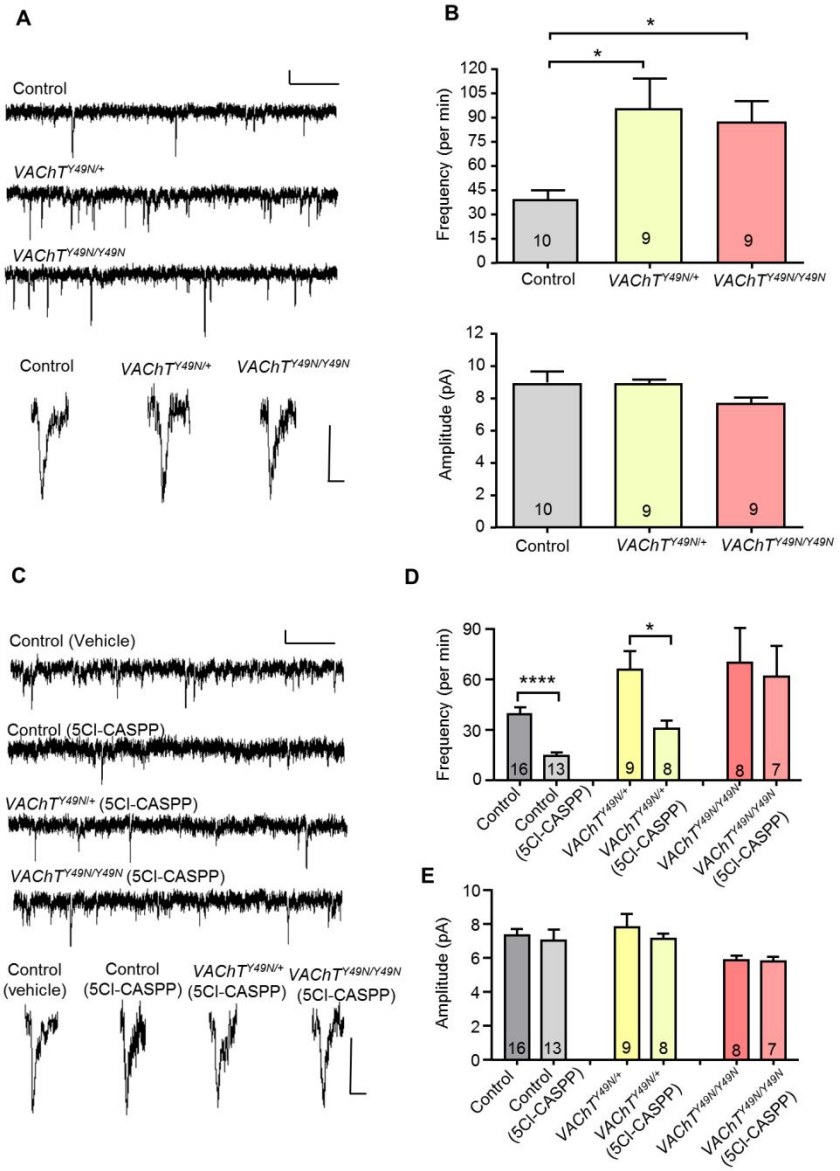

Figure 3.3. *VAChT*^{Y49N} increases mini frequency. (A) Representative traces of cholinergic minis from L3 aCC/RP2 in control (CS + CRISPR control combined, CS presented in trace), *VAChT*$^{Y49N/+}$ and *VAChT*$^{Y49N/Y49N}$ genotypes. Scale Bars (full trace: 10 pA/20 sec, single mini: 5 pA/5 ms). (B) *VAChT*^{Y49N} mutants show a significant increase in mini frequency, compared to control, in both heterozygotes (41.2 ± 6.8 vs. 95.2 ± 19.1 per min, P = 0.02) and homozygotes (87.2 ± 13.3 per min, P = 0.04). However, no effect was observed to mini amplitude (P = 0.32). (C) Representative traces of minis recorded from L3 aCC/RP2 in control (CS and CRISPR control lines combined), *VAChT*$^{Y49N/+}$ and *VAChT*$^{Y49N/Y49N}$ fed either acetone or 10 µg/ml 5Cl-CASPP. Scale Bars (full trace: 10pA/20sec, single mini: 5pA/5ms). (D) Mini frequency in controls is significantly

reduced following ingestion of 10 µg/ml 5Cl-CASPP as opposed to those fed vehicle only (38.8 ± 4.2 vs. 14.3 ± 1.8 per min, vehicle vs. 5Cl-CASPP respectively, P = 1 x 10^{-4}). Mini frequency is also significantly reduced in heterozygous *VAChT*$^{Y49N/+}$ (65.2 ± 10.8 vs. 30.3 ± 4.8 per min, vehicle vs. 5Cl-CASPP respectively, P = 0.01) but to a level that is not significantly different from control values fed vehicle (38.8 ± 4.2 vs. 30.3 ± 4.8 per min, P = 1). Homozygosity of *VAChT*$^{Y49N/Y49N}$ is sufficient to completely prevent 5Cl-CASPP reducing mini frequency (69.3 ± 20.5 vs. 61.0 ± 18.1 per min, vehicle vs. 5Cl-CASPP respectively, P = 0.78). (E) No significant change in mini amplitude was recorded for control (P = 0.67) *VAChT*$^{Y49N/+}$ (P = 0.49) or *VAChT*$^{Y49N/Y49N}$ (P = 0.82). All data points are mean ± sem, n stated in each bar.

3.4.4 Expression of Sytx$^{3\text{-}69}$ or cpx^{SH1} fails to provide resistance to 5Cl-CASPP

To validate the hypothesis that spontaneous release frequency dictates resistance to 5Cl-CASPP, we identified two additional genetic approaches reported to elevate glutamatergic minis at the *Drosophila* NMJ. Larval mortality assays and mini recordings from aCC/RP2 were conducted following expression of *sytx*$^{3\text{-}69}$ or in a *complexin* null mutant, *cpx*^{SH1} (Huntwork and Littleton, 2007, Lagow et al., 2007).

Expression of *sytx*$^{3\text{-}69}$ in cholinergic premotor interneurons (*cha*^{B19}>*sytx*$^{3\text{-}69}$) dramatically increased mini frequency in aCC/RP2 (43.0 ± 15.9 vs. 489.8 ± 115.1 per min, GAL4/+ vs. *cha*^{B19}>*sytx*$^{3\text{-}69}$ respectively, P = 5 x 10^{-3}). In agreement with previous data, exposure to 5Cl-CASPP significantly reduced mini frequency in this genotype (489.8 ± 115.1 vs. 201.4 ± 45.1 per min, vehicle vs. 5Cl-CASPP respectively, P = 0.02), but to a final level ~4.5-fold greater than controls. However, expression of *sytx*$^{3\text{-}69}$ afforded no resistance to 5Cl-CASPP. Observed LD_{50} values to CASPP were: 3.8 ± 0.5, 2.6 ± 0.3 vs. 2.4 ± 0.4 µg/ml, +/*cha*^{B19}, +/*sytx*$^{3\text{-}69}$ vs. *cha*^{B19}> *sytx*$^{3\text{-}69}$ respectively, P = 0.07, Fig. 3.4A).

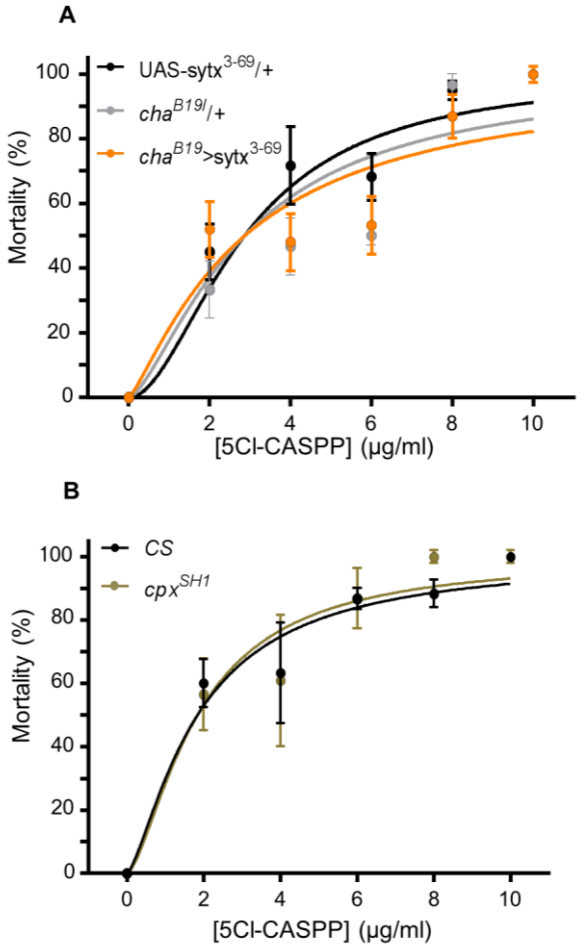

Figure 3.4. Alternative routes that maintain mini release fail to provide resistance to 5Cl-CASPP. (A) Expression of *sytx*$^{3-69}$ in cholinergic neurons is sufficient to increase mini frequency (see text) but does not afford resistance to 5Cl-CASPP. The observed LD_{50} values were: 3.8 ± 0.5, 2.6 ± 0.3 vs. 2.4 ± 0.4 µg/ml, +/*cha*^{B19} (n = 60 larvae tested per concentration), +/*sytx*$^{3-69}$ (n = 60 per concentration) vs. *cha*^{B19}> *sytx*$^{3-69}$ (n = 80 per concentration) respectively, P = 0.07). (B) The *cpx*^{SH1} mutant similarly has no resistance to 5Cl-CASPP. Observed LD_{50} values in this case were: 1.7 ± 0.2 vs. 2.0 ± 0.3, CS vs. *cpx*^{SH1} respectively, n = 60 per concentration, P = 0.73). All data points shown are mean ± sem.

The *complexin* null mutant (*cpx*^{SH1}) similarly increased mini release compared to that observed in CS wildtype (43.3 ± 7.2 vs. 100.4 ± 13.5 per min, CS vs. *cpx*^{SH1} respectively, P = 4 x 10^{-3}). Interestingly, 5Cl-CASPP did not significantly reduce mini frequency in this mutant (100.4 ± 13.5 vs. 81.9 ± 17.7 per min, vehicle vs. 5Cl-CASPP respectively, P =

0.58). Moreover, despite the apparent maintenance of heightened mini release, this did not precipitate any obvious effect to larval survival when challenged with 5Cl-CASPP. Observed LD_{50} values were: 1.7 ± 0.2 vs. 2.0 ± 0.3 µg/ml, CS vs. cpx^{SH1} respectively, P = 0.73, Fig. 3.4B). These data suggest that although a reduction in spontaneous mini frequency is correlated with CASPP-induced toxicity, maintenance of this mode of synaptic release does not confer resistance. We therefore looked towards how $VAChT^{Y49N}$ resistance to CASPP affects action potential-evoked activity (i.e. SRCs).

3.4.5 $VAChT^{Y49N}$ disrupts rhythmicity of cholinergic circuits

To assess how $VAChT^{Y49N}$ influenced motoneuron activity, we examined endogenous bursting activity (as measured by loose patch) of aCC/RP2 motoneurons. The advantage of loose patch is that the interior of the cell is not affected (the membrane remains intact). We measured both frequency of bursts and the number of individual action potentials (APs) per burst. Previous work has shown that a single SRC gives rise to a sustained depolarization (burst) that elicits multiple APs in motoneurons (Baines et al., 2001). Thus, burst frequency represents the evoked release of ACh from premotor interneurons, whilst APs fired is a postsynaptic property of the motoneurons. CS larvae exhibited 27.9 ± 7.5 bursts per minute, with an average of 15.0 ± 1.8 APs per burst. By contrast, $VAChT^{Y49N/Y49N}$ showed significantly reduced burst frequency (9.0 ± 4.2 per min, P=0.04). This is predictive of a decreased ability of the premotor interneurons to maintain a normal synaptic output. However, APs per burst remained constant (12.8 ± 3.0 spikes per burst, P=0.54) indicative that the postsynaptic motoneuron is not affected. Thus, despite an increase in spontaneous mini release (cf. Fig 3B), these data show that the $VAChT^{Y49N}$ point mutation does not support 'normal' presynaptic cholinergic input to motoneurons which, in turn, disrupts motoneuron burst frequency. However, the number of APs fired by motoneurons per burst is unaffected.

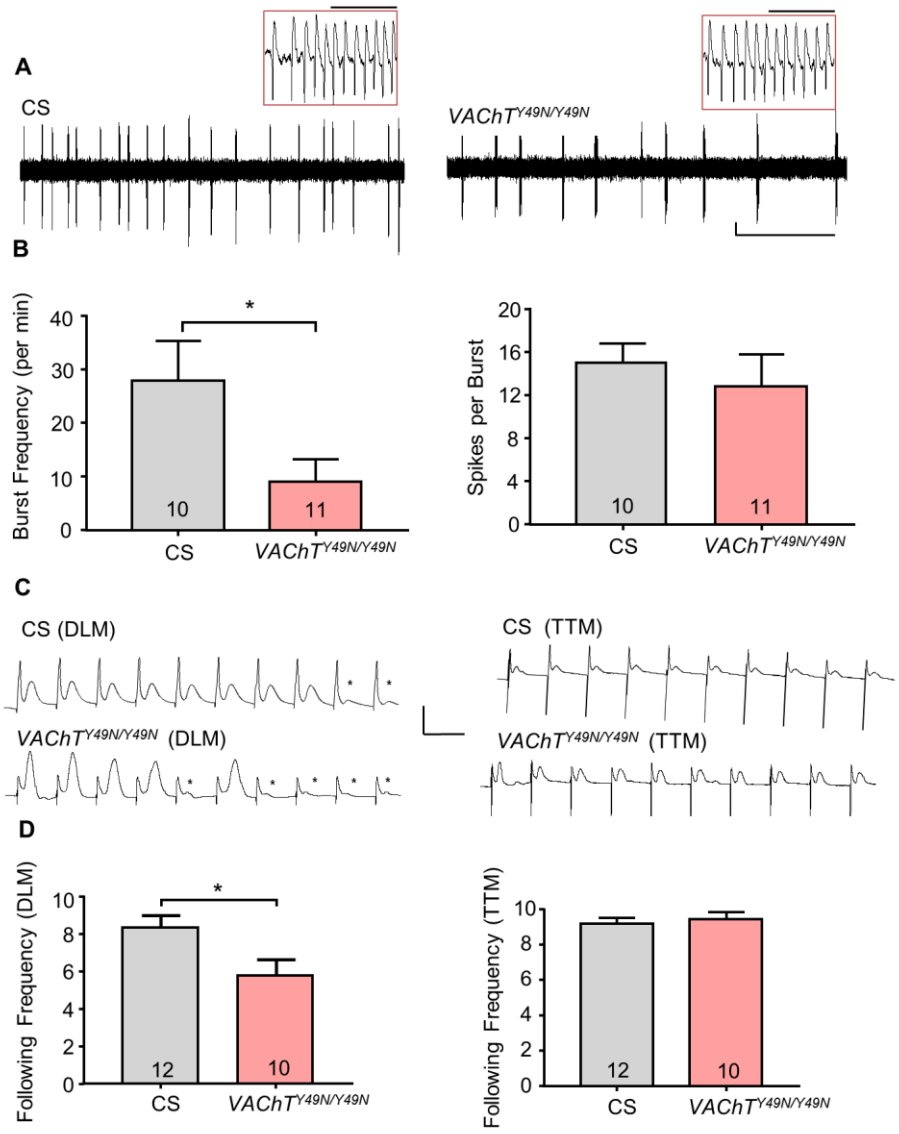

Figure 3.5. *VAChT*^{Y49N}disrupts cholinergic synaptic inputs to motoneurons. (A) Representative traces of extracellular bursting activity recorded from L3 aCC/RP2 in CS or *VAChT*$^{Y49N/Y49N}$. Scale Bar (1 mV/15 sec). A single burst is also shown at an expanded time scale for each recording, inset: 50ms. (B) *VAChT*$^{Y49N/Y49N}$ show a significant reduction in endogenous bursting (27.9 ± 7.5 vs. 9.0 ± 4.2 per min, CS vs. *VAChT*$^{Y49N/Y49N}$ respectively, P = 0.04). However, number of spikes per burst remains consistent (15.0 ± 1.8 vs. 12.8 ± 3.0 spikes per burst, P = 0.54). (C) Representative traces of adult GFS recordings from DLM/TTM in either CS or *VAChT*$^{Y49N/Y49N}$. Scale Bar (30 mV/10 ms). (D) During high frequency stimulation (100Hz), the DLM in *VAChT*$^{Y49N/Y49N}$ are less able to follow a train of 10 stimuli (8.3 ± 0.7 vs. 5.8 ± 0.9, CS vs. *VAChT*$^{Y49N/Y49N}$ respectively, P = 0.03). Dots show synaptic failures. The TTM remains unaffected (9.2 ± 0.3 vs. 9.4 ± 0.4

CS vs. *VAChT*$^{Y49N/Y49N}$ respectively, P = 0.60). All data points are mean ± sem, n stated in each bar.

We next asked whether changes to evoked cholinergic synaptic release are observable in other cholinergic neural circuits. We used the adult giant fibre system (GFS). The physiological output from stimulation of the adult GF is muscular contraction of both the tergotrochanteral muscle (TTM) and the dorsal longitudinal flight muscle (DLM) (King and Wyman, 1980). Although both DLMs and TTMs are directly innervated by glutamatergic synapses, TTM motoneurons are excited via both cholinergic and electrical synapses, whereas DLM motoneurons are excited solely by cholinergic synapses. We find that, during high frequency stimulation (100 Hz), the DLM of *VAChT*^{Y49N} is less able to follow a train of 10 stimuli (8.3 ± 0.7 vs. 5.8 ± 0.9, CS vs. *VAChT*^{Y49N} respectively, P = 0.03, Fig. 3.5C-D). The TTM, by contrast, which has additional electrical synapses, remains unaffected (9.2 ± 0.3 vs. 9.4 ± 0.4 CS vs. *VAChT*^{Y49N} respectively, P = 0.60). These data further support the hypothesis that the *VAChT*^{Y49N} mutation disrupts the ability of cholinergic neurons to maintain sustained evoked release.

3.4.6 The *VAChT*^{Y49N} resistance mutation disrupts evoked vesicle release

A reduction in burst frequency of aCC/RP2 in homozygous *VAChT*^{Y49N} is indicative of an inability to maintain a normal presynaptic cholinergic release. In order to address this question, we tested the ability of motoneurons to follow prolonged stimulation of premotor cholinergic interneurons. We used the blue light-sensitive *ChR* variant, *UAS-ChR*^{ChETA}, expressed in all cholinergic neurons (*ChAT*^{BAC} GAL4), to allow us to stimulate presynaptic activity. Long term stimulation at 1Hz in control lines (CS + CRISPR control)

or *VAChT*$^{Y49N/+}$ resulted in a gradual decline in evoked EPSC amplitude (these EPSPs are equivalent to SRC's but are evoked by optogenetic stimulation). Full failure of transmission occurred at 25.1 ± 1.6 vs. 28.7 ± 2.9 min (control vs. *VAChT*$^{Y49N/+}$, P = 1, Fig. 3.6A-B). By contrast, EPSC amplitude falls off dramatically after the first stimulation in homozygous *VAChT*^{Y49N} (failure of transmission occurring at 2.9 ± 1.3 min, P = 3 x 10^{-4}). A reduction in successive EPSC amplitude is clearly observable between the 1st and 2nd induced EPSCs, which is significantly greater in *VAChT*$^{Y49N/Y49N}$ (90.4 ± 6.5 vs. 52.0 ± 10.6%, control vs. *VAChT*$^{Y49N/Y49N}$ respectively, P = 2 x 10^{-3}). Thus, although the amplitude of the first EPSC is not different, the ability to support a full-size second EPSC is significantly compromised in *VAChT*^{Y49N}. Figure 6C displays ratio (%) of EPSC amplitude difference (2/1) at time intervals 0.1, 1, 2 and 8 seconds following initial stimulation. Regression analysis suggests the minimum time interval required between successive stimulations to generate a second full size EPSC in *VAChT*$^{Y49N/Y49N}$ is approximately doubled compared with control lines (2.4 vs. 4.8 s, control vs. *VAChT*$^{Y49N/Y49N}$ respectively). This is entirely consistent with the reduced frequency of burst activity recorded in these same motoneurons by loose-patch (c.f. Fig. 3.5A-B).

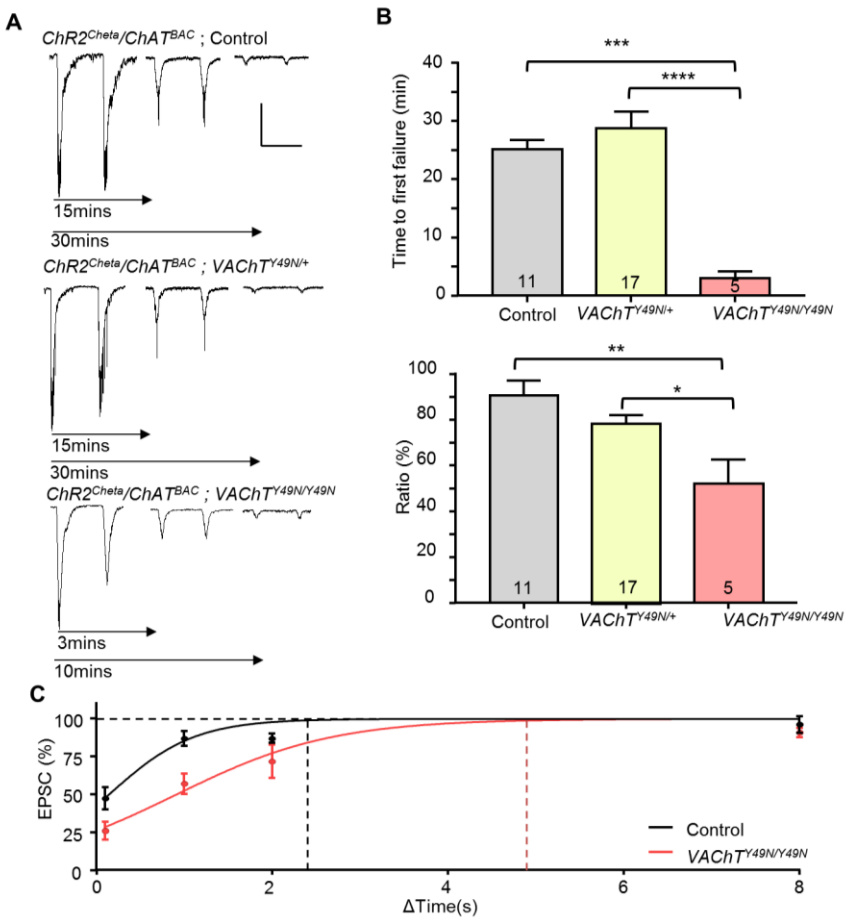

Figure 3.6. *VAChT*^{Y49N} disrupts evoked cholinergic release (A) Representative traces of ChR-activated EPSCs recorded from L3 aCC/RP2 in control, *VAChT*$^{Y49N/+}$ and *VAChT*$^{Y49N/Y49N}$. Scale Bar (100 pA/1 sec) (B) At a stimulation frequency of 1 Hz, homozygous *VAChT*$^{Y49N/Y49N}$ mutants show a significantly reduced time until first synaptic failure compared to controls (25.1 ± 1.6 vs. 0.9 ± 0.4 minutes, control vs. *VAChT*$^{Y49N/Y49N}$ respectively, P = 2 x 10^{-3}). This phenotype is absent in the heterozygote (25.1 ± 1.6 vs. 28.7 ± 2.9 minutes, control vs. *VAChT*$^{Y49N/+}$, P = 1). The ratio change in current density between the 1st and 2nd EPSC is also significantly reduced (90.4 ± 6.5 vs. 48.1 ± 17.8%, control vs. *VAChT*$^{Y49N/Y49N}$ respectively, P = 0.02). (C) Percentage (2/1) EPSC amplitude at time intervals 0.1, 1, 2 and 8 seconds following initial stimulation between control (n = 7, 16, 5, 5 respectively) and *VAChT*$^{Y49N/Y49N}$ (n = 10, 10, 5, 5 respectively). The minimum time interval required between successive stimulations to generate a second full size EPSC at 100% in *VAChT*$^{Y49N/Y49N}$ is approximately doubled compared with control lines (2.4 vs. 4.8 s, control vs. *VAChT*$^{Y49N/Y49N}$ respectively). All data points are mean ± sem, n stated in each bar.

3.4.7 Insecticide resistance and other measures of fitness

We have shown that *VAChT*^{Y49N} perturbs endogenous cholinergic activity. Given the reliance on this neurotransmitter for locomotion, a significant change in behaviour might be expected. We therefore examined larval crawling behaviour. A low 5Cl-CASPP treatment of 5µg/ml was used for crawling assays in order to prevent complete paralysis (observed in control lines at higher CASPP exposure). We found that 5Cl-CASPP treatment of control (CS + CRISPR control) larvae significantly reduced total distance travelled (116.5 ± 8.5 vs. 78.6 ± 12.1 mm, control: vehicle vs. 5Cl-CASPP respectively, P = 0.04, Fig 7A). The presence of *VAChT*^{Y49N} similarly reduces larval total distance (116.5 ± 8.5 vs. 72.7 ± 8.3 mm, vehicle: control vs. *VAChT*$^{Y49N/Y49N}$ respectively, P = 2 x 10^{-3}, Fig. 3.7A). However, *VAChT*^{Y49N} larvae were not further affected when fed 5Cl-CASPP (72.7 ± 8.3 vs. 68.3 ± 7.1 mm, *VAChT*$^{Y49N/Y49N}$, vehicle vs. 5Cl-CASPP respectively, P = 1, Fig. 3.7A).

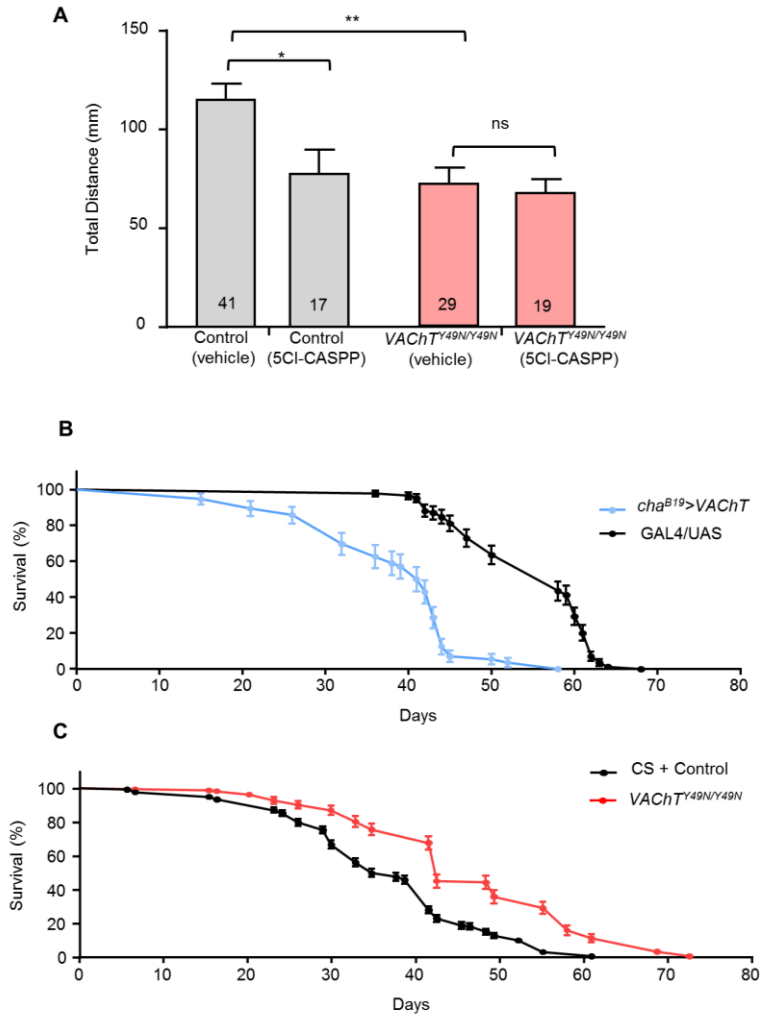

Figure 3.7. *VAChT*^{Y49N} disrupts larval locomotion. (A) 5Cl-CASPP treatment (5 µg/ml) significantly reduces total distance moved (116.5 ± 8.5 vs. 78.6 ± 12.1 mm, control: vehicle vs. 5Cl-CASPP respectively, P = 0.04) in control L3. Reduced distance (116.5 ± 8.5 vs. 72.7 ± 8.3 mm, vehicle: control vs. *VAChT*$^{Y49N/Y49N}$ respectively, P = 2 x 10^{-3}) was also observed in *VAChT*^{Y49N} (0.65 ± 0.05 vs. 0.41 ± 0.05 mm/s, P = 2 x 10^{-3}) in the absence of treatment. However, exposure of *VAChT*^{Y49NY49N} to 5Cl-CASPP does not further affect locomotion (72.7 ± 8.3 vs. 68.3 ± 7.1 mm, *VAChT*$^{Y49N/Y49N}$: vehicle vs. 5Cl-CASPP respectively, P = 1). (B) Transgenic overexpression of *VAChT* (*cha*^{B19}*>VAChT,* light blue*)* elicits a reduction in adult longevity (median survival: 41.5 vs. 58 days, *cha*^{B19}*>VAChT* (n = 56) vs. GAL4/UAS (n = 85) respectively, P = 1 x 10^{-4}). (C) Homozygous *VAChT*^{Y49N} (red) adults show increased longevity (median survival: 36.0 vs. 44.0 days, merged controls (CS + CRISPR control) (n = 400) vs. *VAChT*$^{Y49N/Y49N}$ (n = 150) respectively,

P = 1 x 10^{-4}). All data points are mean ± sem, n stated in each bar or given as individual data points.

Transgenic overexpression of wildtype *VAChT* (*cha^{B19}>VAChT*) elicits a dramatic reduction in adult longevity (median survival: 58.0 vs. 41.5 days, GAL4/UAS vs. *cha^{B19}>VAChT* respectively, P = 1 x 10^{-3}, Fig. 3.7B). The associated hazard ratio of 4.06 indicates that overexpression of *VAChT* results in a 4-fold reduction in survival probability, at any point throughout the longevity assay. Conversely, fly lines homozygous for *VAChT^{Y49N}* exhibit increased longevity (median survival: 36.0 vs. 44.0 days, control vs. *VAChT$^{Y49N/Y49N}$* respectively, P = 1 x 10^{-3}, Fig. 3.7C). In this experiment control lines suffered a hazard ratio of 2.4 relative to *VAChT^{Y49N}*. CS and CRISPR control fly lines did not differ in longevity (median survival: 43.0 vs. 34.0 days, CS vs. CRISPR control respectively, P = 0.07, Fig. 3.7C) and were therefore combined for comparison to *VAChT$^{Y49N/Y49N}$*.

Finally, we measured fecundity in the form of oviposition rate of newly-eclosed mated females. Average oviposition per female remained remarkably similar between all genotypes in either *VAChT* up-regulation (40.7 ± 5.6 vs. 31.2 ± 5.4, GAL4/UAS vs. *cha^{B19}>VAChT* respectively, P = 0.26) or *VAChT$^{Y49N/Y49N}$* (34.2 ± 4.1 vs 33.2 ± 6.6, control vs. *VAChT$^{Y49N/Y49N}$* respectively, P = 0.90).

3.5 Discussion

We report neurophysiological consequences resulting from two potential mechanisms of CASPP-resistance. Resistance obtained through *VAChT* up-regulation correlates to an increase in the availability and/or probability of SV release and not through alteration of the amount of neurotransmitter loaded per vesicle (i.e. quantal size). The lower

bounds of sustainable activity appear to be dictated by a minimum threshold for release frequency, below which normal cholinergic release is unsustainable and the likelihood of mortality increases. However, resistance associated through the second route, endogenous expression of the point mutation *VAChT*^{Y49N}, although showing a similar spontaneous release profile, further uncovers significant deficiencies in evoked neurotransmitter release. We attribute this to an inability of the point mutation to maintain sustained evoked SV release, perhaps indicative of a fitness trade-off between protein functionality and insecticide resistance.

Insecticide resistance alleles commonly produce negative effects on multiple life-traits (including larval development, sex ratio, oviposition/fecundity, mass, embryonic viability and adult longevity) (Jaramillo-O et al., 2014, Li et al., 2002, Martins et al., 2012) and in some cases these are proportional to resistance level (Martins et al., 2012). However, exceptions have been reported suggesting that interactions between resistance modality and target protein functionality dictate complex life-traits (Belinato et al., 2012). We show in this study that although resistance may be attained through *VAChT* up-regulation, adult longevity is reduced. Reduced lifespan is also associated with transgenic up-regulation of *VGLUT*, where adult male longevity is reduced by >50% (Daniels et al., 2011). *VGLUT* mediated excitotoxicity and neurodegeneration may result from increased quantal size (i.e. excess glutamate release) (Daniels et al., 2004, Daniels et al., 2011). Although similar post-synaptic degeneration may occur in central cholinergic neurons following up-regulation of *VAChT*, the degree of excitotoxicity is predicted to be lower due to the inability of this transporter to affect quantal size (only affecting release frequency) (Cash et al., 2015). Following a similar logic, the reduced evoked release of SVs (i.e. SRCs) in *VAChT*^{Y49N} may underlie the increased longevity observed in this genotype; reduced transmission being protective.

The inability to influence quantal size, at central cholinergic synapses, through up-regulation of *VAChT* is indicative that vesicle-loading obeys the proposed "set-point" SV loading model (Cash et al., 2015, Williams, 1997). This model dictates that the level to which SVs are filled is pre-set and, thus, cannot be influenced through an increased loading rate (which might be expected following increased transporter expression). Although several other studies are in agreement with this conclusion (Parsons et al., 1999, Cash et al., 2015), similar studies at cholinergic mouse, rat and nematode NMJ link genetic and pharmacological modulation of *VAChT* activity with corresponding changes in quantal size, conforming to the steady-state SV filling model (Prado et al., 2006, Lima et al., 2010, Searl et al., 1991, Costa et al., 2017). Furthermore, increased *VGLUT* at glutamatergic synapses at the *Drosophila* NMJ is sufficient to increase quantal size through the manipulation of vesicle size (Daniels et al., 2004), an effect also not observed following up-regulation of *VAChT* expression (Cash et al., 2015). Collectively, these studies are indicative of a significant difference between SV loading at central vs. peripheral synapses in *Drosophila* larvae and perhaps more generally. However, additional studies will be required to validate this hypothesis.

Our findings in this study are indicative of a direct relationship between SV release probability and pharmacological and/or genetic regulation of *VAChT*. Our data suggest, moreover, that block of *VAChT* through CASPP results in a reduction in SV release frequency. This agrees with previously published data (Cash et al., 2015) and correlates with CASPP lethality (Sluder et al., 2012). Up-regulation of *VAChT* or expression of $VAChT^{Y49N}$ mediates resistance to CASPP, an effect that is associated with the maintenance of spontaneous SV release above a critical threshold. The resistance effect of up-regulation of wildtype *VAChT* could be simply explained by an increase in the number of vesicles that escape block of *VAChT* by CASPP and are thus able to reach

set-point. The resistance effect of replacing the wildtype *VAChT* with the Y49N mutant form however, might be explained by a combination of different factors: Expression of *VAChT*^{Y49N} may confer resistance to CASPP because binding of the insecticide to the transporter is prevented, because binding of CASPP to *VAChT*^{Y49N} no longer prevents ACh transport and therefore does not critically reduce the number of vesicles reaching set point, and/or because binding and inhibition of *VAChT*^{Y49N} function by CASPP is compensated by an increased release probability conferred by the Y49N mutation. Further experiments would be required to confirm or rule out the individual contributions of these factors.

The expression of *VAChT*^{Y49N} additionally disrupts the ability of the cholinergic system to maintain sustained evoked release. This is evidenced by a reduction in frequency of endogenous bursts of AP firing in motoneurons and by a failure of the DLM to follow high frequency stimulation. The mechanism underlying this may be heightened spontaneous mini release, which in turn reduces the pool of SVs available for evoked release. This conclusion is in agreement with work at the glutamatergic *Drosophila* NMJ which reports *complexin* null mutants display a reduction in EPSPs (equivalent of SRCs) together with increased mini frequency (Huntwork and Littleton, 2007). However, the syntaxin mutant (*syx*$^{3\text{-}69}$) and a SNAP-25 mutant (*SNAP25*^{ts}) maintain higher mini frequency together with EPSPs that are increased in amplitude (Lagow et al., 2007, Rao et al., 2001).

CRISPR-dependent expression of *VAChT*^{Y49N} is sufficient to increase frequency of minis and, also, to prevent a normal pattern of evoked release of ACh from premotor cholinergic interneurons. Only the former results following the up-regulation of wildtype *VAChT* level. In addition to suggesting that the contribution of this transporter

to spontaneous and evoked release may be separable, it identifies a region of the transporter that is seemingly required for sustained evoked release. The *VAChT*^{Y49N} mutation disrupts a region resembling the well-characterized trafficking motif YXXØ (with Ø being any large hydrophobic amino acid): specifically causing a YMVI to NMVI mutation. This motif, amongst others (e.g. YNYY in mammals) is known to be involved in protein sorting, the Y residue being highlighted as the most critical determinant (Bonifacino and Traub, 2003). The positioning of this signal on a cytosolic region of *VAChT* indicates that this region could potentially be involved in trafficking. Disruption of the YNYY motif in mammalian *VAChT* is sufficient to cause mis-localisation and retention of the transporter to the plasma membrane (Kim and Hersh, 2004, Colgan et al., 2007). Whilst mis-localisation or membrane retention of *VAChT* may be sufficient to perturb sustained evoked release, it does not offer a plausible explanation why spontaneous vesicle release is increased in these mutants and following up-regulation of wildtype *VAChT*. It is notable in this regard that a glycine-to-arginine substitution at position 347 (G347R) disrupts a reported *VAChT*-synaptobrevin interaction in *C. elegans* that impacts SV release probability (Sandoval et al., 2006). Glycine is conserved in *Drosophila VAChT* at position 342 suggesting a potential similar involvement in the SNARE assemblage.

Up-regulation of genes relating to insecticide detoxification (e.g. glutathione S-transferase and cytochromes P450s) is a common form of insecticide resistance (Oakeshott et al., 2005, Ranson and Hemingway, 2005, Feyereisen, 2012, Feyereisen et al., 2015). Natural expressional modification of target proteins (expression level or mutation) are rarer but have been found to confer resistance in other cholinergic targets. For example, up-regulation of acetylcholinesterase (*ace-1)* is reported in organophosphate and pyrethroid resistant field populations in the spider mite

(Tetranychus evansi) (Carvalho et al., 2012) in addition to gene duplication of *ace*-1 in mosquito (*Culex pipiens*) (Labbé et al., 2007). This study shows that expressional modification of a target protein (*VAChT*) or the acquisition of a point-mutation (Y49N) is sufficient to confer resistance to CASPP. However, the presence of the Y49N mutation significantly perturbs evoked SV release indicative that this allele would not provide a fitness-advantage for insects in the field. This mutation affects a characterized motif in *VAChT* (YMVI) that is seemingly critical for high frequency SV evoked release. Further characterisation of this motif may provide a better understanding of how this transporter contributes to evoked synaptic release, but may also identify a novel target for insecticidal attack.

3.6 Acknowledgements

We thank members of the Baines group and Syngenta (Jealotts Hill International Research Centre) for their help and advice in completing this study. We also thank colleagues for provision of fly stocks (Steve Stowers, Bing Zhang and Troy Littleton). This work was supported by a Biotechnology and Biological Sciences Research Council (BBSRC) CASE studentship to SWV and by a BBSRC project grant to RAB (BB/L027690/1). Work on this project benefited from the Manchester Fly Facility, established through funds from University and the Wellcome Trust (087742/Z/08/Z). The funders had no role in study design, data collection and analysis, decision to publish, or preparation of the manuscript.

3.7 Appendix 2

3.7.1 The presence of background wild type *VAChT* rescues the effect of *VAChT*^{Y49N}

In order to distinguish any obvious changes to cholinergic physiology when the *VAChT*^{Y49N} mutation is up-regulated, both mini and SRC recordings were conducted from the aCC and RP2 motor using the GAL4/UAS system to overexpress *VAChT*^{Y49N} in cholinergic neurons (*cha*^{B19}).

Figure 3.8 suggests that there are no significant change to mini amplitude (8.05 ± 0.39 vs. 9.81 ± 1.14 pA, GAL4/UAS vs. *cha*^{B19}>*VAChT*^{Y49N} respectively, P = 0.15, Fig 3.8A-B) or frequency (33.39 ± 5.23 vs.44.80 ± 8.77 per min, P = 0.27). Furthermore, there remains no observable change to SRC properties in amplitude (14.06 ± 1.03 vs. 14.89 ± 1.17 pA/pF, GAL4/UAS vs. *cha*^{B19}>*VAChT*^{Y49N} respectively, P = 0.61, Fig. 3.8C-D), duration (528.87 ± 44.23 vs. 528.53 ± 16.99 ms, P = 1) or frequency (22.67 ± 4.21 vs. 23.94 ± 4.72 per min, P = 0.85).

These data suggest there is no obvious change to cholinergic release when the Y49N mutation is up-regulated. We attribute this to the presence of the wildtype VAChT present in the genetic background. This is contradictory to results in Chapter 3 and suggests that the *VAChT*^{Y49N} mutation can be rescued by the presence of endogenous *VAChT* or by an increase in the amount of VAChT^{Y49N} at the synapse.

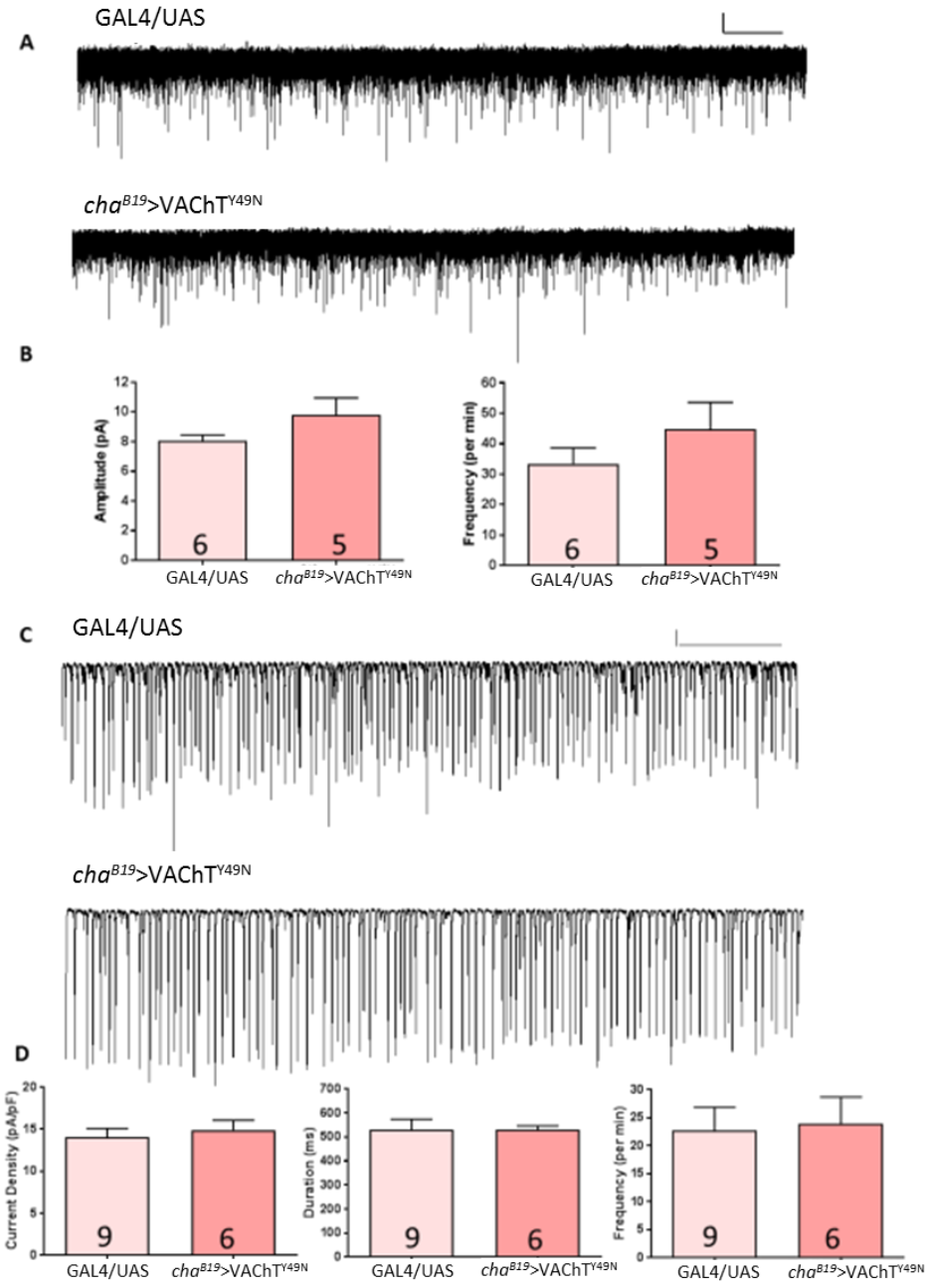

Figure 3.8. Transgenic up-regulation of *VAChT*^{Y49N} shows no obvious implications to cholinergic physiology in the CNS. (A) Representative mini traces of control (GAL4/UAS) and experimental lines (*cha*^{B19}*>VAChT*^{Y49N}). Scale bar (5 pA/ 10sec) (B) no significant change in mini amplitude (P = 0.15) or frequency (P = 0.27). (C) Representative SRC traces of control (GAL4/UAS) and experimental lines (*cha*^{B19}*>VAChT*^{Y49N}) and (D) no observable change to SRC properties in amplitude (P = 0.61), duration (P = 1) or frequency (P = 0.85).

A poly-glutamine region in the *Drosophila* vesicular acetylcholine transporter dictates fill-level of cholinergic synaptic vesicles

Samuel W. Vernon[1], Jim Goodchild[2] and Richard A. Baines[1*]

[1]Division of Neuroscience and Experimental Psychology, School of Biological Sciences, Faculty of Biology, Medicine and Health, University of Manchester, Manchester Academic Health Science Centre, Manchester, M13 9PL, UK. [2]Syngenta Crop Protection Research, Bracknell, Berkshire, UK.

Reference:

Vernon, S. W., Goodchild, J., & Baines, R. A. (2018). A poly-glutamine region in the *Drosophila* vesicular acetylcholine transporter dictates fill-level of cholinergic synaptic vesicles. *Journal of Neuroscience* (in preparation)

4.0 Statement of Contribution.

SV conducted, analysed and interpreted all experiments. SV wrote manuscript with assistance of RAB and JG. Modifications to the text is made in order to incorporate the further relevant data conducted during this project presented in Appendix 3 (section 4.7) and for stylistic consistency for the purpose of this thesis.

4.1 Abstract

Whilst the primary role of vesicular transporters is to load neurotransmitters into synaptic vesicles, accumulating evidence suggests that these proteins also contribute to additional aspects of synaptic function, including vesicle release. In this study, we extend the role of the vesicular acetylcholine transporter (*VAChT*) to include dictating the maximum fill level of synaptic vesicles. We report that manipulation of a C-terminal poly-glutamine (polyQ) region in the *Drosophila VAChT* is sufficient to influence transmitter content and release frequency of cholinergic vesicles from the terminals of premotor interneurons. Specifically, we find that reduction of the polyQ region, by one glutamine residue (*13Q to 12Q*), results in a significant increase in both amplitude and frequency of spontaneous cholinergic mEPSCs recorded in the aCC and RP2 motoneurons. Moreover, this truncation also results in evoked synaptic currents that show increased duration, indicative of increased ACh release. By contrast, extension of the polyQ region by one additional glutamine (*13Q to 14Q*) is sufficient to reduce mEPSC amplitude and frequency and, moreover, prevents evoked synaptic vesicle release. Finally, a complete deletion of the PolyQ region (13Q to 0Q) has no obvious effects on mEPSCs, but again evoked synaptic currents show increased duration. The mechanisms that ensure synaptic vesicles are filled to physiologically-appropriate levels remain unknown. Our study identifies the polyQ region of the insect *VAChT* to be required for correct vesicle transmitter loading and, thus, provides opportunity to increase understanding of this critical aspect of neurotransmission.

4.2 Significance Statement

Neurotransmitter-loading of synaptic vesicles is tightly regulated and underpins the quantal theory of neurotransmission. However, although observed at every synapse studied, the mechanistic basis that ensures vesicle-filling stops at a fixed, pre-determined, level remains poorly understood. In this study we identify a C-terminal poly-glutamine region in the *Drosophila VAChT* as critical for vesicle-loading of ACh. Reduction or extension of this region, by just one glutamine residue, is sufficient to increase or decrease, respectively, the amount of ACh loaded. Our work significantly advances the field of synaptic physiology by identifying a region of a vesicular transporter that regulates the extent to which synaptic vesicles are filled.

4.3 Introduction

Vesicular loading of synaptic vesicles (SV) is dependent on initial acidification mediated by the vATPase pump. This pump generates both a pH gradient (ΔpH) and a voltage gradient (Δψ) across the SV membrane (Takamori, 2016, Edwards, 2007). The relative requirement for these two components for loading is dependent on neurotransmitter: anionic transmitters such as glutamate rely more heavily on Δψ (Maycox et al., 1988, Takamori, 2016, Schenck et al., 2009). Zwitterionic transmitters require both gradients (Takamori, 2016, Edwards, 2007), whereas, cationic transmitters (e.g. ACh) rely predominantly on ΔpH (Parsons, 2000, Parsons et al., 1993, Takamori, 2016). Transport of ACh into a SV involves the exchange of two protons in an antiporter system using the proton-electrochemical gradient (Südhof, 2004, Lawal and Krantz, 2013). The current model suggests that one proton is used to transport ACh into the SV lumen whilst the second proton is needed to re-orientate the *VAChT* substrate binding site back towards the cytoplasm ($2H^+$ for $1ACh^+$) (Parsons, 2000). *In situ*, acidified vesicles exhibit a pH approximately 1.4 units less than un-acidified vesicles (Parsons, 2000). Theoretically, the cholinergic SV lumen has the capacity to concentrate ACh by 100-fold relative to cytoplasmic levels (which range between 1-4mM) (Parsons et al., 1993, Parsons, 2000). However, the maximal reported accumulation of ACh in SV has been found to saturate at ~4 mM suggesting a rather dramatic (and unknown) limiting factor impedes loading (Parsons et al., 1993, Parsons, 2000, Varoqui and Erickson, 1996).

A key limiting factor may be copy number of functional transporter per SV. Murine and *Drosophila* NMJ and mammalian cell culture models suggests vesicular loading is altered following either genetic and/or pharmacological manipulation of *VAChT* activity (Daniels et al., 2004, Prado et al., 2006, Lima et al., 2010, De Castro et al., 2009, Wilson

et al., 2005, Varoqui and Erickson, 1996, Song et al., 1997). However, it is notable that up-regulation of *VAChT* expression fails to show effects on quantal size at either snake NMJ or *Drosophila* motoneurons that receive cholinergic excitation (Parsons et al., 1999, Cash et al., 2015). An inability of increased transporter to affect SV loading is consistent with a set-point model of SV filling (Williams, 1997, Cash et al., 2015). This model posits that SV fill to a pre-determined level independently of filling rate, change in which occurs following manipulation of transporter expression level. We have previously reported that transgenic expression of *VAChT*, which carries a single glutamine truncation in a C-terminal polyQ region (13Q to 12Q), results in an increased quantal size of spontaneously released SV at identified interneuron to motoneuron synapses (Cash et al., 2015). This region, therefore, may contribute to the mechanism that regulates SV loading.

PolyQ regions have been most extensively studied in polyQ-extension disorders such as Huntington's disease (HD) where polyQ regions of disease causing proteins (e.g. Htt for HD) are expanded from a normal range of 6-35 repeats. Individuals who express Htt containing 36 - 40 repeats are considered likely to develop HD, whilst those more than 40 nearly always go on to show HD phenotypes (Fan et al., 2014). The length of the polyQ expansion is, therefore, critical for the onset of the disease and disease severity. The molecular mechanism of HD is complex and not well understood, but length of repeats is associated with the formation of neuronal intracellular aggregates in the nucleus, cell body, dendrites, and nerve terminals (Fan et al., 2014) .

Here, we use electrophysiological characterisation of cholinergic release at *Drosophila* larval and embryonic interneuron→motoneuron synapses to investigate the physiological implications for cholinergic function when the *VAChT* C-terminal polyQ

region is manipulated. We find, in agreement with previously published literature, that expression of a single glutamine truncation *VAChT*^{12Q} increases both amplitude and frequency of spontaneously released cholinergic synaptic vesicles (mEPSCs) recorded from aCC/RP2 motoneurons. Evoked synaptic currents also show an extended duration consistent with an increased ACh load. Conversely, we further show that CRISPR induced single amino acid extension of this region (*VAChT*^{14Q}) results in the opposite effect: reduced mEPSC amplitude and frequency and, moreover, an inability to support evoked release. CRISPR mediated deletion of the polyQ region (*VAChT*$^{\Delta Q}$) has no effect on mEPSC kinetics suggesting that elongation or truncation of the *VAChT* polyQ region is more detrimental to cholinergic functioning than its removal.

4.4 Materials and methods

4.4.1 Fly stocks

Flies were maintained under standard conditions at 25°C. GAL4 drivers used to recapitulate expression of the cholinergic locus were *cha*^{B19} (Salvaterra and Kitamoto, 2001) and *ChAT-BAC* (gifted by Dr. Steve Stowers: Montana State University). These lines were used to drive expression of *UAS-VAChT*^{12Q} (Cash et al., 2015), UAS-*ChR2*^{Cheta} (Bloomington 36354) (Gunaydin et al., 2010) and UAS-*ChR2* (Pulver et al., 2009). CRISPR constructs were prepared as described below and injected into c*as9*-expressing embryos (*yw*; attP40 nos-cas*9*/*CyO*;*+*) by BestGene Inc., (Chino Hills, CA, USA). Control lines were the cleaned CRISPR-injected line lacking construct insertion (*w*$^{-}$; + ; *+*).

4.4.2 gRNA and insert design, template oligo and plasmid construction

The CRISPR Optimal Target Finder tool (http://tools.flycrispr.molbio.wisc.edu/targetFinder/) was used to specify target cut sequence specificity (GATTACCGCTATCAGGTACC). Two guide RNA constructs were made to generate cuts in 5'- and 3'-UTR of *VAChT*, respectively. The gRNA oligonucleotides (5' to 3') are: 5'-UTR: CTTCGAGAGGAAGTCCCAAAGAAAC and AAACGTTTCTTTGGGACTTCCTCTC; 3'-UTR: CTTCGTATTATTACTATAGACATAT and AAACATATGTCTATAGTAATAATAC, sense and antisense, respectively). 100 pmol of each 5' phosphorylated sense and antisense gRNA oligonucleotides were mixed, denatured at 95^{o}C and then reduced to 25^{o}C at a rate of -0.1^{o}C/sec and ligated to the guide RNA expression plasmid, pU6-BbsI-chiRNA (plasmid #45946, Addgene). Oligos used to generate PAM and polyQ site mutations are shown in Table 4.1. Briefly, for 5' PAM site mutagenesis, PCR of primers a+b and c+d (containing TGG to TGC point mutations) were run against *Drosophila* genomic DNA (PAM) or *VAChT* plasmid DNA (polyQ) (PCR1). Following purification, PCR products (a+b and c+d) were used as templates for a second PCR using the most 5' and 3' primers of PCR1 (primers a and d, Table 4.1). This process was repeated for 3' PAM site mutagenesis utilising primers (e+f and g+h), $VAChT^{\Delta Q}$ (i+j and k+l) and $VAChT^{14Q}$ (m+n and o+p). Full UTR sequence with PAM mutations were purified, sequenced and mobilised to pHD-DsRed (plasmid #51434, Addgene) as a dsDNA donor template for CRISPR/Cas9-mediated homology-directed repair (HDR) using restriction digests (5' = *AscI & BssSI*), (3' = *SpeI & XhoI*). PolyQ products were first mobilised to the cloning vector pJET1.2, then to *VAChT* containing pBSII (*BamH1* & *NDe1)* (Cash et al., 2015) then finally to pHD-DsRed with (*EcoR1* and *NDe1*). Sequence was checked by Sanger sequencing at the Manchester Sequencing Facility. Positive progeny were identified by the expression of DsRed in larvae following

the 3xP3 expression pattern. Lines were cleaned and balanced by BestGene. Sequences were re-confirmed at the Manchester Sequencing facility before experimentation.

Table 4.1. Primers used for creation of *Drosophila VAChT* UTR with modified PAM sites (5': a,b,c,d and 3': e,f,g,h). and modified PolyQ regions (5': i,j,k,l and 3': m,n,o,p).

Sequence	Use		
ATCGGGCGCGCCGAATTCATGCTTGGGTCGACTTAAGCTC	a	a+b	5'PAM
ACAAAGTTCTGATGCAGTTTCTTTGG	b		
CCAAAGAAACTGCATCAGAACTTTGT	c	c+d	
CTTAAATAGTCGGGTATAATCGGTACTA	d		
GTACACTAGTTCGTGTTCTTTTGCACACCTCC	e	e+f	3'PAM
ACGTACCACTTGGCTATATGTCTATA	f		
TATAGACATATAGCCAAGTGGTACGT	g	g+h	
GCTACTCGAGAAGTCCGCCACAATGACAACC	h		
GTGCCTACTGGACGGGCT	i	i+j	*VAChT*$^{\Delta Q}$
CAGGACCTCTGCTCTGGACGAAGGGATTGGCCACACGG	j		
CCGTGTGGCCAATCCCTTCGTCCAGAGCAGAGGTCCTG	k	k+l	
GCTATTAATTAACATATGTAGGAGTATCTGTTCGGGGCAA	l		
GTGCCTACTGGACGGGCT	m	m+n	*VAChT14*^{Q}
CTGCTGCTGCTGCTGTTGTTGTTGCTGCTGCTGCTGCTG	n		
CAGCAGCAGCAGCAACAACAACAACAACAGCAGCAGGTCCAGAGC	o	o+p	
GCTATTAATTAACATATGTAGGAGTATCTGTTCGGGGCAA	p		

4.4.3 Larval and embryonic whole-cell patch-clamp recordings

Recordings were performed at room temperature (20-22°C). Third-instar larvae were dissected in external saline (in mM: 135 NaCl, 5 KCl, 4 $MgCl_2 \cdot 6\ H_2O$, 2 $CaCl_2 \cdot 2H_2O$, 5 N-Tris[hydroxymethyl]methyl-2-aminoethanesulfonic acid, and 36 sucrose, pH 7.15). The CNS was removed and secured to a Sylgard (Dow-Corning, Midland, Michigan, USA)-coated cover slip using tissue glue (GLUture; WPI, Hitchin, UK). The neurolemma

surrounding the CNS was partially removed using protease (1% type XIV; Sigma, Dorset, UK) contained in a wide-bore (15 μm) patch pipette. Whole cell recordings were carried out using borosilicate glass electrodes (GC100TF-10; Harvard Apparatus, Edenbridge, UK), fire-polished to resistances of between 7-10MΩ for L3 recordings and 14-18 MΩ for embryonic recordings. The aCC/RP2 motoneurons were identified by characteristic soma size and position within the ventral nerve cord. Cell identity was sporadically confirmed, after recording, by filling with 0.1% Alexa Fluor 488 hydrazyde sodium salt (Invitrogen, Carlsbad, California, USA), included in the internal patch saline (in mM: 140 potassium gluconate, 2 $MgCl_2 \cdot 6H_2O$, 2 EGTA, 5 KCl, and 20 HEPES, pH 7.4). Tetrodotoxin (TTX, 2 μM, Alomone Labs, Hadassah Ein Kerem, Israel) was included in the external saline to block action potential-induced SV release. Recordings were made using a MultiClamp 700B amplifier. Cells were held at -60 mV and recordings were sampled at 100 kHz and lowpass filtered at 0.5 kHz, using pClamp 10.6 (Molecular Devices, Sunnyvale, CA). Only neurons with an input resistance of ≥ 500 MΩ (L3 recordings) or ≥1 GΩ (embryo) were accepted for analysis.

Statistics. Statistical significance between group means was assessed using either a Student's t-test (where a single experimental group is compared to a single control group), a one-way ANOVA followed by Bonferroni's post-hoc test (multiple experimental groups). In all tests, confidence intervals of $*P \leq 0.05$, $**P \leq 0.01$, and $***P \leq 0.001$ and ****P ≤ 0.0001 were used for significance. Data shown is mean ± s.e.m.

4.5 Results

4.5.1 *VAChT*^{12Q} increases SV loading at cholinergic synapses

We undertook patch-clamp recordings from well-characterized aCC/RP2 motoneurons which receive identical cholinergic synaptic input (Baines et al., 1999). We recorded spontaneous mEPSCs, achieved by blocking action potential-dependent activity (termed evoked hereafter) with TTX. We have previously shown that expression of transgenic *VAChT*^{12Q}, in a wildtype background (i.e. *VAChT*^{13Q}) , significantly increases mEPSC amplitude and release frequency (Cash et al., 2015). It should be noted that, unlike the NMJ, mEPSCs recorded in central neurons can (and in this case do) show a range of amplitudes due to filtering of current spread through axonal and dendritic regions. We find transgenic expression of *VAChT*^{12Q} increased mEPSC amplitude (7.8 ± 0.9, 7.5 ± 0.6 vs. 12.0 ± 0.8pA, cha^{B19}/+, UAS/+ vs. *cha*^{B19}>VAChT^{12Q} respectively, P = 3 x 10^{-3} (cha^{B19}/+), P = 2 x 10^{-3} (UAS/+), Fig. 1A-B) and frequency (38.5 ± 6.7, 41.0 ± 11.3 vs. 74.3 ± 6.2 per min, cha^{B19}/+, UAS/+ vs. *cha*^{B19}>VAChT^{12Q} respectively, P = 2 x 10^{-2} (cha^{B19}/+), P = 6 x 10^{-3} (UAS/+).

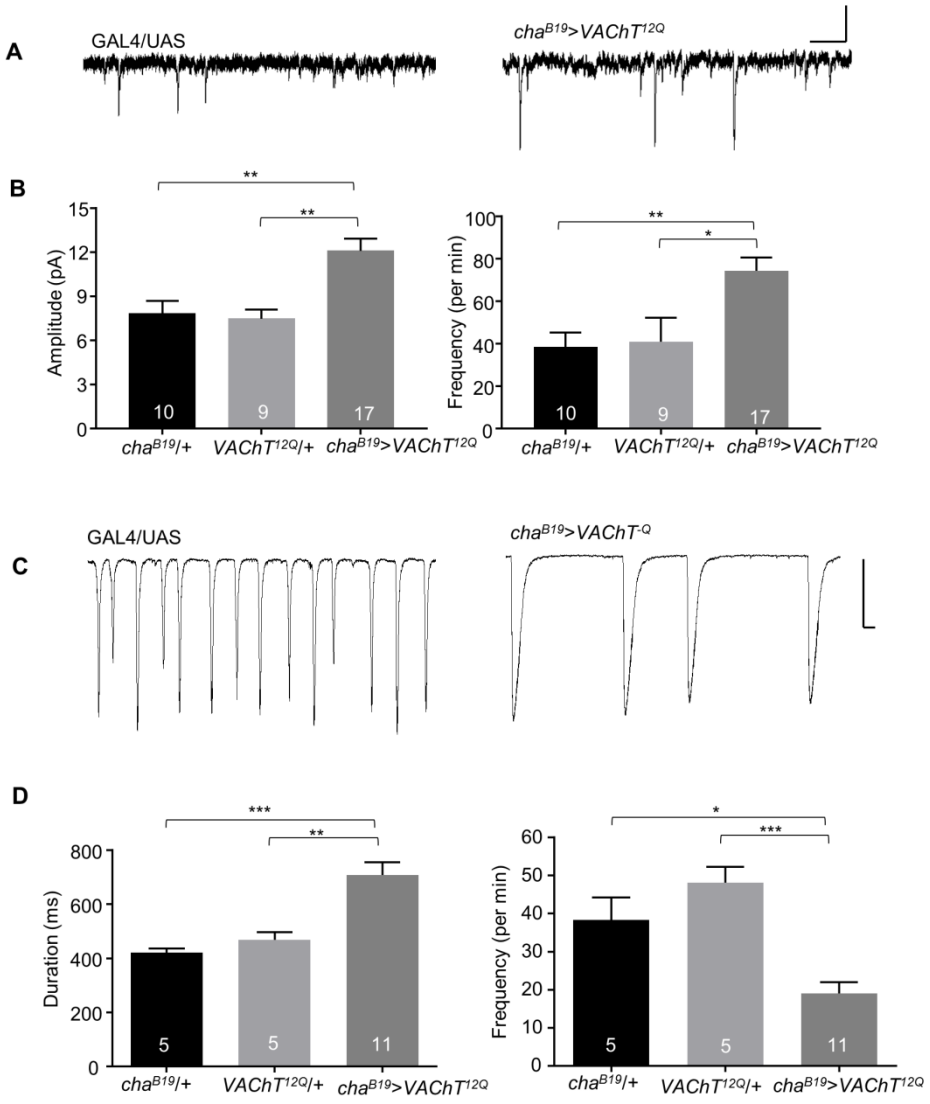

Figure 4.1. Expression of *VAChT^{12Q}* increases mEPSC amplitude. (A) Representative traces of mEPSCs recorded from L3 aCC/RP2 in GAL4 and UAS control and following expression of VAChT^{12Q} in all cholinergic neurons (*cha^{B19}>VAChT^{12Q}*). Scale Bar: 10 pA/30 ms. (B) *VAChT^{12Q}* increases both mEPSC amplitude P = 3 x 10^{-3} (cha^{B19}/+), P = 2 x 10^{-3} (UAS/+) and frequency P = 2 x 10^{-2} (*cha^{B19}*/+), P = 6 x 10^{-3} (UAS/+). GAL4/UAS: N = 10, n = 19. *cha^{B19}>VAChT^{12Q}* N = 11, n = 17. (C) Representative SRCs recorded from L3 aCC/RP2 in GAL4/UAS controls and *cha^{B19}>VAChT^{12Q}*. Scale Bar (400 pA/500 ms) (D) Following expression of *VAChT^{12Q}*, SRCs show significantly increased duration (*cha^{B19}*/+: P = 1 x 10^{-3} , UAS/+ : P = 5 x 10^{-3}) and reduced frequency (*cha^{B19}*/+: P = 1 x 10^{-2} , UAS/+ : P = 3 x 10^{-4}) with no effect to amplitude (P = 0.23). cha^{B19}/+: N = 4 , n = 5. UAS/+: N = 3, n = 5. *cha^{B19}>VAChT^{12Q}:* N = 7, n = 11. All data points are mean ± sem, N = animals, n = cells. n is stated in each bar.

To determine whether the effects we observed in mEPSCs, following expression of *VAChT*^{12Q}, affect evoked release we recorded evoked spontaneous rhythmic currents (SRCs) in aCC/RP2 (i.e. in the absence of TTX). Figure 4.1C-D shows that SRCs are supported, but that they exhibit altered kinetics: specifically showing significantly increased duration (420.3 ± 14.5, 468.8 ± 27.9 vs. 709.2 ± 47.4ms, *cha*^{B19}*/+*, UAS/+ vs. *cha*^{B19}*>VAChT*^{12Q} respectively, P = 1 x 10^{-3} (*cha*^{B19}*/+*) and 5 x 10^{-3} (UAS/+)). SRC frequency was also significantly reduced (38.3 ± 5.9, 48.1 ± 4.2 vs. 19.0 ± 3.0 per min, *cha*^{B19}*/+*, UAS/+ vs. *cha*^{B19}*>VAChT*^{12Q} respectively, P = 1 x 10^{-2} (*cha*^{B19}*/+*) and 3 x 10^{-4} (UAS/+)), whilst amplitude remained unchanged (P = 0.23).

As can be seen in Fig. 4.1C, network-driven SRCs show considerable variability in amplitude due to filtering of current spread through the dendritic regions of motoneurons. To provide a more rigorous baseline (i.e. to reduce variability particularly in amplitude) we used an optogenetic approach. This is sufficient to produce EPSCs that are identical to SRCs (but as these are not spontaneous we term them EPSCs). We expressed ChR2 (Pulver et al., 2009) in all cholinergic neurons. Expression of *VAChT*^{12Q} similarly increased duration of optogenetically-evoked EPSCs (485.4 ± 32.9 vs. 625.9 ± 49.9 ms, *cha*^{B19}*>ChR2* vs. *cha*^{B19}*>ChR2 ; VAChT*^{12Q} respectively, P = 0.03) but again did not influence amplitude (23.4 ± 2.7 vs. 24.5 ± 3.3 pA/pF, *cha*^{B19}*>ChR2* vs. *cha*^{B19}*>ChR2 ; VAChT*^{12Q} respectively, P = 0.81). We also measured the amplitude ratio between the first and second EPSC evoked at a following frequency of 1Hz. The second SRC amplitude was significantly greater in amplitude compared to the equivalent in controls. The resulting ratios (EPSC2 / EPSC1) were 75.2 ± 6.9 vs. 93.0 ± 1.2%, *cha*^{B19}*>ChR2* vs. *cha*^{B19}*>ChR2; VAChT*^{12Q} respectively, P = 0.02 (Fig. 4.2B). This

effect was abrogated when stimulation frequency was reduced to once every 20 seconds (0.05Hz) (84.8 ± 4.2 vs. 89.1 ± 3.0%, *cha^{B19}>ChR2* vs. *cha^{B19}>ChR2 ; VAChT^{12Q}* respectively, P = 0.40). Taken together, our data suggest that expression of *VAChT^{12Q}* is sufficient to increase loading of SV in the terminals of cholinergic central neurons, an effect that was not observed through up-regulation of the wild type (13Q) transporter (Cash et al., 2015). This is sufficient to produce mEPSCs exhibiting larger amplitudes, SRCs/EPSCs exhibiting longer durations and the ability of the presynaptic terminals to resist synaptic depression following continuous 1Hz evoked vesicle release.

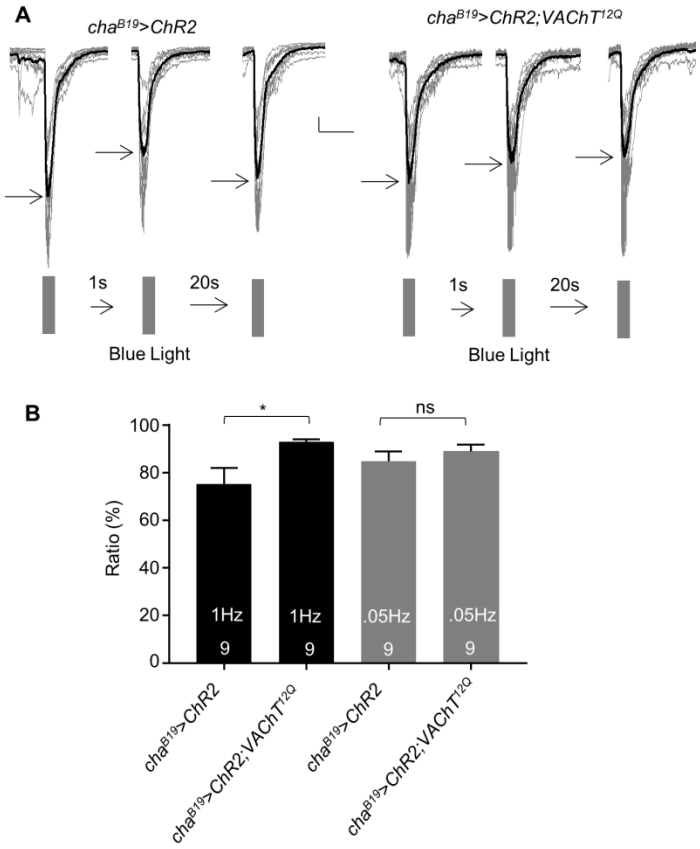

Figure 4.2. Expression of *VAChT^{12Q}* increases optogentically-evoked EPSC duration. (A) Traces of EPSCs recorded from L3 aCC/RP2 in controls (*cha^{B19}>ChR2*) vs. experimental (*cha^{B19}>ChR2 ; VAChT^{12Q}*) conditions. Grey lines are individual recordings whereas the bold black line represents the composite average. Scale Bar: 50 pA/500 ms. (B) Paired-

pulse stimulations, at 1 Hz, show the presence of *VAChT*^{12Q} enables presynaptic release to resist run-down that occurs in the control (P = 0.02). This effect is abrogated when the second stimulus is applied at 0.05 Hz (P = 0.40). All data points are mean ± sem, N is equal to n and stated in each bar.

4.5.2 *VAChT*^{14Q} decreases SV loading at cholinergic synapses

To investigate the contribution to SV loading made by the *VAChT* polyQ region, we created two CRISPR knock-in gene replacements. The first extended the polyQ region by one additional glutamine (*VAChT*^{14Q}), whilst the second deleted the polyQ region (*VAChT*$^{\Delta Q}$). A third CRISPR was attempted containing a single glutamine truncation (*VAChT*^{12Q}) in order to validate our findings using the GAL4/UAS system described above. However, despite several injection attempts (BestGene and Manchester Fly Facility) we were unable to generate transgenic progeny.

Homozygous *VAChT*^{14Q} is embryonic lethal. Embryos develop normally until late stage 17, identified by the presence of inflated trachea, clearly visible mouth hooks, normal gross CNS morphology and body-wall musculature. However, no coordinated peristaltic waves of body-wall muscles were observed indicative of a failure of the central motor network. Recordings from aCC/RP2, in late stage 17 embryos, showed that mEPSC amplitude was significantly reduced (4.0 ± 0.2 vs. 2.9 ± 0.2pA, control *vs.* *VAChT*^{14Q} respectively, P = 1 x 10^{-3}) as was frequency (26.1 ± 4.8 vs. 4.56 ± 1.1per min, control *vs.* *VAChT*^{14Q} respectively, P = 8 x 10^{-4}, Fig. 4.3A-B). This effect was opposite to that observed following expression of *VAChT*^{12Q}. Note: the absolute amplitude and frequency shown in Fig. 4.3 differ from the equivalents shown in Fig. 4.1 (*VAChT*^{12Q}) because the developmental stage differs (embryo vs. L3). Analysis of endogenous SRCs show that knock-in of *VAChT*^{14Q} does not support evoked SRCs (Fig. 4.4A-B). Combining

ChR^{Cheta} in this background was also unable to evoke optogenetically-evoked EPSCs (see appendix 3, section 4.7.1). We rationalise that the reduction in mEPSC amplitude observed, indicative of insufficient loading of cholinergic SV, is sufficient to prevent evoked release.

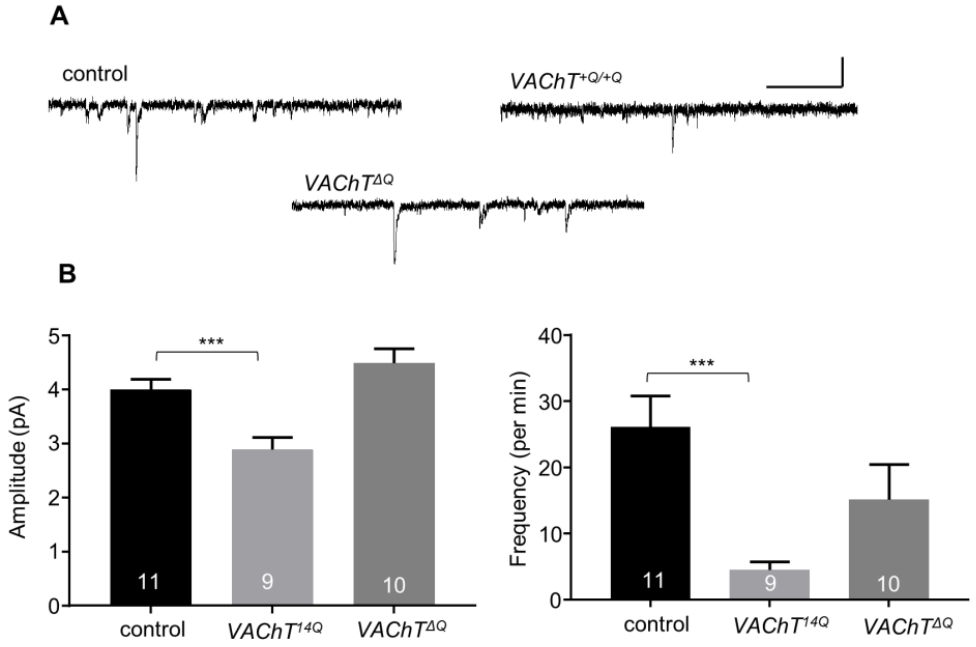

Figure 4.3. *VAChT* polyQ manipulation alters spontaneous neurotransmission. (A) Representative traces of mEPSCs recorded from embryonic late stage 17 aCC/RP2 between control, *VAChT*^{14Q} and *VAChT*$^{\Delta Q}$. Scale Bar: 3 pA/30 ms. (B) *VAChT*^{14Q} mutants display significantly reduced mEPSC amplitude ($P = 1 \times 10^{-3}$) and frequency ($P = 8 \times 10^{-4}$). However, no obvious difference in mEPSC kinetics are observed in *VAChT*$^{\Delta Q}$ mutants for either amplitude (P = 0.13) or frequency (P = 0.14). control: N = 6 , n = 11. *VAChT*^{14Q}: N = 5 , n = 9. *VAChT*$^{\Delta Q}$: N = 6 , n = 10. All data points are mean ± sem, n stated in each bar.

Homozygous knock-in of *VAChT*$^{\Delta Q}$ produces viable larvae. However larval development ceases during L1 after which lethality occurs. Recordings from embryonic aCC/RP2

motoneurons, in homozygous *VAChT*$^{\Delta Q}$, shows no obvious effect on either mEPSC amplitude (4.0 ± 0.2 vs. 4.5 ± 0.26pA, control *vs.* *VAChT*$^{\Delta Q}$ respectively, P = 0.13) or frequency (26.1 ± 4.8 vs. 15.1 ± 5.3 per min, control *vs.* *VAChT*$^{\Delta Q}$, respectively P = 0.14, Fig. 4.3A-B). Unexpectedly, we did observe a change to endogenous SRC kinetics. Specifically, SRC duration was increased (411.7 ± 38.4 vs. 627.93 ± 44.5ms, control *vs.* *VAChT*$^{\Delta Q}$ respectively, P = 3 x 10^{-3}), and frequency reduced (22.4 ± 4.7 vs. 8.3 ± 1.6 per min, control *vs.* *VAChT*$^{\Delta Q}$ respectively, P = 0.01). SRC amplitude was not affected (20.2 ± 2.8 vs. 19.6 ± 4.9pA/pF, control *vs.* *VAChT*$^{\Delta Q}$ respectively, P = 0.91, Fig. 4.4A-B). The lack of effect to mEPSC amplitude suggests that number of glutamines in the polyQ region is the more important determinant, rather than the presence or absence of this region.

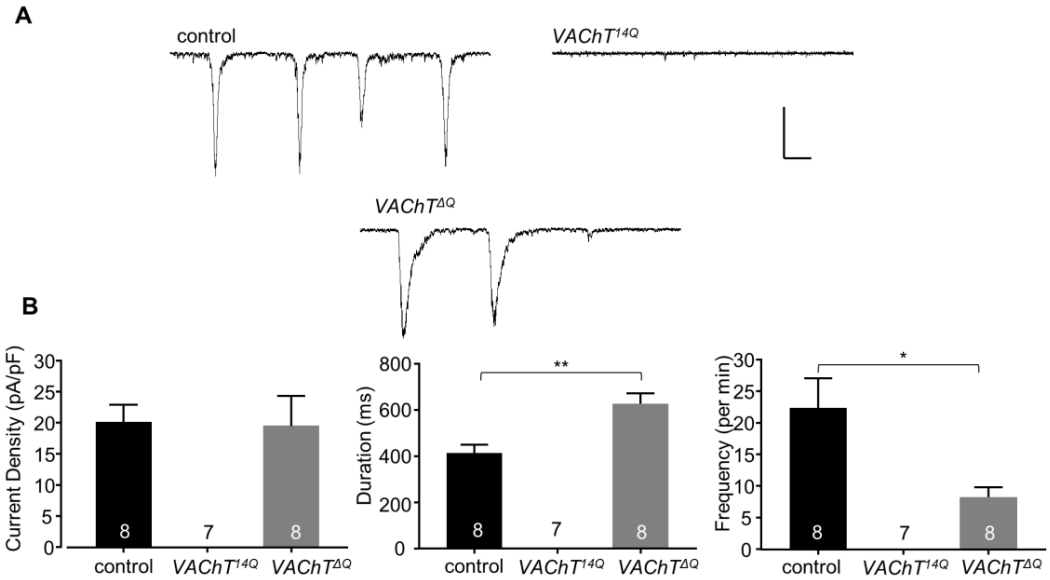

Figure 4.4. *VAChT* polyQ manipulation alters evoked neurotransmission. (A) Representative traces of SRCs recorded from aCC/RP2 between control, *VAChT*^{14Q} and *VAChT*$^{\Delta Q}$. Scale Bar: 50 pA/300 ms. (B) *VAChT*^{14Q} mutants lack any observable SRCs. By contrast, *VAChT*$^{\Delta Q}$ mutants show SRCs with no observable change in amplitude (P = 0.91). However, duration is increased (P = 3 x 10^{-3}) and frequency reduced (P = 0.01).

control: N = 5 , n = 8. *VAChT*^{14Q}: N = 4 , n = 7. *VAChT*$^{\Delta Q}$: N = 4 , n = 8. All data points are mean ± sem, n stated in each bar.

4.6 Discussion

We report neurophysiological consequences arising from the manipulation of the C-terminal *VAChT* polyQ region. We find, in agreement with previously published literature, that the presence of *VAChT*^{12Q} (i.e. truncating the polyQ region by one glutamine) increases both amplitude and frequency of mEPSCs at an identified central cholinergic synapse. This increase in ACh loading may explain the increased duration in evoked SRCs also observed. Conversely, we further show that a CRISPR- induced single amino acid extension of this region (*13Q to 14Q*) results in reduced amplitude and frequency of mEPSCs and an associated inability to support evoked release. Finally, CRISPR mediated deletion of the polyQ region (13Q to 0Q) does not affect mEPSC kinetics showing elongation or truncation of the polyQ region is more detrimental to cholinergic release than removal of this region. This work highlights the *VAChT* polyQ region as an important determinant mediating cholinergic loading in *Drosophila*.

Our results suggest that the length of the polyQ domain is both deterministic for SV filling and for probability of SV release. Reducing glutamines by one residue is sufficient to increase SV load and release probability and *vice versa*. Moreover, addition of a glutamine (14Q) is sufficient to remove the ability of the CNS to generate a rhythmic fictive locomotor pattern, which is reliant on evoked release. We rationalise that *VAChT*^{14Q} disrupts cholinergic loading, generating partially-filled SVs that, in turn, prevent evoked synaptic release. By contrast, increasing SV loading (12Q) results in evoked release events of longer duration. These observations are in agreement with

recent work using a light activated vATPase pump (pHoenix) localised to SVs (Rost et al., 2015). Rost and colleagues used this tool to show that glutamatergic vesicles are only 'nearly full' under normal conditions (i.e. can be further filled) and, moreover, show vesicle load is proportional to release probability (Rost et al., 2015). Our data are supportive of this observation: only increased SV loading supports evoked release. Moreover, our results are also indicative of a set point model, in which vesicles can only release once they surpass a threshold load. This hypothesis, proposed by Williams in 1997, proposed two distinct models of SV loading. The set-point model proposes a mechanism restricting the amount of neurotransmitter per vesicle to a fixed maximum, whereas, the steady state model suggests the amount of neurotransmitter that enters a SV is offset by leakage, but that both are independent variables that can autonomously change to produce SVs with variable levels of filling (Williams, 1997). The set point model is consistent with observations at the snake NMJ and *Drosophila* central neurons (Parsons et al., 1999, Cash et al., 2015), whereas the steady state model better describes loading at murine and *Drosophila* NMJ and in mammalian cell culture models (Daniels et al., 2004, Prado et al., 2006, Lima et al., 2010, De Castro et al., 2009, Wilson et al., 2005, Varoqui and Erickson, 1996, Song et al., 1997).

Analysis of related *Drosophilia spp* reveals polyQ regions of differing lengths (e.g. 9 in *D. willastomi*, 11 in *D. simulans* and 15 in *D. pseudoobscura*). It is tempting to speculate that evolution may have manipulated the length of the polyQ region to alter SV content in these related species. However, recordings from aCC/RP2 in these related species show mEPSC amplitude is remarkably conserved (see Appendix 3, section 4.7.2). Thus, the predicted effect of SV loading due to change in polyQ length, across these related species, may have been abrogated by compensatory mutations in other

regions of the *VAChT*. A comparative analysis may thus be useful to identify such regions for future study.

The *VAChT* polyQ region is specific to insects. A BLAST search comparison also shows no other insect neuronal vesicular transporter possesses a C-terminal polyQ domain (see Appendix 3, section 4.7.2). Mammalian *VAChT* possesses a di-leucine motif in the same approximate location of the insect polyQ domain. The di-leucine motif is well established as a trafficking region (Bonifacino and Traub, 2003). Removal of the full mammalian *VAChT* C-terminal tail, or specific mutation of the di-leucine motif, results in mislocalisation of the transporter to the neuronal membrane (Colgan et al., 2007). Mutant Htt protein containing a polyQ expansion from 20Q to 120Q was found to preferentially bind to synaptic vesicles in murine axon terminals and, further, to displace the binding of Huntington associated protein (HAP1) usually co-localised to SVs (Li et al., 2003). 120Q mutants were also shown to reduce glutamate release suggesting a direct interaction between extended polyQ domains and synaptic release (Li et al., 2003). HAP1 has also been shown to bind synapsin 1 (Mackenzie et al., 2016) which is critical for SV pool mobilisation and formation (Akbergenova and Bykhovskaia, 2010, Rosahl et al., 1995). We therefore theorise that the polyQ region in *VAChT* may play a similar role on trafficking to the SV, plasma membrane and/or SV pool formation.

It is interesting that complete removal of the *VAChT* polyQ region does not influence mEPSCs, although does alter SRC kinetics (increasing their duration). This dichotomy may mirror an increasingly accepted molecular distinction between spontaneous (mEPSCs) and synchronous (SRC/EPSC) release modalities (Kavalali, 2015, Ramirez and Kavalali, 2011, Sara et al., 2005). Other work has shown, for example, that mEPSC release is maintained in the absence of the vesicle associated SNARE protein

synaptobrevin, whilst evoked release is halted (Schoch et al., 2001). Munc-13 has also be shown to influence the spatial localisation of evoked release whilst having no effect on mEPSCs at *C. elegans* NMJ (Zhou et al., 2013). These observations are predictive of a model in which multiple fusion complexes are physiologically separate and dependent on the modality of release. Moreover, a role for *VAChT* in SV release is indicated by a reported interaction between synaptobrevin and *VAChT.* A glycine to arginine substitution (*G342R*) in *VAChT* is sufficient to reduce cholinergic mediated larval motility, an effect that is rescued by a complimentary substitution of an isoleucine to an aspartate in synaptobrevin (Sandoval et al., 2006).

It is curious that, $VAChT^{\Delta Q}$ mutants present early larval mortality (L1) despite being able to produce SRCs. This is further confused by the similarity in SRC kinetics with cha^{B19}>$VAChT^{12Q}$ which produce viable L3 larvae and adults. We attribute early $VAChT^{\Delta Q}$ mortality to the lack of wild type transporter present in the $VAChT^{\Delta Q}$ *genetic* background, which may be consistent with cholinergic deficiencies presented in wider physiological function. In humans, ChAT immunoreactivity and nAChR/mAChR expression is observed in non-neuronal epithelial, endothelial, mesothelial and immune cells (Wessler and Kirkpatrick, 2008) and are shown to modulate multiple cellular processes, including but not exclusive to, cellular migration and apoptosis (Grando et al., 2006), proliferation (Metzen et al., 2003), anti/proinflammatory responses (Shytle et al., 2004, Pavlov and Tracey, 2005) and histamine release (Reinheimer et al., 2000), see Wessler & Kirkpatrick for review (Wessler and Kirkpatrick, 2008). In insects, non-neuronal ACh has been shown to be heavily influential in insect reproduction and larval development (Wessler et al., 2016, Wessler and Kirkpatrick, 2017) and so it remains possible that VAChT modulation may alter wider, as such unknown, physiological aspects of larval development. However, this would require further investigation.

Since the first demonstration of fixed quanta that describes spontaneous release of SVs, the key question of 'how does a SV know when it is full?' remains to be answered. The polyQ region of the *Drosophila VAChT*, that we report here, seemingly orchestrates the filling of cholinergic SVs at central synapses. Future studies to identify the function of this region, including identification of binding partners, provide optimism for understanding how SVs monitor their fill state.

4.7. Appendix 3

4.7.1 *ChR2^{Cheta}* stimulation of *VAChT^{14Q}* mutants suggests failure of evoked vesicle exocytosis.

Figure 4.4 suggests *VAChT^{14Q}* prevents endogenous SRC production. In order to validate this finding we attempted to evoke SRCs in late stage *VAChT^{14Q}* embryos utilising *ChR* (see section 4.4.3). Evoked activity was generated by the expression of *ChR2^{cheta}* driven in all cholinergic neurons (*ChAT^{BAC}>ChR2^{cheta}*) in control (*VAChT*) or mutant (*VAChT^{14Q}*) backgrounds fed 100 µl/vial of 0.1 M all trans-retinal (Sigma, #R2500) in 100% EtOH applied to the surface of standard media and raised in blackout vials in order to prevent ChR2 activation throughout larval development. Stimulation frequency was 1Hz/9 sec (λ470 nm, 100 ms, light intensity 9.65 mW/cm^2).

Figure 4.7 shows that we were able to evoke synaptic currents in control larvae (amplitude: 16.24 ± 1.05pA, N = 4, n = 4, Fig. 4.5A-B), consistent with those produced endogenously (Fig 4.4). However, *VAChT^{14Q}* embryos did not produce obvious synaptic currents. The subtle depolarisation shown in aCC (amplitude: 0.70 ± 0.34pA, VAChT^{14Q}, Fig 4.5A) represents the known expression of the cholinergic GAL4 drivers in aCC and is not indicative of evoked cholinergic release. This is confirmed from recordings from RP2, which do not show GAL4 expression, displaying no post-synaptic current. These data suggest *VAChT^{14Q}* cannot evoke action potential mediated mass vesicle release. We attribute this to a reduction of cholinergic loading.

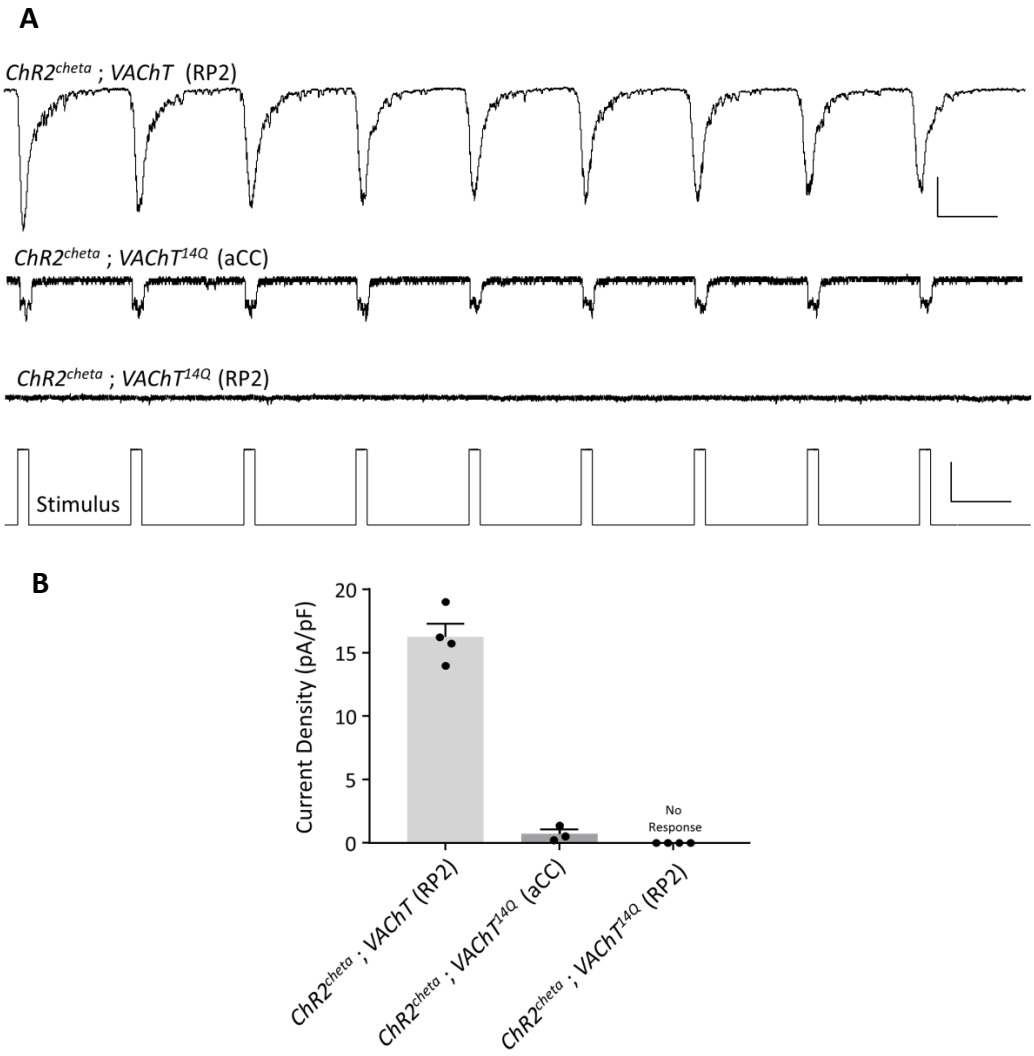

Figure 4.5. *VAChT^{14Q}* does not support evoked vesicle release. (A) representative traces of *ChR2^{Cheta}* evoked synaptic release in *ChAT^{BAC}>ChR2^{cheta}*; *VAChT* (RP2) and *ChAT^{BAC}>ChR2^{cheta}*; *VAChT^{14Q}* (aCC/RP2). Sale bars: (traces: 20 pA/500 ms, stimulus: 1 V/500 ms). (B) Control larvae generate synaptic input representative of endogenous SRC production (amplitude: 16.2 ± 1.1pA, N = 4, n = 4). VAChT^{14Q} produces a small *ChR2^{cheta}* mediated current in aCC (0.7 ± 0.3pA, *VAChT^{14Q}*, N = 3, n = 3). Whereas, no observable current is evoked in RP2 (N = 4, n = 4).

4.7.2. Spontaneous release is remarkably similar across *Drosophila* phylogeny despite variable *VAChT* polyQ regions.

Our previous published observations (Cash et al., 2015), and results presented within this study (Chapter 4) highlight the *VAChT* polyQ region as an important determinant of vesicular loading. Under examination of *VAChT* polyQ regions from different *Drosophila spp* we noticed that this polyQ region is highly variable in length. *D. willastomi*, *D. simulans* and *D. pseudoobscura* display a 9, 11 and 15Q region respectively. We therefore rationalised that we may observe differing mini kinetics between species. However, this was not the case and spontaneous release profile to motoneurons in these phylogenetically distinct species remains remarkably preserved in both amplitude (ANOVA: P = 0.32, Fig. 4.6) and frequency (ANOVA: P = 0.79).

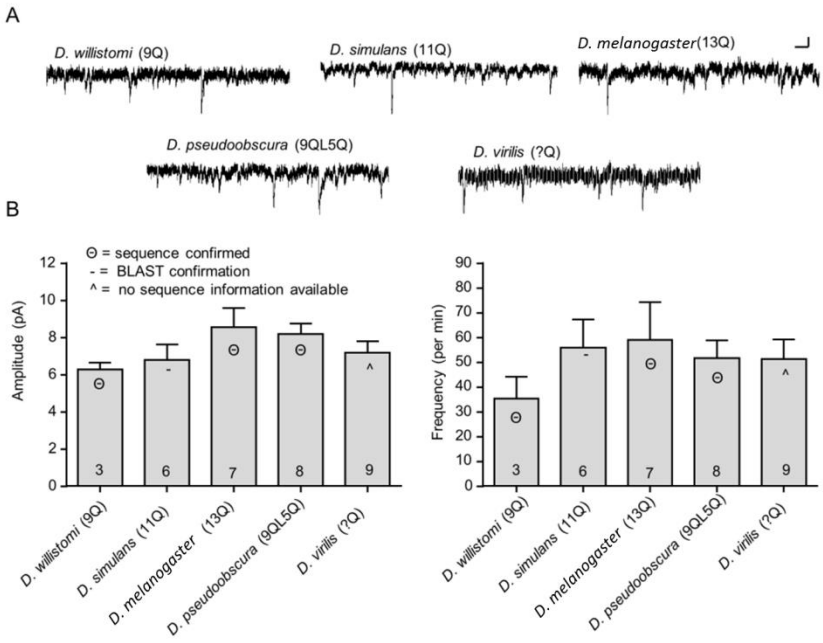

Figure 4.6. Mini kinetics remain remarkably similar throughout *Drosophila* phylogeny. (A) Representative traces of minis recorded from L3 motoneurons between *Drosophila spp*. Scale Bar: 5 pA/10 ms. (B) No obvious differences observed in amplitude (ANOVA:

P = 0.32) or frequency (P = 0.79) of miniature release events despite varied polyQ regions. All data points are mean ± sem, n stated in each bar.

It is noteworthy that although polyQ regions differed, so did other areas of the protein, BLAST comparison with *D. melanogaster* show that *D. willastomi*, *D. simulans*, *D. pseudoobscura* share an 82%, 96% 85% sequence identity respectively (Fig. 4.7). We further find that *D. pseudoobscura* polyQ region differed from that reported in BLAST with one Q within the 15Q region being replaced by a Leucine at position 10 within the region. We rationalised that although polyQ length may be important, compensatory mutations in other protein regions may allow the maintenance of normal cholinergic functioning. We therefore undertook CRISPR mutagenesis of the *Drosophila* PolyQ region in order to study polyQ mutations in an otherwise wild type background (Fig 4.3 and 4.4).

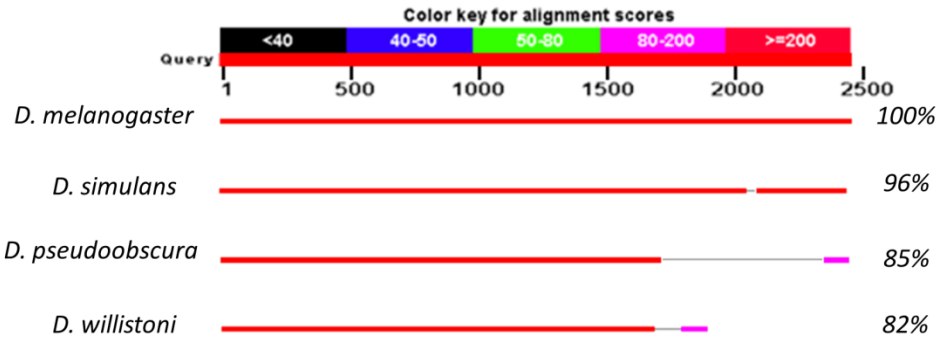

Figure 4.7. BLAST search reveals differentiated *VAChT* sequence identities between *Drosophila spp*. BLAST sequence comparison vs. *D. melanogaster VAChT* full sequence suggests wider regions of the *VAChT* are not conserved between species.

General Discussion

5.0 Evolution has shaped two modalities of vesicular loading

The set point model of SV filling is consistent with observations at the snake NMJ and our observations at *Drosophila* central synapses (Parsons et al., 1999, Cash et al., 2015), whereas the steady state model better describes loading in almost every other model studied to date: mammalian, *C. elegans, Xenopus* and *Drosophila* NMJ (Daniels et al., 2004, Daniels et al., 2011, Lima et al., 2010, Prado et al., 2006, Sugita et al., 2016, Costa et al., 2017, Song et al., 1997) and in cultured mammalian central neurons and cell models (Wilson et al., 2005, Varoqui and Erickson, 1996). Overwhelmingly then, it would appear fair to conclude that systems following a steady state model would seem to be comparatively dominant in the light of this information, or would it? One consideration to take into account is, with exception from the work presented within this thesis, no other study has investigated vesicular loading kinetics in a living, intact CNS. One may argue that, although informative, reductionist models and culture conditions may be missing key components that central neurons require for true endogenous loading kinetics to be observed. With this in mind, and in light of the work presented in this thesis, one may open an interesting discussion regarding key differences between synaptic vesicle loading at central and peripheral synapses.

Synaptic machinery localised to the NMJ needs to constantly modulate dynamic, highly plastic, motor output with high evolutionary selectivity. For example, short but intense bouts of activity when escaping predation are followed by the organism's eventual escape and subsequent rest or imminent death. Therefore, synaptic input to the NMJ should be sufficiently dynamic in order to support these functional requirements. Fast synaptic plasticity is well documented at NMJ synapses (Davis et al., 1998; Frank et al.,

2006; Davis and Müller, 2015; Yeates et al.,2017). Blocking postsynaptic glutamate receptors with the glutamate receptor antagonist philanthrotoxin, results in an initial decrease in mini amplitude (indicative of quantal size) together with a subsequent increase in the number of vesicles released per stimulation (quantal content) occurring from 2 - 10 minutes following pharmacological challenge and mini amplitude degradation (Frank et al., 2006, Yeates et al., 2017). This phenomenon is termed presynaptic homeostatic plasticity/potentiation (PHP) (Frank et al., 2006, Davis and Müller, 2015). PHP can also be initiated at NMJ synapses by dampening glutamate receptor response through mutagenesis of GluTIIA (Petersen et al., 1997), manipulation of PKA activity (Davis et al., 1998) and muscle hyperpolarisation (Paradis et al., 2001) and has recently been found to be modulated by a semaphorin-plexin signalling cascade (Orr et al., 2017). However, no data exist for this phenomenon in an intact CNS. In dissociated rat hippocampal and visual cortical pyramidal neuron cultures, blockade of glutamate receptors with APV or NQBX was shown to increase mini amplitude, but curiously not until after 18-48 h of incubation and is strictly attributed to longer term changes in postsynaptic glutamate receptor expression rather than PHP itself (Sutton et al., 2006, Thiagarajan et al., 2005, Turrigiano et al., 1998). These data suggest that central neurons are less able to dynamically regulate quantal kinetics. We find that direct manipulation of presynaptic loading machinery, in central neurons, influences the ability of vesicles to release rather than produce direct modifications to quantal size (i.e mini amplitude).

5.1 *VAChT* modulation highlights a univesicular release model at aCC/RP2 pre-motor synapses.

Much of the work through this thesis appears to suggest that central neurons have tight control over the number of full vesicles docked at active zones, disruption of which produces wider synaptic deficits. Reducing the number of full vesicles, through CASPP treatment, reduces both mini and SRC frequency (Chapters 2, Fig.2D & 3 Fig. 2D), whereas up-regulation of the CASPP target (*cha*^{B19}>*VAChT*) restores SRC frequency to wildtype levels, presumably facilitated by increased loading via the increased presence of *VAChT*. This is reciprocated further in Chapter 2 where the incorporation of the *VAChT*^{Y49N} mutation seemingly exhausts the RRP through enhanced mini release. The *VAChT*^{Y49N} phenotype is detrimental to wider synaptic function, showing clear motor deficits manifesting itself as a reduction in SRC frequency and an inability to sustain prolonged synaptic release (Chapter 2, Fig. 5A-B & Fig. 6A-B). This phenotype was rescued by up-regulation of the *VAChT*^{Y49N} using the GAL4/UAS system, again presumably mediated via increased *VAChT* (Appendix 2). Further, Chapter 3 shows that a direct reduction in loading kinetics through manipulation of the *VAChT* polyQ region (*VAChT*^{14Q}) results in an inability to produce SRCs leading to embryonic lethality. Taken together, these data are consistent with a model in which insufficiently loaded or docked active zones halt the initiation of synchronous, evoked release. Such a model is dictated by how many SVs are docked and loaded at each active zone and how many release per evoked release event.

Initial work suggested most synapses follow univesicular release (UVR). Thus, although many vesicles may be docked, only one SV at most is released per stimulation in a stochastic fashion from each active zone (Rudolph et al., 2015). This was rationalised

because post synaptic responses always equated to equal or less than the number of identified synapses (Redman and Walmsley, 1983, Gulyás et al., 1993, Rudolph et al., 2015). However, UVR suggests an "all or nothing model" in which variability of evoked amplitudes should be small. However, other studies have highlighted large variability in evoked amplitudes in mammalian central synapses and thus suggested vesicle release could also be facilitated by multiple active sites from the same synapse following a "multivesicular release model" (MVR) (Tong and Jahr, 1994, Auger et al., 1998, Christie and Jahr, 2006, Huang et al., 2010, Conti and Lisman, 2003).

MVR is hypothesised to occur when the postsynaptic response to single quanta is low and thus the relative receptor occupancy, meaning the proportional stimulation of postsynaptic receptor from one quantum, is also low (Rudolph et al., 2015). Thus multiple quanta can release simultaneously to strengthen postsynaptic responses by acting on the same receptor pool (Rudolph et al., 2015). Increasing the probability of vesicle release is known to saturate relative receptor occupancy and increase amplitudes of EPSPs occurring at synapses displaying both low and high spontaneous release frequencies (Foster et al., 2005, Tong and Jahr, 1994). However, receptor occupancy is known to be highly variable (Rudolph et al., 2015). Interestingly, increased release probability through *VAChT* transgenic expression and the *VAChT*^{Y49N} mutation shows no obvious difference to SRC amplitudes. This would be expected from a model in which full receptor site saturation occurs from a single quantum i.e. a UVR model. This observation is supported by the observation of increased loading kinetics through the expression of *VAChT*^{12Q}. *VAChT*^{12Q} does not influence amplitude of SRCs but does increase duration. Again, if receptor saturation is already at or close to 100%, further increased quanta will only be sufficient to increase cholinergic tone through *AChE* saturation and thus an observed prolonged duration of EPSPs/SRCs. A UVR model at

aCC/RP2 pre-motor synapses also agrees with recent observations of ChR2 stimulation of individually identified premotor interneurons giving significantly reduced postsynaptic response than perhaps expected or none at all (Baines Lab, unpublished data).

Despite two decades of research, very few studies have shown dramatic increases in the amplitude of SRCs in *Drosophila* without modulating post-synaptic excitability (Marley and Baines, 2011, Baines, 2003) or larval stage (Zwart et al., 2013). Indeed reduced SRC amplitudes have been seen amongst a reduction in synaptic inputs (Baines et al., 2002) but not when vesicle release is reduced through TeTxLC expression (Baines et al., 2001). Increased SRC amplitude have exclusively been found in mutants known to modulate retrograde signalling pathways such as glass bottomed boat (gbb) and bone morphogenic protein (BMP) and dystrophin mutants (Baines, 2004, Fradkin et al., 2008). Possibly indicative of a retrograde control mechanism. Natural variation between SRCs, within one recording exist, however, may be explained through a combination of dendritic filtering and differential activation of pre-motor interneurons during endogenous activity.

In the context of UVR/MVR theory, an MVR model appears to instead correlate with NMJ kinetics. Syntaxin ($syx^{3\text{-}69}$) and SNAP-25 ($SNAP25^{ts}$) mutants maintain a heightened mini frequency and EPSPs are greater in amplitude (Lagow et al., 2007, Rao et al., 2001). $syx^{3\text{-}69}$ mutants were shown to possess increased quantal content and therefore can be attributable to increased receptor occupancy per stimulation indicative of the MVR model and, in the context of this discussion, highlights another key difference between loading and release at central and peripheral synapses. However, exceptions to this general rule exist; increased spontaneous release through complexin null

mutations decreases EPSP amplitude (Huntwork and Littleton, 2007). Complexin null up-regulation is more severe than previously described syntaxin and SNAP-25 mutants and so active zone depletion may be explained by RRP depletion, as is the case for *VAChT*^{Y49N}.

5.2 Outlook

Several lines of further investigation generated by this thesis would further our understanding of synaptic release and loading at cholinergic synapses. One that would appear most obvious is a direct investigation of loading and release between central and peripheral synapses. An alternate explanation for the differences addressed through this discussion is not localisation or quantal kinetics, but the underlying difference between the predominant excitatory neurotransmitter present between synapses. *Drosophila* NMJ and central synapses are predominantly glutamatergic and cholinergic, respectively, whereas this is reversed at mammalian synapses. This issue is exacerbated when examining the lack of functionally characterised cholinergic peripheral synapses in *Drosophila* or glutamatergic central synapses and thus hampered this line of investigation through this thesis. However, with the recent advancements of morphological characterisation of the whole *Drosophila* CNS (Zheng et al., 2017), functional characterisation is soon to follow. Knowledge of identified central glutamatergic neurons accessible *in vivo* may ease this line of investigation.

A further line of investigation is that of *VAChT* localisation. As discussed in chapters 3 and 4, both the *VAChT*^{Y49N} and *VAChT* polyQ region may be involved in vesicular trafficking. The tyrosine (Y) in Y49N is a known important trafficking motif but is yet to be clarified for *VAChT* and evidence exists for polyQ manipulations to effect interactions with synaptic vesicles. Further work would clarify whether *VAChT*

trafficking deficits underlies the observed physiological abnormalities and if so, which pathways are involved.

Further the *VAChT* polyQ domain is an entirely novel region in regards to modulation of SV loading at insect cholinergic synapses. One avenue would be to further explore the wider implications of these polyQ mutants. For example, it is unknown whether or not the *VAChT* polyQ region binds an important synaptic protein to modulate localisation or loading, this may have wider implications to other neuronal polyQ disruptions in other proteins. A pull down assay utilising the *VAChT*$^{\Delta Q}$ vs. wild type and *VAChT*^{14Q} generated in this project may provide important insights into protein-protein polyQ binding partners. Further, if polyQ regions functionally act as spacers for other important C-terminal domains, then the examination of polyQ flanking domains may give insights into other important regions that modulates loading. Finally, direct measurement of ACh loading in isolated synaptic vesicles, utilising tritiated ACh (Erickson et al., 1994), is another potential route of investigation to further elicit exact loading changes due to polyQ manipulations.

6.0 Bibliography

AGUILAR, J. I., DUNN, M., MINGOTE, S., KARAM, C. S., FARINO, Z. J., SONDERS, M. S., CHOI, S. J., GRYGORUK, A., ZHANG, Y. & CELA, C. 2017. Neuronal depolarization drives increased dopamine synaptic vesicle loading via VGLUT. *Neuron,* 95**,** 1074-1088. e7.

AKBERGENOVA, Y. & BYKHOVSKAIA, M. 2010. Synapsin regulates vesicle organization and activity-dependent recycling at *Drosophila* motor boutons. *Neuroscience,* 170**,** 441-452.

ARBAS, E. A. & CALABRESE, R. L. 1987. Ionic conductances underlying the activity of interneurons that control heartbeat in the medicinal leech. *Journal of Neuroscience,* 7**,** 3945-3952.

AUBREY, K. R. 2016. Presynaptic control of inhibitory neurotransmitter content in *VIAAT* containing synaptic vesicles. *Neurochemistry international,* 98**,** 94-102.

AUGER, C., KONDO, S. & MARTY, A. 1998. Multivesicular release at single functional synaptic sites in cerebellar stellate and basket cells. *Journal of Neuroscience,* 18**,** 4532-4547.

BAARS, T. L., PETRI, S., PETERS, C. & MAYER, A. 2007. Role of the V-ATPase in regulation of the vacuolar fission–fusion equilibrium. *Molecular biology of the cell,* 18**,** 3873-3882.

BAINES, R. A. 2003. Postsynaptic protein kinase A reduces neuronal excitability in response to increased synaptic excitation in the *Drosophila* CNS. *Journal of Neuroscience,* 23**,** 8664-8672.

BAINES, R. A. 2004. Synaptic strengthening mediated by bone morphogenetic protein-dependent retrograde signaling in the *Drosophila* CNS. *Journal of Neuroscience,* 24**,** 6904-6911.

BAINES, R. A. & BATE, M. 1998. Electrophysiological development of central neurons in the *Drosophila* embryo. *Journal of Neuroscience,* 18**,** 4673-4683.

BAINES, R. A., ROBINSON, S. G., FUJIOKA, M., JAYNES, J. B. & BATE, M. 1999. Postsynaptic expression of tetanus toxin light chain blocks synaptogenesis in *Drosophila*. *Current biology,* 9**,** 1267-S1.

BAINES, R. A., SEUGNET, L., THOMPSON, A., SALVATERRA, P. M. & BATE, M. 2002. Regulation of synaptic connectivity: levels of Fasciclin II influence synaptic growth in the *Drosophila* CNS. *Journal of Neuroscience,* 22**,** 6587-6595.

BAINES, R. A., UHLER, J. P., THOMPSON, A., SWEENEY, S. T. & BATE, M. 2001. Altered electrical properties in *Drosophila* neurons developing without synaptic transmission. *Journal of Neuroscience,* 21**,** 1523-1531.

BARBOSA, J., FERREIRA, L. T., MARTINS-SILVA, C., SANTOS, M. S., TORRES, G. E., CARON, M. G., GOMEZ, M. V., FERGUSON, S. S., PRADO, M. A. & PRADO, V. F. 2002. Trafficking of the vesicular acetylcholine transporter in SN56 cells: a dynamin-sensitive step

and interaction with the AP-2 adaptor complex. *Journal of neurochemistry,* 82**,** 1221-1228.

BARKER, L., DOWDALL, M. & WHITTAKER, V. 1972. Choline metabolism in the cerebral cortex of guinea pigs. Stable-bound acetylcholine. *Biochemical Journal,* 130**,** 1063-1075.

BARNSTEDT, O., OWALD, D., FELSENBERG, J., BRAIN, R., MOSZYNSKI, J.-P., TALBOT, C. B., PERRAT, P. N. & WADDELL, S. 2016. Memory-relevant mushroom body output synapses are cholinergic. *Neuron,* 89**,** 1237-1247.

BASS, C., DENHOLM, I., WILLIAMSON, M. S. & NAUEN, R. 2015. The global status of insect resistance to neonicotinoid insecticides. *Pesticide Biochemistry and Physiology,* 121**,** 78-87.

BAYER, M. J., REESE, C., BÜHLER, S., PETERS, C. & MAYER, A. 2003. Vacuole membrane fusion: V0 functions after trans-SNARE pairing and is coupled to the Ca^{2+}-releasing channel. *J Cell Biol,* 162**,** 211-222.

BELINATO, T. A. & MARTINS, A. J. 2016. Insecticide resistance and fitness cost. *Insecticides Resistance.* InTech.

BELINATO, T. A., MARTINS, A. J. & VALLE, D. 2012. Fitness evaluation of two Brazilian *Aedes aegypti* field populations with distinct levels of resistance to the organophosphate temephos. *Memorias do Instituto Oswaldo Cruz,* 107**,** 916-922.

BLACQUIERE, T., SMAGGHE, G., VAN GESTEL, C. A. & MOMMAERTS, V. 2012. Neonicotinoids in bees: a review on concentrations, side-effects and risk assessment. *Ecotoxicology,* 21**,** 973-992.

BONIFACINO, J. S. & TRAUB, L. M. 2003. Signals for sorting of transmembrane proteins to endosomes and lysosomes. *Annual review of biochemistry,* 72**,** 395-447.

BOWMAN, E. J., SIEBERS, A. & ALTENDORF, K. 1988. Bafilomycins: a class of inhibitors of membrane ATPases from microorganisms, animal cells, and plant cells. *Proceedings of the National Academy of Sciences,* 85**,** 7972-7976.

BROWN, T. G. The intrinsic factors in the act of progression in the mammal. Proc. R. Soc. Lond. B, 1911. The Royal Society, 308-319.

CAMACHO, M., BASU, J., TRIMBUCH, T., CHANG, S., PULIDO-LOZANO, C., CHANG, S.-S., DULUVOVA, I., ABO-RADY, M., RIZO, J. & ROSENMUND, C. 2017. Heterodimerization of Munc13 C 2 A domain with RIM regulates synaptic vesicle docking and priming. *Nature communications,* 8**,** 15293.

CARBINI, L. A., MAINES, V. J. M. & SALVATERRA, P. M. 1990. Developmental expression of choline acetyltransferase mRNA in *Drosophila*. *Neurochemical research,* 15**,** 1089-1096.

CARVALHO, R., YANG, Y., FIELD, L. M., GORMAN, K., MOORES, G., WILLIAMSON, M. S. & BASS, C. 2012. Chlorpyrifos resistance is associated with mutation and amplification

of the acetylcholinesterase-1 gene in the tomato red spider mite, *Tetranychus evansi*. *Pesticide biochemistry and physiology,* 104**,** 143-149.

CASH, F., VERNON, S. W., PHELAN, P., GOODCHILD, J. & BAINES, R. A. 2015. Central cholinergic synaptic vesicle loading obeys the set-point model in *Drosophila*. *Journal of neurophysiology,* 115**,** 843-850.

CASIDA, J. E. & DURKIN, K. A. 2013. Neuroactive insecticides: targets, selectivity, resistance, and secondary effects. *Annual review of entomology,* 58**,** 99-117.

CASSAYRE, J., HUGHES, D. J., ROBERTS, R. S., WORTHINGTON, P. A., CEDERBAUM, F., MAIENFISCH, P. & MOLLEYRES, L.-P. Spiroindolines: Discovery of a novel class of insecticides. Abstracts of papers of the american chemical society, 2010. Amer chemical soc 1155 16th St, NW, Washington, DC 20036.

CASSAYRE, J., MAIENFISCH, P., ROBERTS, R. S., WORTHINGTON, P. A., HUGHES, D. J., MOLLEYRES, L.-P., CEDERBAUM, F., HILLESHEIM, E., SLUDER, A. & EARLEY, F. Discovery of spiroindolines: A new class of insecticides with a novel mode of action. Abstracts of papers of the american chemical society, 2011. Amer chemical soc 1155 16th St, NW, Washington, DC 20036.

CECCARELLI, B., HURLBUT, W. & MAURO, A. 1973. Turnover of transmitter and synaptic vesicles at the frog neuromuscular junction. *The Journal of Cell Biology,* 57**,** 499-524.

CHAMAON, K., SMALLA, K. H., THOMAS, U. & GUNDELFINGER, E. D. 2002. Nicotinic acetylcholine receptors of *Drosophila*: three subunits encoded by genomically linked genes can co-assemble into the same receptor complex. *Journal of neurochemistry,* 80**,** 149-157.

CHRISTIE, J. M. & JAHR, C. E. 2006. Multivesicular release at Schaffer collateral-CA1 hippocampal synapses. *Journal of Neuroscience,* 26**,** 210-216.

CHUNG, S. & KACZMAREK, L. K. 1995. Modulation of the inactivation of voltage-dependent potassium channels by cAMP. *Journal of Neuroscience,* 15**,** 3927-3935.

COHEN, A. H. & WALLÉN, P. 1980. The neuronal correlate of locomotion in fish. *Experimental brain research,* 41**,** 11-18.

COLEMAN, M., HEMINGWAY, J., GLEAVE, K. A., WIEBE, A., GETHING, P. W. & MOYES, C. L. 2017. Developing global maps of insecticide resistance risk to improve vector control. *Malaria journal,* 16**,** 86.

COLGAN, L., LIU, H., HUANG, S. Y. & LIU, Y. J. 2007. Dileucine motif is sufficient for internalization and synaptic vesicle targeting of vesicular acetylcholine transporter. *Traffic,* 8**,** 512-522.

COLLIN, C., HAUSER, F., DE VALDIVIA, E. G., LI, S., REISENBERGER, J., CARLSEN, E. M., KHAN, Z., HANSEN, N. Ø., PUHM, F. & SØNDERGAARD, L. 2013. Two types of muscarinic acetylcholine receptors in *Drosophila* and other arthropods. *Cellular and molecular life sciences,* 70**,** 3231-3242.

CONTI, R. & LISMAN, J. 2003. The high variance of AMPA receptor- and NMDA receptor-mediated responses at single hippocampal synapses: Evidence for multiquantal release. *Proceedings of the National Academy of Sciences of the United States of America,* 100**,** 4885-4890.

CORRINGER, P.-J., NOVÈRE, N. L. & CHANGEUX, J.-P. 2000. Nicotinic receptors at the amino acid level. *Annual review of pharmacology and toxicology,* 40**,** 431-458.

COSTA, W. S., YU, S.-C., LIEWALD, J. F. & GOTTSCHALK, A. 2017. Fast cAMP modulation of neurotransmission via neuropeptide signals and vesicle loading. *Current Biology,* 27**,** 495-507.

CROSS, R. L. & MÜLLER, V. 2004. The evolution of A-, F-, and V-type ATP synthases and ATPases: reversals in function and changes in the H+/ATP coupling ratio. *FEBS letters,* 576**,** 1-4.

CUBELOS, B., LEITE, C., GIMÉNEZ, C. & ZAFRA, F. 2014. Localization of the glycine transporter *GLYT1* in glutamatergic synaptic vesicles. *Neurochemistry international,* 73**,** 204-210.

DANIELS, R. W., COLLINS, C. A., CHEN, K., GELFAND, M. V., FEATHERSTONE, D. E. & DIANTONIO, A. 2006. A single vesicular glutamate transporter is sufficient to fill a synaptic vesicle. *Neuron,* 49**,** 11-16.

DANIELS, R. W., COLLINS, C. A., GELFAND, M. V., DANT, J., BROOKS, E. S., KRANTZ, D. E. & DIANTONIO, A. 2004. Increased expression of the *Drosophila* vesicular glutamate transporter leads to excess glutamate release and a compensatory decrease in quantal content. *Journal of Neuroscience,* 24**,** 10466-10474.

DANIELS, R. W., MILLER, B. R. & DIANTONIO, A. 2011. Increased vesicular glutamate transporter expression causes excitotoxic neurodegeneration. *Neurobiology of disease,* 41**,** 415-420.

DAVIS, G. W., DIANTONIO, A., PETERSEN, S. A. & GOODMAN, C. S. 1998. Postsynaptic PKA controls quantal size and reveals a retrograde signal that regulates presynaptic transmitter release in Drosophila. *Neuron,* 20**,** 305-315.

DAVIS, G. W. & MÜLLER, M. 2015. Homeostatic control of presynaptic neurotransmitter release. *Annual review of physiology,* 77**,** 251-270.

DE CASTRO, B., PEREIRA, G., MAGALHAES, V., ROSSATO, J., DE JAEGER, X., MARTINS-SILVA, C., LELES, B., LIMA, P., GOMEZ, M. & GAINETDINOV, R. 2009. Reduced expression of the vesicular acetylcholine transporter causes learning deficits in mice. *Genes, Brain and Behavior,* 8**,** 23-35.

DEDERER, H., WERR, M. & ILG, T. 2011. Differential sensitivity of *Ctenocephalides felis* and *Drosophila melanogaster* nicotinic acetylcholine receptor α1 and α2 subunits in recombinant hybrid receptors to nicotinoids and neonicotinoid insecticides. *Insect biochemistry and molecular biology,* 41**,** 51-61.

DELVOLVÉ, I., BRANCHEREAU, P., DUBUC, R. & CABELGUEN, J.-M. 1999. Fictive rhythmic motor patterns induced by NMDA in an in vitro brain stem–spinal cord preparation from an adult urodele. *Journal of Neurophysiology,* 82**,** 1074-1077.

DICKSON, B. J. & GILESTRO, G. F. 2006. Regulation of commissural axon pathfinding by slit and its Robo receptors. *Annu. Rev. Cell Dev. Biol.,* 22**,** 651-675.

DOMANSKA, U. M., KRUIZINGA, R. C., NAGENGAST, W. B., TIMMER-BOSSCHA, H., HULS, G., DE VRIES, E. G. & WALENKAMP, A. M. 2013. A review on CXCR4/CXCL12 axis in oncology: no place to hide. *European journal of cancer,* 49**,** 219-230.

DRACHMAN, D. A. 2005. Do we have brain to spare? *Neurology,* 64**,** 2004-2005.

DUFFY, J. B. 2002. GAL4 system in *Drosophila*: a fly geneticist's Swiss army knife. *genesis,* 34**,** 1-15.

DUPUIS, J., LOUIS, T., GAUTHIER, M. & RAYMOND, V. 2012. Insights from honeybee (*Apis mellifera*) and fly (*Drosophila melanogaster*) nicotinic acetylcholine receptors: from genes to behavioral functions. *Neuroscience & Biobehavioral Reviews,* 36**,** 1553-1564.

EDWARDS, R. H. 2007. The neurotransmitter cycle and quantal size. *Neuron,* 55**,** 835-858.

EL MESTIKAWY, S., WALLÉN-MACKENZIE, Å., FORTIN, G. M., DESCARRIES, L. & TRUDEAU, L.-E. 2011. From glutamate co-release to vesicular synergy: vesicular glutamate transporters. *Nature Reviews Neuroscience,* 12**,** 204.

ERICKSON, J. D., VAROQUI, H., SCHÄFER, M., MODI, W., DIEBLER, M.-F., WEIHE, E., RAND, J., EIDEN, L. E., BONNER, T. I. & USDIN, T. B. 1994. Functional identification of a vesicular acetylcholine transporter and its expression from a" cholinergic" gene locus. *Journal of Biological Chemistry,* 269**,** 21929-21932.

FAN, H.-C., HO, L.-I., CHI, C.-S., CHEN, S.-J., PENG, G.-S., CHAN, T.-M., LIN, S.-Z. & HARN, H.-J. 2014. Polyglutamine (PolyQ) diseases: genetics to treatments. *Cell transplantation,* 23**,** 441-458.

FATT, P. & KATZ, B. 1950. Some observations on biological noise. *Nature,* 166**,** 597.

FATT, P. & KATZ, B. 1952. Spontaneous subthreshold activity at motor nerve endings. *The Journal of physiology,* 117**,** 109-128.

FEI, H. & KRANTZ, D. 2009. Vesicular neurotransmitter transporters. *Handbook of Neurochemistry and Molecular Neurobiology.* Springer.

FERREIRA-VIEIRA, T., GUIMARAES, I., SILVA, F. & RIBEIRO, F. 2016. Alzheimer's disease: targeting the cholinergic system. *Current neuropharmacology,* 14**,** 101-115.

FEYEREISEN, R. 2012. 8 - Insect CYP Genes and P450 Enzymes A2 - Gilbert, Lawrence I. *Insect Molecular Biology and Biochemistry.* San Diego: Academic Press.

FEYEREISEN, R., DERMAUW, W. & VAN LEEUWEN, T. 2015. Genotype to phenotype, the molecular and physiological dimensions of resistance in arthropods. *Pesticide Biochemistry and Physiology,* 121**,** 61-77.

FORIEL, S., WILLEMS, P., SMEITINK, J., SCHENCK, A. & BEYRATH, J. 2015. Mitochondrial diseases: *Drosophila melanogaster* as a model to evaluate potential therapeutics. *The international journal of biochemistry & cell biology,* 63**,** 60-65.

FOSTER, K. A., CROWLEY, J. J. & REGEHR, W. G. 2005. The influence of multivesicular release and postsynaptic receptor saturation on transmission at granule cell to Purkinje cell synapses. *Journal of Neuroscience,* 25**,** 11655-11665.

FRADKIN, L. G., BAINES, R. A., VAN DER PLAS, M. C. & NOORDERMEER, J. N. 2008. The dystrophin Dp186 isoform regulates neurotransmitter release at a central synapse in *Drosophila*. *Journal of Neuroscience,* 28**,** 5105-5114.

FRANK, C. A., KENNEDY, M. J., GOOLD, C. P., MAREK, K. W. & DAVIS, G. W. 2006. Mechanisms underlying the rapid induction and sustained expression of synaptic homeostasis. *Neuron,* 52**,** 663-677.

FREMEAU, R. T., BURMAN, J., QURESHI, T., TRAN, C. H., PROCTOR, J., JOHNSON, J., ZHANG, H., SULZER, D., COPENHAGEN, D. R. & STORM-MATHISEN, J. 2002. The identification of vesicular glutamate transporter 3 suggests novel modes of signaling by glutamate. *Proceedings of the National Academy of Sciences,* 99**,** 14488-14493.

FUSHIKI, A., ZWART, M. F., KOHSAKA, H., FETTER, R. D., CARDONA, A. & NOSE, A. 2016. A circuit mechanism for the propagation of waves of muscle contraction in *Drosophila*. *Elife,* 5.

GERMAN, C. L., BALADI, M. G., MCFADDEN, L. M., HANSON, G. R. & FLECKENSTEIN, A. E. 2015. Regulation of the dopamine and vesicular monoamine transporters: pharmacological targets and implications for disease. *Pharmacological reviews,* 67**,** 1005-1024.

GODA, Y. & STEVENS, C. F. 1994. Two components of transmitter release at a central synapse. *Proceedings of the National Academy of Sciences,* 91**,** 12942-12946.

GORCZYCA, M. G. & HALL, J. C. 1987. Immunohistochemical localization of choline acetyltransferase during development and in Chats mutants of *Drosophila melanogaster*. *Journal of Neuroscience,* 7**,** 1361-1369.

GOULSON, D. 2013. An overview of the environmental risks posed by neonicotinoid insecticides. *Journal of Applied Ecology,* 50**,** 977-987.

GRANDISON, R. C., PIPER, M. D. & PARTRIDGE, L. 2009. Amino-acid imbalance explains extension of lifespan by dietary restriction in *Drosophila*. *Nature,* 462**,** 1061.

GRANDO, S. A., PITTELKOW, M. R. & SCHALLREUTER, K. U. 2006. Adrenergic and cholinergic control in the biology of epidermis: physiological and clinical significance. *Journal of Investigative Dermatology,* 126**,** 1948-1965.

GRAUSO, M., REENAN, R., CULETTO, E. & SATTELLE, D. 2002. Novel putative nicotinic acetylcholine receptor subunit genes, Dα5, Dα6 and Dα7, in *Drosophila melanogaster* identify a new and highly conserved target of adenosine deaminase acting on RNA-mediated A-to-I pre-mRNA editing. *Genetics,* 160**,** 1519-1533.

GRILLNER, S. 1985. Neurobiological bases of rhythmic motor acts in vertebrates. *Science,* 228**,** 143-149.

GULYÁS, A., MILES, R., SIK, A., TOTH, K., TAMAMAKI, N. & FREUND, T. 1993. Hippocampal pyramidal cells excite inhibitory neurons through a single release site. *Nature,* 366**,** 683.

GUNAYDIN, L. A., YIZHAR, O., BERNDT, A., SOHAL, V. S., DEISSEROTH, K. & HEGEMANN, P. 2010. Ultrafast optogenetic control. *Nature neuroscience,* 13**,** 387.

GUO, F., WANG, Y., LIU, J., MOK, S., XUE, F. & ZHANG, W. 2016a. CXCL12/CXCR4: a symbiotic bridge linking cancer cells and their stromal neighbors in oncogenic communication networks. *Oncogene,* 35**,** 816.

GUO, Z., LUCCHETTA, E., RAFEL, N. & OHLSTEIN, B. 2016b. Maintenance of the adult *Drosophila* intestine: all roads lead to homeostasis. *Current opinion in genetics & development,* 40**,** 81-86.

HARTENSTEIN, V. & WODARZ, A. 2013. Initial neurogenesis in *Drosophila*. *Wiley Interdisciplinary Reviews: Developmental Biology,* 2**,** 701-721.

HECKSCHER, E. S., LOCKERY, S. R. & DOE, C. Q. 2012. Characterization of *Drosophila* larval crawling at the level of organism, segment, and somatic body wall musculature. *Journal of Neuroscience,* 32**,** 12460-12471.

HECKSCHER, E. S., ZARIN, A. A., FAUMONT, S., CLARK, M. Q., MANNING, L., FUSHIKI, A., SCHNEIDER-MIZELL, C. M., FETTER, R. D., TRUMAN, J. W. & ZWART, M. F. 2015. Even-skipped+ interneurons are core components of a sensorimotor circuit that maintains left-right symmetric muscle contraction amplitude. *Neuron,* 88**,** 314-329.

HEUSER, J. & REESE, T. 1973. Evidence for recycling of synaptic vesicle membrane during transmitter release at the frog neuromuscular junction. *The Journal of cell biology,* 57**,** 315-344.

HEUSER, J., REESE, T., DENNIS, M., JAN, Y., JAN, L. & EVANS, L. 1979. Synaptic vesicle exocytosis captured by quick freezing and correlated with quantal transmitter release. *The Journal of cell biology,* 81**,** 275-300.

HORIUCHI, Y., KIMURA, R., KATO, N., FUJII, T., SEKI, M., ENDO, T., KATO, T. & KAWASHIMA, K. 2003. Evolutional study on acetylcholine expression. *Life Sciences,* 72**,** 1745-1756.

HOYER, R. F. & PLAPP JR, F. W. 1966. A gross genetic analysis of two DDT-resistant house fly strains. *Journal of economic entomology,* 59**,** 495-501.

HUA, Z., LEAL-ORTIZ, S., FOSS, S. M., WAITES, C. L., GARNER, C. C., VOGLMAIER, S. M. & EDWARDS, R. H. 2011. v-SNARE composition distinguishes synaptic vesicle pools. *Neuron,* 71**,** 474-487.

HUANG, C.-H., BAO, J. & SAKABA, T. 2010. Multivesicular release differentiates the reliability of synaptic transmission between the visual cortex and the somatosensory cortex. *Journal of Neuroscience,* 30**,** 11994-12004.

HUNTWORK, S. & LITTLETON, J. T. 2007. A complexin fusion clamp regulates spontaneous neurotransmitter release and synaptic growth. *Nature neuroscience,* 10**,** 1235.

HURTADO-LORENZO, A., SKINNER, M., EL ANNAN, J., FUTAI, M., SUN-WADA, G.-H., BOURGOIN, S., CASANOVA, J., WILDEMAN, A., BECHOUA, S. & AUSIELLO, D. A. 2006. V-ATPase interacts with ARNO and Arf6 in early endosomes and regulates the protein degradative pathway. *Nature cell biology,* 8**,** 124.

IREMONGER, K. J. & BAINS, J. S. 2016. Asynchronous presynaptic glutamate release enhances neuronal excitability during the post-spike refractory period. *The Journal of physiology,* 594**,** 1005-1015.

JANICKOVA, H., PRADO, V. F., PRADO, M. A., EL MESTIKAWY, S. & BERNARD, V. 2017. Vesicular Acetylcholine Transporter (*VAChT*) overexpression induces major modifications of striatal cholinergic interneuron morphology and function. *Journal of neurochemistry*.

JARAMILLO-O, N., FONSECA-GONZALEZ, I. & CHAVERRA-RODRÍGUEZ, D. 2014. Geometric morphometrics of nine field isolates of *Aedes aegypti* with different resistance levels to lambda-cyhalothrin and relative fitness of one artificially selected for resistance. *PLoS One,* 9**,** e96379.

JIN, Y., TIAN, N., CAO, J., LIANG, J., YANG, Z. & LV, J. 2007. RNA editing and alternative splicing of the insect nAChR subunit alpha6 transcript: evolutionary conservation, divergence and regulation. *BMC Evolutionary Biology,* 7**,** 98.

JONES, A. K., RAYMOND-DELPECH, V., THANY, S. H., GAUTHIER, M. & SATTELLE, D. B. 2006. The nicotinic acetylcholine receptor gene family of the honey bee, *Apis mellifera*. *Genome research,* 16**,** 1422-1430.

KAESER, P. S. & REGEHR, W. G. 2014. Molecular mechanisms for synchronous, asynchronous, and spontaneous neurotransmitter release. *Annual review of physiology,* 76**,** 333-363.

KANE, P. M. 1995. Disassembly and reassembly of the yeast vacuolar H+-ATPase in vivo. *Journal of Biological Chemistry,* 270**,** 17025-17032.

KAVALALI, E. T. 2015. The mechanisms and functions of spontaneous neurotransmitter release. *Nature Reviews Neuroscience,* 16**,** 5.

KETTNER, C., BERTL, A., OBERMEYER, G., SLAYMAN, C. & BIHLER, H. 2003. Electrophysiological analysis of the yeast V-type proton pump: variable coupling ratio and proton shunt. *Biophysical journal,* 85**,** 3730-3738.

KIM, M.-H. & HERSH, L. B. 2004. The vesicular acetylcholine transporter interacts with clathrin-associated adaptor complexes AP-1 and AP-2. *Journal of Biological Chemistry,* 279**,** 12580-12587.

KING, D. G. & WYMAN, R. J. 1980. Anatomy of the giant fibre pathway in *Drosophila*. I. Three thoracic components of the pathway. *Journal of neurocytology,* 9**,** 753-770.

KITAMOTO, T., WANG, W. & SALVATERRA, P. M. 1998. Structure and Organization of the *Drosophila* Cholinergic Locus. *Journal of Biological Chemistry,* 273**,** 2706-2713.

KITAMOTO, T., XIE, X., WU, C. F. & SALVATERRA, P. M. 2000. Isolation and characterization of mutants for the vesicular acetylcholine transporter gene in *Drosophila melanogaster*. *Developmental Neurobiology,* 42**,** 161-171.

KUHAR, M. J. & MURRIN, L. C. 1978. SODIUM-DEPENDENT, HIGH AFFINITY CHOLINE UPTAKE. *Journal of neurochemistry,* 30**,** 15-21.

KUROMI, H. & KIDOKORO, Y. 1998. Two distinct pools of synaptic vesicles in single presynaptic boutons in a temperature-sensitive *Drosophila* mutant, shibire. *Neuron,* 20**,** 917-925.

KUROMI, H. & KIDOKORO, Y. 2000. Tetanic stimulation recruits vesicles from reserve pool via a cAMP-mediated process in *Drosophila* synapses. *Neuron,* 27**,** 133-143.

LABBÉ, P., BERTHOMIEU, A., BERTICAT, C., ALOUT, H., RAYMOND, M., LENORMAND, T. & WEILL, M. 2007. Independent Duplications of the Acetylcholinesterase Gene Conferring Insecticide Resistance in the Mosquito *Culex pipiens*. *Molecular Biology and Evolution,* 24**,** 1056-1067.

LABRADOR, J. P., O'KEEFE, D., YOSHIKAWA, S., MCKINNON, R. D., THOMAS, J. B. & BASHAW, G. J. 2005. The homeobox transcription factor even-skipped regulates netrin-receptor expression to control dorsal motor-axon projections in *Drosophila*. *Current biology,* 15**,** 1413-1419.

LAGOW, R. D., BAO, H., COHEN, E. N., DANIELS, R. W., ZUZEK, A., WILLIAMS, W. H., MACLEOD, G. T., SUTTON, R. B. & ZHANG, B. 2007. Modification of a hydrophobic layer by a point mutation in syntaxin 1A regulates the rate of synaptic vesicle fusion. *PLoS biology,* 5**,** e72.

LANDGRAF, M. & THOR, S. Development of *Drosophila* motoneurons: specification and morphology. Seminars in cell & developmental biology, 2006. Elsevier, 3-11.

LAWAL, H. O. & KRANTZ, D. E. 2013. SLC18: Vesicular neurotransmitter transporters for monoamines and acetylcholine. *Molecular aspects of medicine,* 34**,** 360-372.

LAYDEN, M. J., ODDEN, J. P., SCHMID, A., GARCES, A., THOR, S. & DOE, C. Q. 2006. Zfh1, a somatic motor neuron transcription factor, regulates axon exit from the CNS. *Developmental biology,* 291**,** 253-263.

LEE, D. & O'DOWD, D. K. 1999. Fast excitatory synaptic transmission mediated by nicotinic acetylcholine receptors in *Drosophila* neurons. *Journal of Neuroscience,* 19**,** 5311-5321.

LEMON, W. C., PULVER, S. R., HÖCKENDORF, B., MCDOLE, K., BRANSON, K., FREEMAN, J. & KELLER, P. J. 2015. Whole-central nervous system functional imaging in larval *Drosophila*. *Nature communications,* 6**,** 7924.

LI, H., WYMAN, T., YU, Z. X., LI, S. H. & LI, X. J. 2003. Abnormal association of mutant huntingtin with synaptic vesicles inhibits glutamate release. *Human Molecular Genetics,* 12**,** 2021-2030.

LI, X., MA, L., SUN, L. & ZHU, C. 2002. Biotic characteristics in the deltamethrin-susceptible and resistant strains of *Culex pipiens pallens* (Diptera: Culicidae) in China. *Applied entomology and zoology,* 37**,** 305-308.

LI, Y. C. & KAVALALI, E. T. 2017. Synaptic vesicle-recycling machinery components as potential therapeutic targets. *Pharmacological reviews,* 69**,** 141-160.

LIANG, Z., BROOKS, J., WILLARD, M., LIANG, K., YOON, Y., KANG, S. & SHIM, H. 2007. CXCR4/CXCL12 axis promotes VEGF-mediated tumor angiogenesis through Akt signaling pathway. *Biochemical and biophysical research communications,* 359**,** 716-722.

LICURSI, M., CHRISTIAN, S., PONGNOPPARAT, T. & HIRASAWA, K. 2011. In vitro and in vivo comparison of viral and cellular internal ribosome entry sites for bicistronic vector expression. *Gene therapy,* 18**,** 631.

LIMA, R. D. F., PRADO, V. F., PRADO, M. A. & KUSHMERICK, C. 2010. Quantal release of acetylcholine in mice with reduced levels of the vesicular acetylcholine transporter. *Journal of neurochemistry,* 113**,** 943-951.

LINK, E., EDELMANN, L., CHOU, J. H., BINZ, T., YAMASAKI, S., EISEL, U., BAUMERT, M., SÜDHOF, T. C., NIEMANN, H. & JAHN, R. 1992. Tetanus toxin action: inhibition of neurotransmitter release linked to synaptobrevin proteolysis. *Biochemical and biophysical research communications,* 189**,** 1017-1023.

MA, C., SU, L., SEVEN, A. B., XU, Y. & RIZO, J. 2013. Reconstitution of the vital functions of Munc18 and Munc13 in neurotransmitter release. *Science,* 339**,** 421-425.

MACKENZIE, K. D., LUMSDEN, A. L., GUO, F., DUFFIELD, M. D., CHATAWAY, T., LIM, Y., ZHOU, X. F. & KEATING, D. J. 2016. Huntingtin-associated protein-1 is a synapsin I-binding protein regulating synaptic vesicle exocytosis and synapsin I trafficking. *Journal of neurochemistry,* 138**,** 710-721.

MAIENFISCH, P., CASSAYRE, J., CEDERBAUM, F., CORSI, C., MOLLEYRES, L.-P., PITTERNA, T. & HILLESHEIM, E. Design, synthesis, and properties of acyclic spiroindoline insecticides. Abstracts of papers of the american chemical society, 2011a. Amer chemical soc 1155 16th St, NW, Washington, DC 20036.

MAIENFISCH, P., CASSAYRE, J. C., MOLLEYRES, L.-P., ROBERTS, R. S., HUGHES, D. J. & HILLESHEIM, E. Effect of halogen and trifluoromethyl substituents on the biological activity of spiroindolines. Abstracts of papers of the american chemical society, 2011b. Amer chemical soc 1155 16th St, NW, Washington, DC 20036.

MAIENFISCH, P., ROBERTS, R. S., CASSAYRE, J., MOLLEYRES, L.-P., WINKLER, T. & HILLESHEIM, E. Synthesis and biological activity of spiroindoline N-oxides. Abstracts of papers of the american chemical society, 2011c. Amer chemical soc 1155 16th St, NW, Washington, DC 20036.

MALLET, J., HOUHOU, L., PAJAK, F., ODA, Y., CERVINI, R., BEJANIN, S. & BERRARD, S. 1998. The cholinergic locus: *ChAT* and *VAChT* genes. *Journal of Physiology-paris,* 92**,** 145-147.

MARDER, E. & BUCHER, D. 2001. Central pattern generators and the control of rhythmic movements. *Current biology,* 11**,** R986-R996.

MARDER, E. & BUCHER, D. 2007. Understanding circuit dynamics using the stomatogastric nervous system of lobsters and crabs. *Annu. Rev. Physiol.,* 69**,** 291-316.

MARLEY, R. & BAINES, R. A. 2011. Increased persistent Na^+ current contributes to seizure in the slamdance bang-sensitive *Drosophila* mutant. *Journal of neurophysiology,* 106**,** 18-29.

MARTIN, C. A. & KRANTZ, D. E. 2014. *Drosophila melanogaster* as a genetic model system to study neurotransmitter transporters. *Neurochemistry international,* 73**,** 71-88.

MARTINS, A. J., BELLINATO, D. F., PEIXOTO, A. A., VALLE, D. & LIMA, J. B. P. 2012. Effect of insecticide resistance on development, longevity and reproduction of field or laboratory selected *Aedes aegypti* populations. *PLoS One,* 7**,** e31889.

MAXSON, M. E. & GRINSTEIN, S. 2014. The vacuolar-type H+-ATPase at a glance–more than a proton pump. The Company of Biologists Ltd.

MAYCOX, P., DECKWERTH, T., HELL, J. & JAHN, R. 1988. Glutamate uptake by brain synaptic vesicles. Energy dependence of transport and functional reconstitution in proteoliposomes. *Journal of Biological Chemistry,* 263**,** 15423-15428.

MAZERE, J., SIBON, I., MESSNER, W., MAYO, W., BARRET, O., GUILLOTEAU, D., TISON, F. & ALLARD, M. 2009. Cholinergic impairment in Parkinson Plus Syndrome: A molecular imaging study. *Alzheimer's & Dementia: The Journal of the Alzheimer's Association,* 5**,** P489.

MCGUIRE, S. E., DESHAZER, M. & DAVIS, R. L. 2005. Thirty years of olfactory learning and memory research in *Drosophila melanogaster*. *Progress in neurobiology,* 76**,** 328-347.

MCINTIRE, S. L., REIMER, R. J., SCHUSKE, K., EDWARDS, R. H. & JORGENSEN, E. M. 1997. Identification and characterization of the vesicular GABA transporter. *Nature,* 389**,** 870.

MERKULOVA, M., BAKULINA, A., THAKER, Y. R., GRÜBER, G. & MARSHANSKY, V. 2010. Specific motifs of the V-ATPase a2-subunit isoform interact with catalytic and regulatory domains of ARNO. *Biochimica et Biophysica Acta (BBA)-Bioenergetics,* 1797**,** 1398-1409.

METCALF, R. L. 1989. Insect resistance to insecticides. *Pest Management Science,* 26**,** 333-358.

METZEN, J., BITTINGER, F., KIRKPATRICK, C. J., KILBINGER, H. & WESSLER, I. 2003. Proliferative effect of acetylcholine on rat trachea epithelial cells is mediated by nicotinic receptors and muscarinic receptors of the M1-subtype. *Life Sciences,* 72**,** 2075-2080.

MILJKOVIC-LICINA, M., GAUCHAT, D. & GALLIOT, B. 2004. Neuronal evolution: analysis of regulatory genes in a first-evolved nervous system, the hydra nervous system. *Biosystems,* 76**,** 75-87.

MITTELSTAEDT, T., ALVARÉZ-BARON, E. & SCHOCH, S. 2010. RIM proteins and their role in synapse function. *Biological chemistry,* 391**,** 599-606.

MUMM, J. S. & KOPAN, R. 2000. Notch signaling: from the outside in. *Developmental biology,* 228**,** 151-165.

NAQQASH, M. N., GÖKÇE, A., BAKHSH, A. & SALIM, M. 2016. Insecticide resistance and its molecular basis in urban insect pests. *Parasitology research,* 115**,** 1363-1373.

NEFF, R. A., CONROY, W. G., SCHOELLERMAN, J. D. & BERG, D. K. 2009. Synchronous and asynchronous transmitter release at nicotinic synapses are differentially regulated by postsynaptic PSD-95 proteins. *Journal of Neuroscience,* 29**,** 15770-15779.

NGUYEN, M. L., COX, G. D. & PARSONS, S. M. 1998. Kinetic parameters for the vesicular acetylcholine transporter: two protons are exchanged for one acetylcholine. *Biochemistry,* 37**,** 13400-13410.

NICHOLS, C. D. 2006. *Drosophila melanogaster* neurobiology, neuropharmacology, and how the fly can inform central nervous system drug discovery. *Pharmacology & therapeutics,* 112**,** 677-700.

NÚÑEZ, E., PÉREZ-SILES, G., RODENSTEIN, L., ALONSO-TORRES, P., ZAFRA, F., JIMÉNEZ, E., ARAGÓN, C. & LÓPEZ-CORCUERA, B. 2009. Subcellular localization of the neuronal glycine transporter *GLYT2* in brainstem. *Traffic,* 10**,** 829-843.

OAKESHOTT, J., CLAUDIANOS, C., CAMPBELL, P., NEWCOMB, R., RUSSELL, R. & GILBERT, L. 2005. Biochemical genetics and genomics of insect esterases. *Comprehensive molecular insect science. Volume,* 5.

OERKE, E.-C. 2006. Crop losses to pests. *The Journal of Agricultural Science,* 144**,** 31-43.

OKUDA, T., HAGA, T., KANAI, Y., ENDOU, H., ISHIHARA, T. & KATSURA, I. 2000. Identification and characterization of the high-affinity choline transporter. *Nature neuroscience,* 3**,** 120.

OLIVEIRA, C., AUAD, A., MENDES, S. & FRIZZAS, M. 2014. Crop losses and the economic impact of insect pests on Brazilian agriculture. *Crop Protection,* 56**,** 50-54.

ORR, B. O., FETTER, R. D. & DAVIS, G. W. 2017. Retrograde semaphorin–plexin signalling drives homeostatic synaptic plasticity. *Nature,* 550**,** 109.

OWEN, M. D. 2000. Current use of transgenic herbicide-resistant soybean and corn in the USA. *Crop Protection,* 19**,** 765-771.

PACK-CHUNG, E., KURSHAN, P. T., DICKMAN, D. K. & SCHWARZ, T. L. 2007. A *Drosophila* kinesin required for synaptic bouton formation and synaptic vesicle transport. *Nature neuroscience,* 10**,** 980.

PAIN, V. M. 1996. Initiation of protein synthesis in eukaryotic cells. *The FEBS Journal,* 236**,** 747-771.

PAK, W. L. 1995. *Drosophila* in vision research. The Friedenwald Lecture. *Investigative Ophthalmology & Visual Science,* 36**,** 2340-2357.

PARADIS, S., SWEENEY, S. T. & DAVIS, G. W. 2001. Homeostatic control of presynaptic release is triggered by postsynaptic membrane depolarization. *Neuron,* 30**,** 737-749.

PARSONS, R. L., CALUPCA, M. A., MERRIAM, L. A. & PRIOR, C. 1999. Empty synaptic vesicles recycle and undergo exocytosis at vesamicol-treated motor nerve terminals. *Journal of neurophysiology,* 81**,** 2696-2700.

PARSONS, S. M. 2000. Transport mechanisms in acetylcholine and monoamine storage. *The FASEB Journal,* 14**,** 2423-2434.

PARSONS, S. M., PRIOR, C. & MARSHALL, I. G. 1993. Acetylcholine transport, storage, and release. *International review of neurobiology.* Elsevier.

PAVLOV, V. A. & TRACEY, K. J. 2005. The cholinergic anti-inflammatory pathway. *Brain, behavior, and immunity,* 19**,** 493-499.

PEARSON, K. G. 1995. Proprioceptive regulation of locomotion. *Current opinion in neurobiology,* 5**,** 786-791.

PETERS, J., WALSH, M. & FRANKE, W. 1990. An abundant and ubiquitous homo-oligomeric ring-shaped ATPase particle related to the putative vesicle fusion proteins Sec18p and NSF. *The EMBO journal,* 9**,** 1757-1767.

PETERSEN, S. A., FETTER, R. D., NOORDERMEER, J. N., GOODMAN, C. S. & DIANTONIO, A. 1997. Genetic analysis of glutamate receptors in *Drosophila* reveals a retrograde signal regulating presynaptic transmitter release. *Neuron,* 19**,** 1237-1248.

PING, Y. & TSUNODA, S. 2012. Inactivity-induced increase in nAChRs upregulates Shal K+ channels to stabilize synaptic potentials. *Nature neuroscience,* 15**,** 90.

POËA-GUYON, S., AMMAR, M. R., ERARD, M., AMAR, M., MOREAU, A. W., FOSSIER, P., GLEIZE, V., VITALE, N. & MOREL, N. 2013. The V-ATPase membrane domain is a sensor of granular pH that controls the exocytotic machinery. *J Cell Biol,* 203**,** 283-298.

POTTER, C. J., TURENCHALK, G. S. & XU, T. 2000. *Drosophila* in cancer research: an expanding role. *TRENDS in Genetics,* 16**,** 33-39.

PRADO, V. F., MARTINS-SILVA, C., DE CASTRO, B. M., LIMA, R. F., BARROS, D. M., AMARAL, E., RAMSEY, A. J., SOTNIKOVA, T. D., RAMIREZ, M. R. & KIM, H.-G. 2006. Mice deficient for the vesicular acetylcholine transporter are myasthenic and have deficits in object and social recognition. *Neuron,* 51**,** 601-612.

PRADO, V. F., ROY, A., KOLISNYK, B., GROS, R. & PRADO, M. A. 2013. Regulation of cholinergic activity by the vesicular acetylcholine transporter. *Biochemical Journal,* 450**,** 265-274.

PULVER, S. R., BAYLEY, T. G., TAYLOR, A. L., BERNI, J., BATE, M. & HEDWIG, B. 2015. Imaging fictive locomotor patterns in larval *Drosophila*. *Journal of neurophysiology,* 114**,** 2564-2577.

PULVER, S. R., PASHKOVSKI, S. L., HORNSTEIN, N. J., GARRITY, P. A. & GRIFFITH, L. C. 2009. Temporal dynamics of neuronal activation by Channelrhodopsin-2 and TRPA1 determine behavioral output in *Drosophila* larvae. *Journal of neurophysiology,* 101**,** 3075-3088.

RAMIREZ, D. M. & KAVALALI, E. T. 2011. Differential regulation of spontaneous and evoked neurotransmitter release at central synapses. *Current opinion in neurobiology,* 21**,** 275-282.

RAMIREZ, D. M., KHVOTCHEV, M., TRAUTERMAN, B. & KAVALALI, E. T. 2012. *Vti1a* identifies a vesicle pool that preferentially recycles at rest and maintains spontaneous neurotransmission. *Neuron,* 73**,** 121-134.

RANSON, H. & HEMINGWAY, J. 2005. 5.11 - Glutathione Transferases A2 - Gilbert, Lawrence I. *Comprehensive Molecular Insect Science.* Amsterdam: Elsevier.

RAO, S. S., STEWART, B. A., RIVLIN, P. K., VILINSKY, I., WATSON, B. O., LANG, C., BOULIANNE, G., SALPETER, M. M. & DEITCHER, D. L. 2001. Two distinct effects on neurotransmission in a temperature-sensitive SNAP-25 mutant. *The EMBO Journal,* 20**,** 6761-6771.

REDMAN, S. & WALMSLEY, B. 1983. Amplitude fluctuations in synaptic potentials evoked in cat spinal motoneurones at identified group Ia synapses. *The Journal of physiology,* 343**,** 135-145.

REINHEIMER, T., MOHLIG, T., ZIMMERMANN, S., HOHLE, K.-D. & WESSLER, I. 2000. Muscarinic control of histamine release from airways: inhibitory M1-receptors in human bronchi but absence in rat trachea. *American journal of respiratory and critical care medicine,* 162**,** 534-538.

REN, G. R., FOLKE, J., HAUSER, F., LI, S. & GRIMMELIKHUIJZEN, C. J. 2015. The A-and B-type muscarinic acetylcholine receptors from *Drosophila melanogaster* couple to different second messenger pathways. *Biochemical and biophysical research communications,* 462**,** 358-364.

RICHMOND, J. E., WEIMER, R. M. & JORGENSEN, E. M. 2001. An open form of syntaxin bypasses the requirement for UNC-13 in vesicle priming. *Nature,* 412**,** 338.

RIZO, J. & SÜDHOF, T. C. 2012. The membrane fusion enigma: SNAREs, Sec1/Munc18 proteins, and their accomplices—guilty as charged? *Annual review of cell and developmental biology,* 28**,** 279-308.

RIZZOLI, S. O. & BETZ, W. J. 2005. Synaptic vesicle pools. *Nature Reviews Neuroscience,* 6**,** 57.

ROBERTS, A., SOFFE, S. R., WOLF, E. S., YOSHIDA, M. & ZHAO, F. Y. 1998. Central circuits controlling locomotion in young frog tadpoles. *Annals of the New York Academy of Sciences.*

RODRIGUES, H. A., FONSECA, M. D. C., CAMARGO, W. L., LIMA, P. M., MARTINELLI, P. M., NAVES, L. A., PRADO, V. F., PRADO, M. A. & GUATIMOSIM, C. 2013. Reduced expression of the vesicular acetylcholine transporter and neurotransmitter content affects synaptic vesicle distribution and shape in mouse neuromuscular junction. *PLoS One,* 8**,** e78342.

ROHRBOUGH, J. & BROADIE, K. 2002. Electrophysiological analysis of synaptic transmission in central neurons of *Drosophila* larvae. *Journal of neurophysiology,* 88**,** 847-860.

ROSAHL, T. W., SPILLANE, D., MISSLER, M., HERZ, J., SELIG, D. K., WOLFF, J. R., HAMMER, R. E., MALENKA, R. C. & SÜDHOF, T. C. 1995. Essential functions of synapsins I and II in synaptic vesicle regulation. *Nature,* 375**,** 488-493.

ROST, B. R., SCHNEIDER, F., GRAUEL, M. K., WOZNY, C., BENTZ, C. G., BLESSING, A., ROSENMUND, T., JENTSCH, T. J., SCHMITZ, D. & HEGEMANN, P. 2015. Optogenetic acidification of synaptic vesicles and lysosomes. *Nature neuroscience,* 18**,** 1845.

RUDOLPH, S., TSAI, M.-C., VON GERSDORFF, H. & WADICHE, J. I. 2015. The ubiquitous nature of multivesicular release. *Trends in neurosciences,* 38**,** 428-438.

SACHS, J. & MALANEY, P. 2002. The economic and social burden of malaria. *Nature,* 415**,** 680.

SAGNÉ, C., EL MESTIKAWY, S., ISAMBERT, M.-F., HAMON, M., HENRY, J.-P., GIROS, B. & GASNIER, B. 1997. Cloning of a functional vesicular GABA and glycine transporter by screening of genome databases. *FEBS letters,* 417**,** 177-183.

SAKAMOTO, T. 2006. Phytohormones and rice crop yield: strategies and opportunities for genetic improvement. *Transgenic research,* 15**,** 399-404.

SALVATERRA, P. M. & KITAMOTO, T. 2001. *Drosophila* cholinergic neurons and processes visualized with GAL4/UAS–GFP. *Gene Expression Patterns,* 1**,** 73-82.

SANDOVAL, G. M., DUERR, J. S., HODGKIN, J., RAND, J. B. & RUVKUN, G. 2006. A genetic interaction between the vesicular acetylcholine transporter *VAChT/UNC-17* and synaptobrevin/SNB-1 in C. elegans. *Nature neuroscience,* 9**,** 599.

SARA, Y., VIRMANI, T., DEÁK, F., LIU, X. & KAVALALI, E. T. 2005. An isolated pool of vesicles recycles at rest and drives spontaneous neurotransmission. *Neuron,* 45**,** 563-573.

SATTELLE, D., JONES, A., SATTELLE, B., MATSUDA, K., REENAN, R. & BIGGIN, P. 2005. Edit, cut and paste in the nicotinic acetylcholine receptor gene family of *Drosophila* melanogaster. *Bioessays,* 27**,** 366-376.

SAWRUK, E., SCHLOSS, P., BETZ, H. & SCHMITT, B. 1990. Heterogeneity of *Drosophila* nicotinic acetylcholine receptors: SAD, a novel developmentally regulated alpha-subunit. *The EMBO journal,* 9**,** 2671-2677.

SCHAEFER, M. H., WANKER, E. E. & ANDRADE-NAVARRO, M. A. 2012. Evolution and function of CAG/polyglutamine repeats in protein–protein interaction networks. *Nucleic acids research,* 40**,** 4273-4287.

SCHENCK, S., WOJCIK, S. M., BROSE, N. & TAKAMORI, S. 2009. A chloride conductance in VGLUT1 underlies maximal glutamate loading into synaptic vesicles. *Nature neuroscience,* 12**,** 156.

SCHIAVO, G. G., BENFENATI, F., POULAIN, B., ROSSETTO, O., DE LAURETO, P. P., DASGUPTA, B. R. & MONTECUCCO, C. 1992. Tetanus and botulinum-B neurotoxins block neurotransmitter release by proteolytic cleavage of synaptobrevin. *Nature,* 359**,** 832.

SCHOCH, S., DEÁK, F., KÖNIGSTORFER, A., MOZHAYEVA, M., SARA, Y., SÜDHOF, T. C. & KAVALALI, E. T. 2001. SNARE function analyzed in synaptobrevin/VAMP knockout mice. *Science,* 294**,** 1117-1122.

SEARL, T., PRIOR, C. & MARSHALL, I. 1991. Acetylcholine recycling and release at rat motor nerve terminals studied using (-)-vesamicol and troxpyrrolium. *The Journal of physiology,* 444**,** 99-116.

SHARP, A. A., SKINNER, F. K. & MARDER, E. 1996. Mechanisms of oscillation in dynamic clamp constructed two-cell half- center circuits. *Journal of Neurophysiology,* 76**,** 867-883.

SHONO, T., KASAI, S., KAMIYA, E., KONO, Y. & SCOTT, J. G. 2002. Genetics and mechanisms of permethrin resistance in the YPER strain of house fly. *Pesticide biochemistry and physiology,* 73**,** 27-36.

SHYTLE, R. D., MORI, T., TOWNSEND, K., VENDRAME, M., SUN, N., ZENG, J., EHRHART, J., SILVER, A. A., SANBERG, P. R. & TAN, J. 2004. Cholinergic modulation of microglial activation by α7 nicotinic receptors. *Journal of neurochemistry,* 89**,** 337-343.

SLUDER, A., SHAH, S., CASSAYRE, J., CLOVER, R., MAIENFISCH, P., MOLLEYRES, L.-P., HIRST, E. A., FLEMMING, A. J., SHI, M. & CUTLER, P. 2012. Spiroindolines identify the vesicular acetylcholine transporter as a novel target for insecticide action. *PLoS One,* 7**,** e34712.

SONG, H.-J., MING, G.-L., FON, E., BELLOCCHIO, E., EDWARDS, R. H. & POO, M.-M. 1997. Expression of a putative vesicular acetylcholine transporter facilitates quantal transmitter packaging. *Neuron,* 18**,** 815-826.

SOREQ, H. & SEIDMAN, S. 2001. Acetylcholinesterase—new roles for an old actor. *Nature Reviews Neuroscience,* 2**,** 294.

STREIT, A. K., FAN, Y. N., MASULLO, L. & BAINES, R. A. 2016. Calcium imaging of neuronal activity in *Drosophila* can identify anticonvulsive compounds. *PloS one,* 11**,** e0148461.

SÜDHOF, T. C. 2004. The synaptic vesicle cycle. *Annu. Rev. Neurosci.,* 27**,** 509-547.

SÜDHOF, T. C. 2013. Neurotransmitter release: the last millisecond in the life of a synaptic vesicle. *Neuron,* 80**,** 675-690.

SÜDHOF, T. C. & ROTHMAN, J. E. 2009. Membrane fusion: grappling with SNARE and SM proteins. *Science,* 323**,** 474-477.

SUGITA, S., FLEMING, L. L., WOOD, C., VAUGHAN, S. K., GOMES, M. P., CAMARGO, W., NAVES, L. A., PRADO, V. F., PRADO, M. A. & GUATIMOSIM, C. 2016. VAChT overexpression increases acetylcholine at the synaptic cleft and accelerates aging of neuromuscular junctions. *Skeletal muscle,* 6**,** 31.

SUTTON, M. A., ITO, H. T., CRESSY, P., KEMPF, C., WOO, J. C. & SCHUMAN, E. M. 2006. Miniature neurotransmission stabilizes synaptic function via tonic suppression of local dendritic protein synthesis. *Cell,* 125**,** 785-799.

SUZUKI, M., DESMOND, T. J., ALBIN, R. L. & FREY, K. A. 2001. Vesicular neurotransmitter transporters in Huntington's disease: initial observations and comparison with traditional synaptic markers. *Synapse,* 41**,** 329-336.

TABB, J., KISH, P. E., VAN DYKE, R. & UEDA, T. 1992. Glutamate transport into synaptic vesicles. Roles of membrane potential, pH gradient, and intravesicular pH. *Journal of Biological Chemistry,* 267**,** 15412-15418.

TAKAGI, S., COCANOUGHER, B. T., NIKI, S., MIYAMOTO, D., KOHSAKA, H., KAZAMA, H., FETTER, R. D., TRUMAN, J. W., ZLATIC, M. & CARDONA, A. 2017. Divergent Connectivity of Homologous Command-like Neurons Mediates Segment-Specific Touch Responses in *Drosophila*. *Neuron,* 96**,** 1373-1387. e6.

TAKAMORI, S. 2016. Presynaptic molecular determinants of quantal size. *Frontiers in synaptic neuroscience,* 8.

TAKAMORI, S., RHEE, J. S., ROSENMUND, C. & JAHN, R. 2000. Identification of a vesicular glutamate transporter that defines a glutamatergic phenotype in neurons. *Nature,* 407**,** 189-194.

TAKAMORI, S., RHEE, J. S., ROSENMUND, C. & JAHN, R. 2001. Identification of differentiation-associated brain-specific phosphate transporter as a second vesicular glutamate transporter (*VGLUT2*). *Journal of Neuroscience,* 21**,** RC182-RC182.

TAN, P. K., WAITES, C., LIU, Y., KRANTZ, D. E. & EDWARDS, R. H. 1998. A leucine-based motif mediates the endocytosis of vesicular monoamine and acetylcholine transporters. *Journal of Biological Chemistry,* 273**,** 17351-17360.

TAYLOR, P. & RADIC, Z. 1994. The cholinesterases: from genes to proteins. *Annual review of pharmacology and toxicology,* 34**,** 281-320.

THIAGARAJAN, T. C., LINDSKOG, M. & TSIEN, R. W. 2005. Adaptation to synaptic inactivity in hippocampal neurons. *Neuron,* 47**,** 725-737.

THIELE, A. 2013. Muscarinic signaling in the brain. *Annual review of neuroscience,* 36**,** 271-294.

TONG, G. & JAHR, C. E. 1994. Multivesicular release from excitatory synapses of cultured hippocampal neurons. *Neuron,* 12**,** 51-59.

TSUKIYAMA-KOHARA, K., IIZUKA, N., KOHARA, M. & NOMOTO, A. 1992. Internal ribosome entry site within hepatitis C virus RNA. *Journal of virology,* 66**,** 1476-1483.

TURRIGIANO, G. G., LESLIE, K. R., DESAI, N. S., RUTHERFORD, L. C. & NELSON, S. B. 1998. Activity-dependent scaling of quantal amplitude in neocortical neurons. *Nature,* 391**,** 892.

USDIN, T. B., EIDEN, L. E., BONNER, T. I. & ERICKSON, J. D. 1995. Molecular biology of the vesicular ACh transporter. *Trends in neurosciences,* 18**,** 218-224.

VAN DER KLOOT, W. 2003. Loading and recycling of synaptic vesicles in the Torpedo electric organ and the vertebrate neuromuscular junction. *Progress in neurobiology,* 71**,** 269-303.

VAN LIEFFERINGE, J., MASSIE, A., PORTELLI, J., DI GIOVANNI, G. & SMOLDERS, I. 2013. Are vesicular neurotransmitter transporters potential treatment targets for temporal lobe epilepsy? *Frontiers in cellular neuroscience,* 7**,** 139.

VAROQUI, H. & ERICKSON, J. D. 1996. Active transport of acetylcholine by the human vesicular acetylcholine transporter. *Journal of Biological Chemistry,* 271**,** 27229-27232.

WEN, H., LINHOFF, M. W., MCGINLEY, M. J., LI, G.-L., CORSON, G. M., MANDEL, G. & BREHM, P. 2010. Distinct roles for two synaptotagmin isoforms in synchronous and asynchronous transmitter release at zebrafish neuromuscular junction. *Proceedings of the National Academy of Sciences,* 107**,** 13906-13911.

WESSLER, I., GÄRTNER, H.-A., MICHEL-SCHMIDT, R., BROCHHAUSEN, C., SCHMITZ, L., ANSPACH, L., GRÜNEWALD, B. & KIRKPATRICK, C. J. 2016. Honeybees produce millimolar concentrations of non-neuronal acetylcholine for breeding: possible adverse effects of neonicotinoids. *PLoS One,* 11**,** e0156886.

WESSLER, I. & KIRKPATRICK, C. 2008. Acetylcholine beyond neurons: the non-neuronal cholinergic system in humans. *British journal of pharmacology,* 154**,** 1558-1571.

WESSLER, I. K. & KIRKPATRICK, C. J. 2017. Non-neuronal acetylcholine involved in reproduction in mammals and honeybees. *Journal of neurochemistry,* 142**,** 144-150.

WILLIAMS, J. 1997. How does a vesicle know it is full? *Neuron,* 18**,** 683-686.

WILSON, D. M. 1961. The central nervous control of flight in a locust. *Journal of Experimental Biology,* 38**,** 471-490.

WILSON, N. R., KANG, J., HUESKE, E. V., LEUNG, T., VAROQUI, H., MURNICK, J. G., ERICKSON, J. D. & LIU, G. 2005. Presynaptic regulation of quantal size by the vesicular glutamate transporter *VGLUT1*. *Journal of Neuroscience,* 25**,** 6221-6234.

XU, T. & FORGAC, M. 2001. Microtubules are involved in glucose-dependent dissociation of the yeast vacuolar [H+]-ATPase in vivo. *Journal of Biological Chemistry,* 276**,** 24855-24861.

YAMAMURA, H. I. & SNYDER, S. H. 1972. Choline: high-affinity uptake by rat brain synaptosomes. *Science,* 178**,** 626-628.

YAN, J., ZHAO, W., GUO, M., HAN, X. & FENG, Z. 2016. CXCL12 Regulates the Cholinergic Locus and *CHT1* Through *Akt* Signaling Pathway. *Cellular Physiology and Biochemistry,* 40**,** 982-992.

YANG, H. & KUNES, S. 2004. Non-vesicular release of acetylcholine is required for axon targeting in the *Drosophila* visual system. *Proceedings of the National Academy of Sciences of the United States of America,* 101**,** 15213-15218.

YASUYAMA, K. & SALVATERRA, P. M. 1999. Localization of choline acetyltransferase-expressing neurons in *Drosophila* nervous system. *Microscopy research and technique,* 45**,** 65-79.

YEATES, C. J., ZWIEFELHOFER, D. J. & FRANK, C. A. 2017. The Maintenance of Synaptic Homeostasis at the *Drosophila* Neuromuscular Junction Is Reversible and Sensitive to High Temperature. *eNeuro***,** ENEURO. 0220-17.2017.

ZHANG, J. 2003. Evolution by gene duplication: an update. *Trends in ecology & evolution,* 18**,** 292-298.

ZHENG, Z., LAURITZEN, J. S., PERLMAN, E., ROBINSON, C. G., NICHOLS, M., MILKIE, D., TORRENS, O., PRICE, J., FISHER, C. B. & SHARIFI, N. 2017. A complete electron microscopy volume of the brain of adult *Drosophila melanogaster*. *BioRxiv***,** 140905.

ZHOU, K., STAWICKI, T. M., GONCHAROV, A. & JIN, Y. 2013. Position of UNC-13 in the active zone regulates synaptic vesicle release probability and release kinetics. *Elife,* 2.

ZHOU, Q., ZHOU, P., WANG, A. L., WU, D., ZHAO, M., SÜDHOF, T. C. & BRUNGER, A. T. 2017. The primed SNARE–complexin–synaptotagmin complex for neuronal exocytosis. *Nature,* 548**,** 420.

ZWART, M. F., RANDLETT, O., EVERS, J. F. & LANDGRAF, M. 2013. Dendritic growth gated by a steroid hormone receptor underlies increases in activity in the developing *Drosophila* locomotor system. *Proceedings of the National Academy of Sciences,* 110**,** E3878-E3887.